STRUCTURE FUNCTION RELATIONSHIP OF PLANT ADP-GLUCOSE PYROPHOSPHORYLASE

by

Ayşe Bengisu Seferoğlu

A Thesis Submitted to the

Graduate School of Sciences and Engineering

in Partial Fulfillment of the Requirements for

the Degree of

Doctor of Philosophy

in

Chemical and Biological Engineering

Koç University

December 2014

Koç University

Graduate School of Sciences and Engineering

This is

To certify that I have examined this copy of Ph.D thesis by

Ayşe Bengisu Seferoğlu

and have found that it is complete and satisfactory in all respects,

and that any and all revisions required by the final

examining committee have been made.

Committee Members:

_____

İ. Halil Kavaklı, Ph. D.(Advisor)

_____

Özlem Keskin, Ph. D.

_____

Funda Şar, Ph. D.

_____

Gül Cevahir, Ph. D.

_____

Mahmut Çalışkan, Ph. D.

Date: 09. 12. 2014

to my beloved family…

ABSTRACT

Starch is the main storage polysaccharide of plants. It constitutes not only the majority of the human diet but also is used in many industrial applications. There have been significant efforts to increase the starch yield of plants in order to meet the nutritional and industrial requirements of a growing population. ADP glucose pyrophosphorylase (AGPase) is one of the target enzymes of many research studies focusing on the improvement of the starch yield in crop plants. AGPase catalyzes first committed step of bacterial glycogen and plant starch synthesis as it controls carbon flux via its allosteric regulatory behavior. Plant AGPase is a heterotetrameric enzyme ($\alpha_2\beta_2$), composed of two identical large (LS) and two identical small (SS) subunits, which requires both subunits for proper functioning and regulation. Structure-function relationship of AGPase gets much of the attention in order to modulate its activity to increase starch yield of plants. This PhD thesis is focused on two main aspects of AGPase. The first one is exploring the correlation between day length and transcriptional regulation of AGPase isoforms in long day plant lentil (*Lens culinaris,* Medic.). It is known that starch synthesis and degradation are strictly regulated according to day and night-time. In this thesis, transcriptional regulation of AGPase isoforms in lentil leaf and stem under long and short photoperiod was elucidated. To this end, lentil AGPase cDNAs belonging to two isoforms of LS and two isoforms of SS were isolated. Expression profiles of lentil AGPase isoforms, which were analyzed by quantitative real time PCR, were found to be distinct in long-day and short-day grown plants. The distinctive transcriptional profiles led us to explore kinetic properties of the plant exposed to different photoperiod conditions. The second aspect of this thesis is to study subunit-subunit interaction of potato AGPase in order to enhance heterotetrameric assembly thus, in turn, to generate more stable AGPase variants. Computational and experimental studies indicate that heterotetrameric assembly of AGPase is thermodynamically weak. To modulate the subunit-subunit interaction and to find novel variants of AGPase, random mutagenesis and site directed mutagenesis techniques were applied to the LS of potato tuber AGPase. By using reverse genetics approach we improved heterotetrameric assembly of potato AGPase by subjecting LS-R88A cDNA

to error-prone PCR, and selecting second-site revertants according to their ability to restore glycogen accumulation, as assessed by iodine staining, in bacterial cells lacking their own AGPase. Novel mutants of AGPase were characterized by biochemical techniques including native polyacrylamide gel electrophoresis, purification and enzymatic assays. As a result, specific amino acids on the LS which interact with the SS stronger than wild-type LS were identified. The next objective was to analyze physiological effects of novel AGPases in transgenic rice plants. First, identical replacements of the residues found on the LS of potato AGPase have been generated in the LS of rice endosperm (OsAGPL2) in order to analyze *in vitro* enzymatic and structural properties of recombinant AGPases. Then, plant expression vectors carrying mutant LSs of rice endosperm AGPase were constructed for *Agrobacterium* mediated transformation of rice. First generation of transgenic plants was obtained successfully. In future, stable homozygous lines of transgenic rice plants will be analyzed for their starch content and AGPase activity.

ÖZET

Nişasta, bitkilerin temel depo polisakkariti olup hem insanların temel besin maddelerinden biri olarak hem de birçok endüstriyel uygulamada ham madde olarak kullanılmaktadır. ADP glikoz pirofosforilaz (AGPaz), giderek artan dünya nüfusunun besin ve endüstriyel ihtiyaçlarını karşılayabilmek amacıyla bitkilerin nişasta verimini artırmak için üzerinde yoğun çalışmalar yapılan enzimlerden biridir. AGPaz, bakterilerde glikojen ve bitkilerde nişasta sentezinin ilk adımını katalizleyerek allosterik düzenlemeye tabii yapısı ile karbon akışını kontrol eden enzimdir. Bitkilerdeki AGPaz, iki tane büyük (LS) ve iki tane küçük (SS) alt birimin bir araya gelmesinden oluşan heterotetramerik bir enzim olup doğru bir şekilde çalışabilmesi ve regüle edilebilmesi için her iki alt birimine de ihtiyaç duyan bir enzimdir. Bitkilerde nişasta verimini artırmak üzere AGPaz aktivitesini iyileştirmek için enzimin yapı-işlev ilişkisi ile ilgili çalışmalar dikkat çekmektedir. Bu doktora tezi AGPaz enziminin iki ana özelliğini ele almaktadır. Birincisi, uzun gün bitkisi olan mercimekte (*Lens cullinaris,* Medic.) AGPaz izoformlarinin gün uzunluğu ve enzimin transkripsiyonel regülasyonu arasındaki ilişkiyi incelemektir. Nişasta sentezi ve yıkımının gündüz ve gece süresine bağlı olarak sıkı bir şekilde düzenlendiği bilinmektedir. Bu tez çalışmasında, mercimeğin AGPaz izoformlarinin uzun gün ve kısa gün koşulları altındaki transkripsiyon seviyesindeki değişimler incelenmiştir. Bunun için mercimek AGPaz'ına ait olan iki tane LS iki tane SS izoformunun cDNA'ları izole edilmiştir. Kantitatif gerçek zamanlı PCR ile ifade analizi yapılan mercimek AGPaz izoformlarinin uzun gün ve kısa gün koşulları altında farklı olduğu belirlenmiştir. Bu farklı transkripsiyon profili, bizi farklı foto-periyot koşullarında enzimin kinetik özelliklerini incelemeye yöneltmiştir. Bu tezin ikinci olarak ele aldığı konu AGPaz'ın heterotetramerik olarak bir araya gelişini iyileştirmek ve dolayısıyla daha kararlı AGPaz çeşitleri elde etmek amacıyla patates AGPaz'ının alt birimleri arasındaki ilişkiyi incelemektir. Hesaplamalı ve deneysel çalışmalar AGPaz enziminin heterotetramer oluşturmasının termodinamik olarak zayıf olduğunu göstermektedir. Alt birimleri arası ilişkiyi güçlendirmek ve yeni AGPaz varyantları elde etmek için patates AGPaz'ının büyük alt birimi üzerinde rastgele ve bölge-hedefli mutajenez yöntemleri uygulanmıştır. Ters genetik yaklaşımı

ile patates AGPaz'ının heterotetramer oluşumu iyileştirmek için, heterotetramer oluşumunu engelleyen R88A mutasyonunu taşıyan LS cDNA'sı üzerinde hata meyilli PCR yapılarak AGPazı eksik bakteri hücre hattında yapılan iyot boyama tekniği ile heterotetramer oluşturma özelliğini dolayısıyla glikojen sentezini geri kazandıran mutasyonları taşıyan AGPaz'lar seçilmiştir. Yeni elde edilen mutant AGPaz'lar doğal poliakrilamid jel elektroforezi, saflaştırma ve enzimatik analizler gibi biyokimyasal yöntemlerle karakterize edilmiştir. Sonuç olarak, LS üzerinde SS ile yabanıl tipe kıyasla daha güçlü etkileşmesini sağlayan spesifik amino asitler tespit edilmiştir. Bir sonraki amaç olarak bulunan yeni AGPaz'ların fizyolojik etkilerini transgenik çeltik bitkilerinde incelemek hedeflenmiştir. İlk olarak, rekombinant AGPaz'ların enzimatik ve yapısal özelliklerini analiz etmek üzere çeltik endosperm AGPaz LS'i üzerindeki eş bölgelerde patates AGPaz LS'i üzerinde bulunan mutasyonlar yapıldı. Daha sonra Agrobakteri aracılığıyla çeltik tranformasyonunu yapabilmek için çeltik endosperm AGPaz mutant LS'lerini taşıyan bitki ifade vektörleri hazırlandı. Birinci nesil transgenik bitkiler başarı ile elde edildi. Kararlı ve homozigot transgenik çeltik bitkilerinin elde edildikten sonra nişasta miktarı ve AGPaz aktiviteleri gelecek çalışmalarda araştırılacaktır.

ACKNOWLEDGEMENTS

I would like to gratefully acknowledge the following people, who were instrumental in the writing and publication of this dissertation.

Foremost, I would like to thank my thesis advisor Assoc. Prof. Halil Kavakli for his training, endless support and the many opportunities he provided for me during the course of my time here. I am grateful to him being so generous for sharing his time, knowledge and ideas.

I am also thankful to Prof. Thomas W. Okita at Washington State University, who gave me the opportunity to conduct part of my research in his lab. During my visit to Prof. Okita's laboratory, I have learned rice transformation experiments from Dr. Salvinder Singh and I appreciate his assistance.

I am grateful to my thesis committee members, Prof. Özlem Keskin and Assist. Prof. Funda Şar, they always kept track of my PhD study, carefully. It would be incomplete if I do not mention the names of PhD dissertation jury members; Prof. Gül Cevahir and Prof. Mahmut Çalışkan from Istanbul University. I would like to thank them for their supportive comments.

I am grateful to Assoc. Prof. İbrahim Barış for his guidance and support whenever I need.

I would like to give my special thanks to my dear friend Hande Asımgil, for sharing her knowledge and for her endless support in my studies and in my personal life. She is like a sister to me.

My dear lab mate, office mate and friend Selma Bulut, and the loveliest couple I have ever met Derya Yarparvar and Hadi Nozari. Thank you for the endless humor, encouragement and great times.

Thank you, Anı Akpınar. My best friend, my colleague… Words are not enough to express my gratitude for your precious friendship.

I would like to give my special thanks to my former housemates Zeynep Ülker Demir and Melis Yavuz Müren who made me feel always at home. I will never forget their endless support and friendship.

A hearty thank you to all the former and current lab mates and friends who helped me a lot. This list includes, but is not limited to: Kaan Koper, Fatma Betul Can, Şeref Gül, Ehsan Sarayloo, Eylem Külköylüoğlu, Derya Kabacaoğlu, Sibel Çal, Berke Gürkan, Mehmet Tardu, Elif Muku, Engin Çukuroglu and Oytun Aygün.

I also appreciate Aytuğ Tuncel's and Bilal Çakır's help during my research visit in Washington State University.

Last but not least I would like to thank my family for their continuous support, patience and endless love during every step of my education.

I acknowledge the financial support from the Scientific and Technological Research Council (TÜBİTAK) for the 2211 and 2214A scholarships during my whole graduate study and my visit to the Washington State University, respectively. In addition, a part of studies was supported by TUBITAK-TBAG 110T058 fund.

TABLE OF CONTENTS

LIST OF TABLES

LIST OF FIGURES

NOMENCLATURE

AGPase	ADP glucose pyrophosphorylase
ADPGlc	ADP glucose
BE	Branching enzyme
CFE	Cell free extract
DEAE	Diethylaminoethyl
DTT	Dithiothreitol
GBSS	Granule bound starch synthase
G1P	Glucose 1 phosphate
HRP	Horseradish peroxidase
LB	Luria Bertani
LS	Large subunit
NAD	Nicotinamide adenine dinucleotide
PCR	Polymerase chain reaction
PMSF	Phenylmethanesulfonylfluoride
P_i	Inorganic phosphate
PP_i	Pyrophosphate
SDS-PAGE	Sodium dodecyl sulfate polyacrylamide gel electrophoresis
SS	Small subunit
WT	Wild type
3PGA	3-Phosphoglyceric acid

CHAPTER 1

INTRODUCTION

Starch is the main storage carbohydrate in many plants. It serves as a primary source of calories in human diet as well as being an inexpensive and environmentally friendly polymer for various industrial processes [1]

In higher plants starch is synthesized in both photosynthetic and non-photosynthetic tissues. Cereal seeds (rice, maize, barley, wheat), roots (cassava) and tubers (potato) are the main plant sources for starch production with an overall supply of 2.7 billion tons annually. Seventy-five million tons are used for industrial purposes according to 2012 data published by the International Starch Institute (http://www.starch.dk). Both from nutritional and industrial perspectives, improving starch yield in plants is crucial due to increasing population and industrial demand.

In food sector starch is commonly used as a thickener, confectioner and emulsifier. Starch can be used as a sizing agent in textile and paper industries. Its adhering texture is used in adhesive industry. Moreover, it is an environment friendly raw material for the production of biodegradable plastics. Being a cheap and renewable polymer, makes starch a valuable source for various industrial processes. In recent years, biofuel industry made by fermentation of starch and sugars has also grown rapidly. Improving starch content of crop yields would be one of the most important achievements to enhance sustainability of biofuel crops [2].

ADP glucose pyrophosphorylase (AGPase) is one of the target enzymes of many research studies focusing on the improvement of the starch yield in crop plants. AGPase catalyzes first committed step of bacterial glycogen and plant starch synthesis as it controls carbon flux via its allosteric regulatory behavior. Plant AGPase is a heterotetrameric enzyme ($\alpha_2\beta_2$), composed of two identical large (LS) and two identical small (SS) subunits, which requires both subunits for proper functioning and regulation. Structure-function relationship of AGPase gets much of the attention in order to modulate its activity to increase starch yield of plants.

The outline of this dissertation is as follows:

In Chapter 2, structure and biosynthesis of starch is described, the role of the key enzyme ADP-glucose pyrophosphorylase is highlighted and approaches to increase starch yield in plants is summarized.

Chapter 3 focuses on the transcriptional regulation and enzyme kinetics of AGPase in long-day plant lentil. For this purpose, cDNA clones of two LS isoforms and two SS isoforms were isolated from plants grown under long-day and short-day conditions and their RNA expression level was determined with quantitative real time PCR. In addition, kinetic and allosteric properties of native lentil AGPase were characterized for the first time. The content of Chapter 2 was published as Seferoglu, A.B., et al., *Transcriptional regulation of the ADP-glucose pyrophosphorylase isoforms in the leaf and the stem under long and short photoperiod in lentil.* Plant Sci, 2013. **205-206**: p. 29-37.

In Chapter 4, LS-SS subunit interaction of potato tuber AGPase was analyzed in an effort to improve heterotetrameric assembly of enzyme focusing on subunit interface residues. By using reverse genetics approach interaction between monomers and dimers of AGPase were increased so that heterotetrameric assembly of enzyme is favored *in vitro* conditions. Results of this study was published as Seferoglu, A.B., et al., *Enhanced heterotetrameric assembly of potato ADP-glucose pyrophosphorylase using reverse genetics.* Plant Cell Physiol, 2014. **55**(8): p. 1473-83

Chapter 5 describes works performed to elucidate structural and physiological effects of better assembling potato AGPase LS variants in rice endosperm AGPase. To this end, identical replacements of the residues found on the LS of potato AGPase have been generated in the LS of rice endosperm (OsAGPL2) for *in vitro* analyses. Next, transgenic rice plant lines were generated carrying mutant LS variants of rice endosperm AGPase for future investigations.

Chapter 6 comprehends the results that are put forward in this dissertation and the major conclusions about the topics as well as the future directions.

CHAPTER 2

LITERATURE REVIEW

2.1 Starch and its structure

Starch granules have a semi-crystalline form, which are composed of amylose and amylopectin molecules. Amylose and amylopectin are polymers of alpha-D-glucose units. The major difference between them is their branching pattern. Amylopectin has a highly branched structure via α-1, 6-glycoside bonds, whereas amylose has a slightly branched structure [3]. Amylopectin not only forms 75% of the starch but also is responsible for its granular structure. This granular structure is mainly composed of tree like patterns of amylopectin clusters. The tree-like structure depends on the chain lengths and branching patterns of the amylopectin clusters. Branching points in amylopectin clusters are not randomly distributed. Typically, chains formed by 12-15 glucosyl residues interconnect two clusters. There are also chains containing 35-40 residues. Adjacent chains within clusters form double helices giving rise to the semi-crystalline structure of starch which is a highly conserved structure among plant species [4]. Estimated molecular weight of amylopectin varies between 10^7 and 10^9 Daltons [3].

Amylose is a smaller molecule than amylopectin with a molecular weight between 10^5 and 10^6 Daltons. Approximately 25% of a starch granule is composed of lightly branched amylose molecules [3], which are mainly, exists in the amorphous regions of the starch granules [5].

2.2 Main enzymes of starch biosynthesis

ADP-glucose pyrophosphorylase (AGPase) catalyzes first committed step of starch biosynthesis and produces the soluble precursor molecule ADP-glucose (Figure 2-1). AGPase is subject to different levels of post-translational modification including redox and allosteric regulation, which will be described in the following sections. The

subsequent step is transfer of glucose residue from ADP-glucose by starch synthases. This glucose residue is added to the 4-position of the terminal glucose residue of elongating glucan chain (Figure 2-1). Plants have multiple isoforms of starch synthases. Those isoforms can split into two groups based on their roles in amylose/amylopectin synthesis. Granule bound starch synthases (GBSS) involves in the amylose synthesis. GBSS family includes GBSSI and GBSSII isoforms. GBSSI is mainly found in the storage tissues, whereas GBSSII is thought to be responsible for amylose synthesis in source tissues [6-8]. Studies in sweet potato and *Arabidopsis* have shown that transcript abundance and protein expression levels of GBSS show strong diurnal fluctuation [9, 10].

The second group of starch synthases involves in amylopectin synthesis (SSI, SSII, SSIII and SSIV). Activity of those isoforms shows significantly plant and tissue specificity [11]. In rice, for example, multiple isoforms of starch synthase not only show tissue specificity but also have temporal expression pattern [12]. Studies suggest that SSI catalyzes formation of short glucan chains and plants lacking SSI do not have significant changes in terms of starch structure [13]. SSII and SSIII catalyze further extension of longer chains. Combined reduction of SSII and SSIII in potato revealed that those isoforms are responsible for the amylopectin synthesis and they also depend each other for production of a proper starch granule [14, 15].

Branches in the tree-like structure of starch are formed by starch branching and debranching enzymes. Starch branching enzymes (SBE) cleaves the α-(1,4) bonds at specific chain lengths and transfer free reducing ends to C6 hydroxyls to form the branched structure (Figure 2-2). Similar to starch synthase SBE also has multiple isoforms showing tissue and temporal specificity [13]. SBEI and SBEII are two major classes of branching enzymes. There are two main differences between SBEI an SBEII isoforms. SBEII catalyzes branching on shorter glucan chains and it has a higher affinity to amylopectin than amylose as a substrate. SBEII mutant plant studies resulted in formation of high-amylose starch [16, 17].

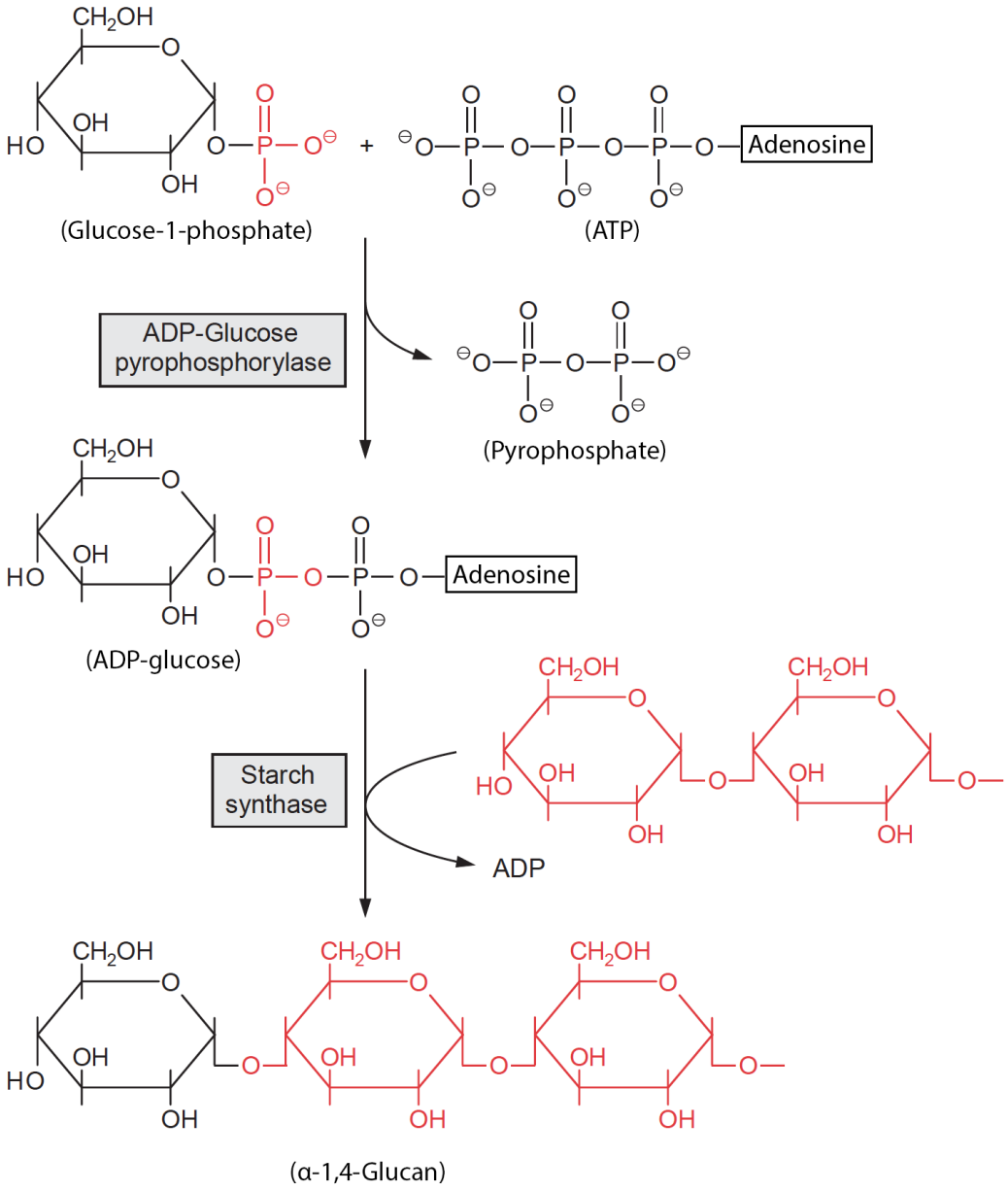

Figure 2 - 1 Starch biosynthesis. First step is catalyzed by ADP-glucose pyrophosphorylase, which produces ADP-glucose and pyrophosphate from the reaction of ATP and Glucose-1-phosphate. Glucose from ADP-glucose is transferred by starch synthase for the elongation of glucan chain. Adapted from [18].

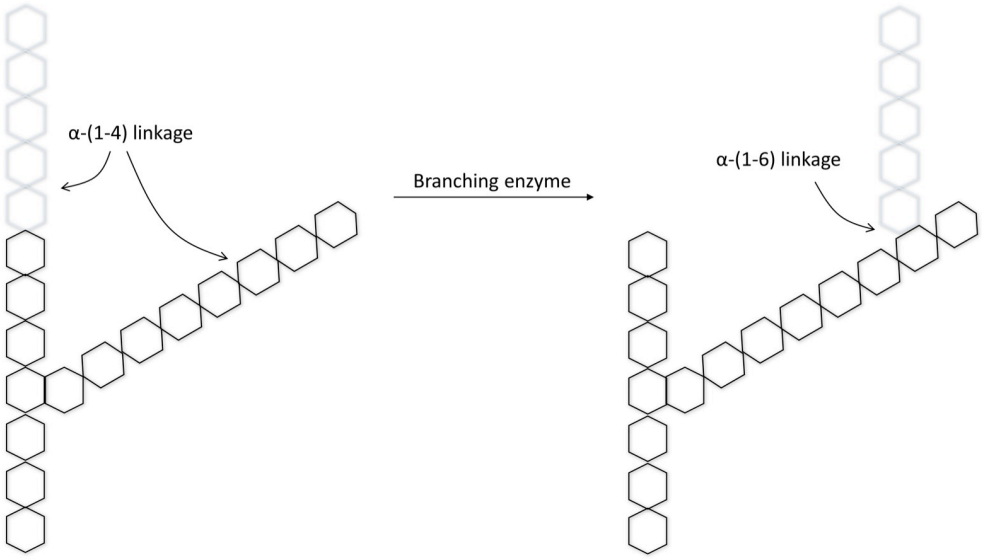

Figure 2 - 2 Starch branching enzymes cleaves α-(1-4) linkage and links disconnected chain to a neighboring chain by a α-(1-6) linkage. Adapted from [18].

In the formation of starch granule, debranching enzymes also play a significant role. Plants have two types of debranching enzymes; isoamylase-type and pullunase-type. Exact roles of debranching enzymes in starch biosynthesis are not fully known. Mutant and transgenic plants studies showed that plants lacking functional debranching ezyme accumulated phytoglycogen instead of starch granule [19, 20]. There are two proposed models for the role of debranching enzymes in starch synthesis. The first one proposes that debranching enzymes prevent amylopectin aggregation by trimming glucans [21, 22]. The second model suggests that debranching enzymes removes soluble glucan chains that are not attached to the starch granule [23].

2.3 Overview of starch synthesis in plants

Starch production occurs in both photosynthetic (source) and non-photosynthetic (sink) plant tissues. Starch biosynthesis in source tissues, which are mainly leaves, regulates plant growth [24]. Starch metabolism follows a diurnal synthesis and breakdown cycle and is, therefore, named transitory starch. Although much of the fixed carbon is exported to the cytosol for sucrose synthesis; a significant portion is used for starch synthesis in the chloroplast. The first committed step in the synthesis of starch is catalyzed by AGPase, an enzyme which utilizes glucose-1-phosphate (G1P) and ATP to produce ADP-glucose, sugar donor molecule used by starch synthase [25] (See Figure 2-1).

On the other hand, production of storage starch takes place in non-photosynthetic sink tissues such as tubers, roots and seeds. For the production of storage starch, ADP-glucose is synthesized in amyloplasts in most plants. In cereal endosperm, the storage tissue of seeds, however, the major AGPase form is located in the cytoplasm [26, 27] where newly synthesized ADP-glucose is subsequently imported to the amyloplast via ADP-glucose transporters for starch synthesis [28].

2.3.1 Starch metabolism in source tissues

In leaves, products of photosynthesis partitioned for starch and sucrose synthesis. Transitory starch storage in leaves is an essential sugar source for continued metabolism and growth at night. Mutant *Arabidopsis* studies with reduced activities of phosphoglucoisomerase (PGI), phosphoglucomutase (PGM) or AGPase indicate that starch biosynthesis in leaves takes place in plastids [29-31].

The precursor molecule of starch synthesis, ADPglucose, is linked to the Calvin-Benson cycle via three enzymatic steps (Figure 2-3). First step is catalyzed by PGI, which convert fructose-6-phosphate (F6P) to glucose-6-phosphate (G6P). Then, PGM converts G6P to G1P. Third step is production of ADP-glucose from G1P and ATP by AGPase catalyzed reaction. This reaction liberates inorganic pyrophosphate (PP_i), which is hydrolyzed by plastidial alkaline pyrophosphatase. This hydrolysis makes the reversible reaction of AGPase irreversible in physiological conditions. Remaining steps of starch biosynthesis are catalyzed by starch synthases, branching and debranching enzymes as indicated in previous section.

Although AGPase is the main producer of ADP-glucose, recent studies have shown that, sucrose synthase (SuSy) can also produce some amount of ADP-Glucose [32] but no transporter is known to mediate its import from cytosol to plastid [33].

Plants are able to tune transitory starch synthesis and breakdown according to the day length. Both starch synthesis and starch breakdown occurs in a near-linear manner, during the day and the night, respectively [33]. *Arabidopsis* studies have shown that in short-day conditions starch synthesis is faster than in long-day conditions [34, 35]. In addition, when plants are exposed to an unexpected extended night period, starch synthesis is also accelerated [36]. Currently, the exact mechanism behind this regulation is not known. It was shown in a recent study, allosteric regulatory properties of AGPase are crucial for the regulation of the rate of starch synthesis according to day length [37].

The rate of starch breakdown in source tissues determines the energy budget of plants for growth and metabolic activities. Enzymes involved in starch breakdown works

cooperatively. Starch breakdown begins with the glucan phosphorylation catalyzed by glucan water dikinase (GWD) and phosphoglucan water dikinase (PWD). This phosphorylation disrupts granule surface. Most important enzymes involved in glucan degradation are β-amylases and debranching enzymes [5]. Hydrolysis of transitory starch produces maltose and glucose, which are than exported from chloroplast to cytosol [38, 39].

2.3.2 Starch metabolism in sink tissues

Sucrose produced in source tissues is transferred to sink tissues to supply energy and starch synthesis in the amyloplast. One of the major differences of starch synthesis between source and sink tissues is the precursor molecule entering to the plastid. Although chloroplasts and amyloplasts are ontogenically related, chloroplasts use triose phosphates (C-3), whereas amyloplasts use a C-6 molecule (G6P or ADP-glucose) entering to the amyloplast [40, 41]. Another major difference is the presence of ATP. Since amyloplasts are not capable of generating ATP via photosynthesis, they have to import ATP from cytosol for the AGPase catalyzed reaction. Amyloplasts have ATP/ADP translocator in the envelope membrane [42, 43] (Figure 2-4A). Starch biosynthesis in sink tissues also differs between dicotyledonous and monocotyledonous plants depending on the major localization of AGPase (Figure 2-4). In dicots, AGPase is localized in amyloplasts, whereas most of AGPase in cereal endosperm cell are cytosolic. In dicots, sucrose is broken down by SuSy to produce fructose and UDP-glucose. UDP-gluose is converted to the G1P and PP_i by UGPases. Next, G1P is converted to G6P, which is then transported to the amyloplast. In amyloplast, starch synthesis continues with stepwise reactions catalyzed by PGM, AGPase and starch synthase as indicated previously (Figure 2-4A). In monocot plants ADP-glucose is produced in cytosol and transferred to amyloplast for starch biosynthesis. Studies have shown that Bt1 proteins drive ADP-glucose transfer [28, 44, 45]. SuSy, UGPase and AGPase catalyzed reactions takes place in cytosol. ADP-glucose enters amyloplast and is utilized as a glucosyl donor for starch synthesis (Figure 2-4B).

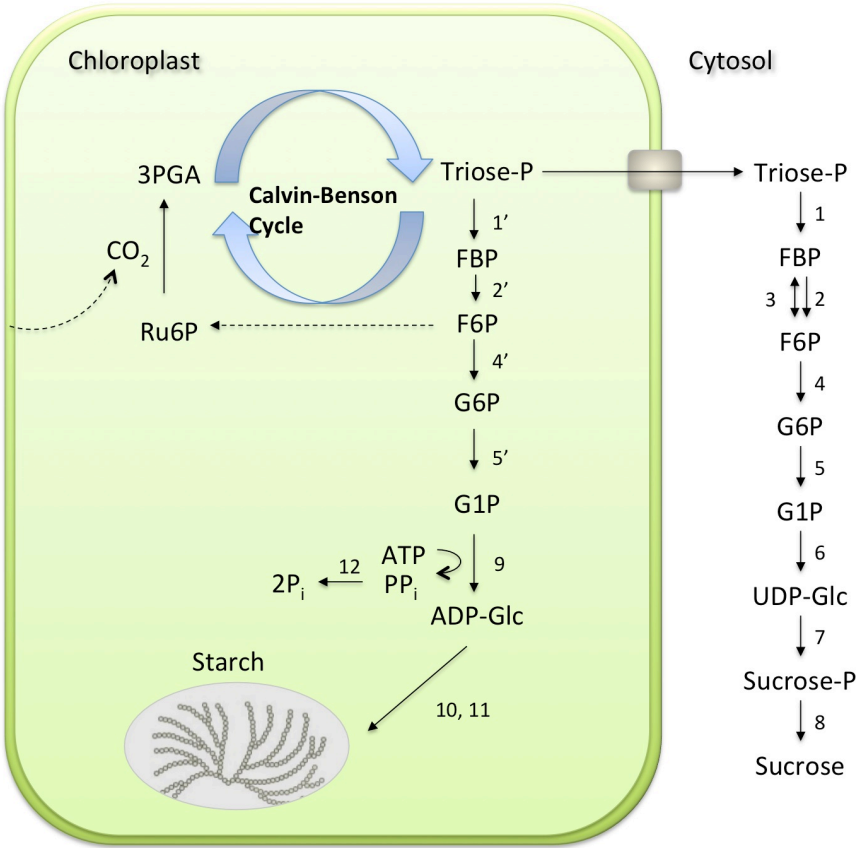

Figure 2 - 3 Starch and sucrose synthesis in leaves. Calvin-Benson cycle product, 3PGA, is converted to Triose-P which is either used for starch synthesis in chloroplast or transported to cytosol and converted to sucrose by a series of reactions. The enzymes are numbered as follows: 1, 1', fructose-1,6-bisphosphate aldolase; 2, 2′, fructose-1,6-bisphosphatase; 3, fructose-6-P 1-phosphotransferase; 4, 4′, phosphoglucose isomerase; 5, 5', phosphoglucomutase; 6, UGPase; 7, sucrose-phosphate-synthase; 8, sucrose phosphate phosphatase; 9, AGPase; 10, starch synthase; 11, brancing and debranching enzymes; 12, inorganic pyrophosphatase. Adapted from [46]

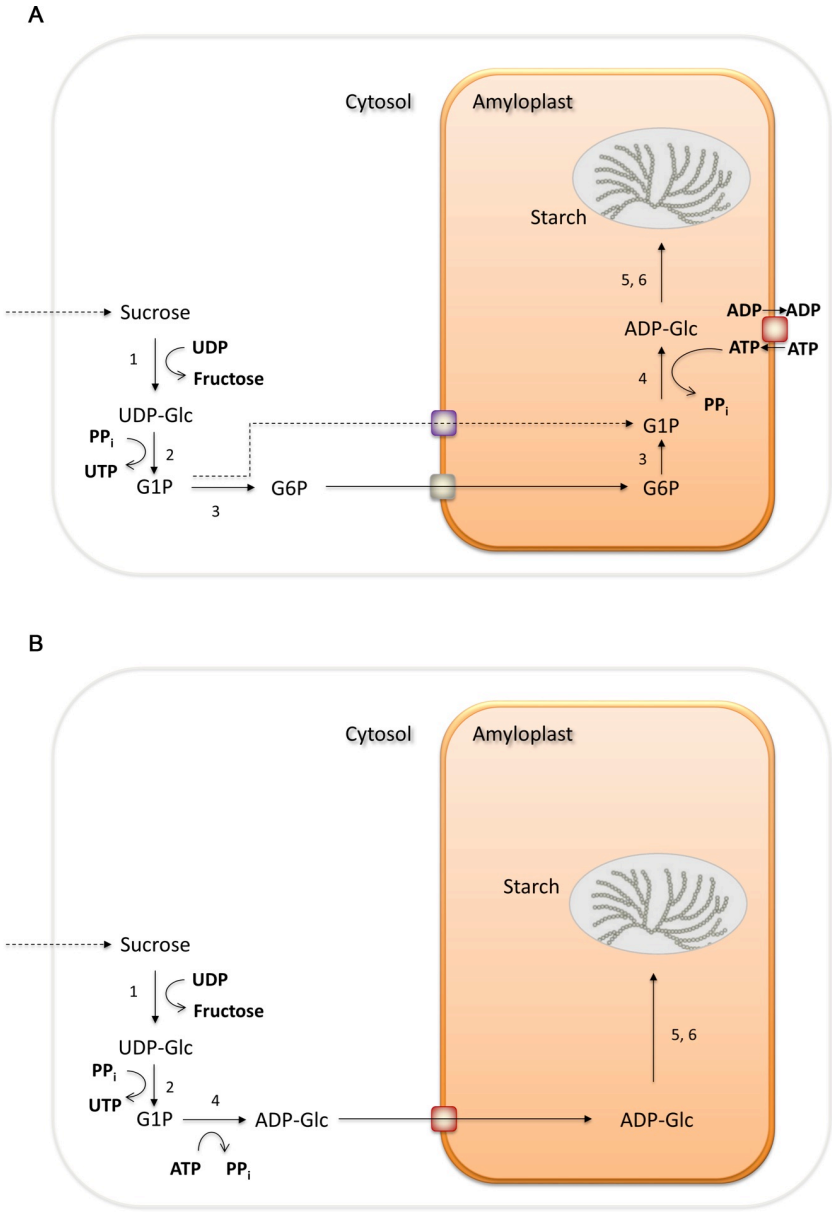

Figure 2 - 4 Starch biosynthesis in sink organs. (A) Heterotrophic cells of dicotyledonous plants where AGPase is exclusively located in the plastid. (B) Cereal endosperm cells where most of AGPase is localized in cytosol. ADP-glucose transporters transport ADP-glucose from cytosol to plastid where starch synthesis is completed. Enzyme numberings are same as in figure legend 1-3. Adapted from [46]

2.4 ADP-glucose pyrophosphorylase

The reaction catalyzed by AGPase plays an important role in starch synthesis is not only being the first committed step of the reaction but also because it is extensively controlled allosterically by small effector molecules. Therefore, modulating the activity of this pivotal enzyme has a potential to increase starch yield in crop plants.

AGPase catalyzed reaction was first identified in soybean extracts [47]. Then it has been shown that other plant and bacteria extracts also have AGPase [48, 49]. AGPase catalyzes the first committed step of glycogen and starch biosynthesis in bacteria and plants, respectively (see Figure 2-1). Plant AGPases are structurally more complex than bacterial AGPase. The prokaryotic AGPase is a homotetrameric enzyme composed of four identical subunits, while plant AGPase is a heterotetrameric enzyme composed of two identical large subunits (LS) and two identical small subunits (SS). Moreover, plants possess multiple isoforms for LS and/or SS of AGPase, which can be differentially expressed in different tissues. For example, *Arabidopsis* has four LS isoforms (APL1 to APL4), and two SS isoforms (APS1 and APS2). Large subunit isoforms show tissue specific expression such as APL1 for leaf and APL3 for seed [50]. Among small subunits *Arabidopsis* APS2 is not the functional one which has not displayed any catalytic activity by itself or when coexpressed with the other LS isoforms of *Arabidposis* [51].

Phylogenetic analysis shows that SSs are more conserved between different species than LSs. This difference stems from faster evolution rate of LS than SS. In general SSs are less tissue specific, have less gene copies and therefore have to interact with multiple LS isoforms [52]. Studies indicate that since there is fewer SS isoforms than LS isoforms, SS is under the pressure of being and remaining catalytic [53]. As displaying more flexibility, modulating LS structure can be a way to fine-tune the subunit interaction, catalytic and allosteric properties of AGPase.

Allosteric regulation is one of the most important posttranslational regulations of AGPase as it significantly changes activity of enzyme and in turn starch biosynthesis. Plant AGPases are allosterically activated by 3PGA and inhibited by P_i. Activation and

inhibition of AGPase to these allosteric effector molecules depend on tissue and plastid type. Chloroplast AGPases, for example, are much more sensitive to the allosteric effector molecules than cytoplasmic AGPases [13]. On the other hand, AGPase activities of bean cotyledon [54] and pea embryo [55] show much less response to 3PGA. Many studies have been focused on modulating allosteric regulatory behavior of AGPase. Pyridoxal-P labeling facilitated to identify residues involved in the binding of allosteric effector molecules in AGPase in which specific lysine residues were found to be regulatory binding sites [56, 57]. Random mutagenesis and site directed mutagenesis studies have also provided useful information about allosteric regulatory behavior of AGPase. Upregulated variants of potato AGPase, for example, were obtained by the conversion of Glu38 to Lys [58] or Gly101 to Asn [59] in the LS of potato AGPase. A random mutagenesis study has found that D413 residue on the LS of potato tuber AGPase is crucial for the normal activation by 3PGA [60]. Similarly, another *in vitro* random mutagenesis strategy on the potato tuber LS have identified three residues, Lys197, Pro261, Lys420, on the LS showing altered affinities to the allosteric effector molecules [61]. A DNA shuffling approach identified regions of the primary sequence on the SS of potato tuber AGPase involved in allosteric effector binding [62].

Previously, it has been suggested that the SS and the LS have different roles in enzyme function. The SS is regarded as the main catalytic subunit, whereas the LS modulates allosteric properties of AGPase [63]. When the SS of potato tuber AGPase expressed alone, it is capable of forming active homotetramers requiring high concentrations of activator 3PGA [64]. In addition, earlier studies indicated that the LS was capable of binding activator molecules, which supports the regulatory subunit role attributed to the LS [56]. Although the SS was regarded as the main catalytic subunit, later, a study with mosaic enzymes composed of primary sequences of maize endosperm and potato tuber AGPase revealed that both subunits are required for the catalyctic activity and allosteric regulation [65, 66]. Similarly, in another study, kinetic analyses of combination of mutant LSs and SSs have shown that allosteric regulation requires contribution of both subunits [67]. When six proline residues on the N-terminal region of potato AGPase LS were subjected to scanning mutagenesis, the importance of the LS for the catalytic

activity of enzyme was revealed. In addition to that photolabelling studies suggested the LS also binds to ATP with similar affinity as the SS [68]. More recently, it has been found that in tomato L3 isoform of AGPase is active alone as a monomer although it is inefficiently catalytic [69]. On the whole, LS is not the most catalytically efficient subunit, nonetheless it involves in catalysis and allosteric regulation of AGPase substantially.

Kinetic studies from many different AGPases such as barley [70], *Rhodospirillum rubrum* [71] revealed that AGPase follows Theorell-Chance bi bi mechanism with minor modifications. A recent study made a detail kinetic characterization of AGPase using, maize, potato and maize/potato chimeric AGPases. This study also indicated that AGPase exhibits Theorell-Chance bi bi mechanism in which in the presence of 3PGA substrate ATP binds first and releases ADP-glucose last [72]. Collectively, results indicate that ATP or ADP glucose is the first substrate to bind to the enzyme. Then, the other substrate G1P or PP_i binds to the enzyme in the forward and reverse direction reactions, respectively.

AGPase is also subject to the post-translational redox regulation. Redox regulation of AGPase was first shown in potato tubers where SS dimerization is related to enzyme activity, sugar levels and starch synthesis. Reductive environment leads to the monomerization of SSs through breakage of intermolecular disulfide bridge between Cys12 of the two SSs of potato tuber AGPase [73, 74]. Other studies have also shown that leaf AGPases of pea, potato and *Arabidopsis* are subject to redox regulation depending on the sugar and light levels [75, 76]. It has been shown that increased levels of trehalose-6-phosphate lead to the redox activation of AGPase and stimulation of starch synthesis in plants [77].

Although cytosolic isoform of cereal endosperm AGPases lacks the conserved Cys12 residue, recent studies suggest that they are also subject to redox regulation. A proteomics study has shown that wheat endosperm AGPase interacts with thioredoxin indicating a potential redox regulation [78]. A recent study has revealed that rice

endosperm cytosolic AGPase is also controlled by redox regulation through showing more affinity to the activator 3PGA under reduced conditions [79].

2.4.1 Structure of AGPase

As described above, AGPase is a heterotetrameric enzyme composed of pairs of LS and SS. The first atomic structure resolution of AGPase was determined based on crystals obtained from SS homotetramers of potato tuber AGPase [80]. This 2.1Å resolution crystal structure belongs to an inhibited state of the enzyme (PDB ID 1YP2). Two more structures were extracted in that study: the enzyme in complex with ATP and ADP-glucose, with resolutions, 2.2Å and 2.6Å, respectively. According to the homotetrameric crystal structure, catalytic N-terminus is composed of mostly parallel but mixed seven stranded β-sheets covered by α-helices resulting a strong hydrophobic interaction area (Figure 2-5). N-terminus interacts with β-helix domain of C-terminus through a 20 amino acid long loop [80]. Although determined crystal structure is not in its native form, it gives valuable structural information about the assembly of subunits and insights into the heterotetrameric structure of AGPase. Atomic resolution structure of heterotetrameric AGPase is not currently available, since it is difficult to obtain a highly pure and stable form of heterotetrameric native enzyme.

Another 3D structural data for AGPase belongs to the homotetrameric *Agrobacterium tumefaciens*' AGPase [81]. Although SS of potato tuber AGPase and *A. tumefaciens* AGPase share 31% primary sequence identity, N-terminal and C-terminal domains exhibit very different sequence homology.

Computational and mutagenesis studies provide valuable data to interpret LS-SS interaction profile of heterotetrameric AGPases. Approximately 50% similarity between SS and LS primary amino acid sequences makes homology modeling feasible to construct heterotetrameric models of AGPase. To elucidate heterotetrameric structure of AGPase, the first homology modeling study was conducted for potato AGPase [82] (Figure 2-6). Later, homology models of heterotetrameric enzyme for maize, rice and wheat AGPases were also built up [83-85].

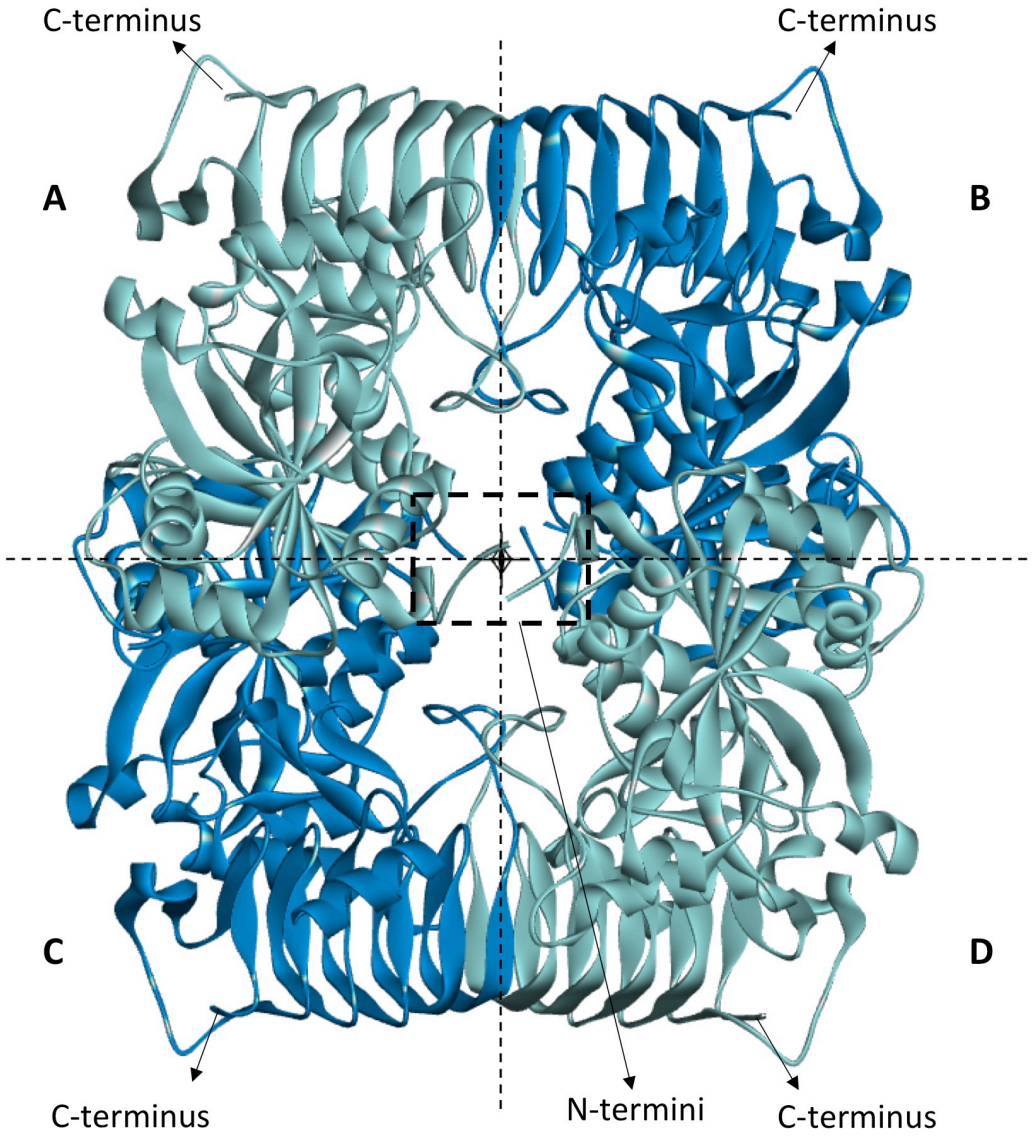

Figure 2 - 1 Crystal structure of the homotetrameric potato tuber AGPase composed of four chains (A to D) of the SS (PDB ID: 1YP2). Structure was visualized by BIOVIA Discovery Studio.

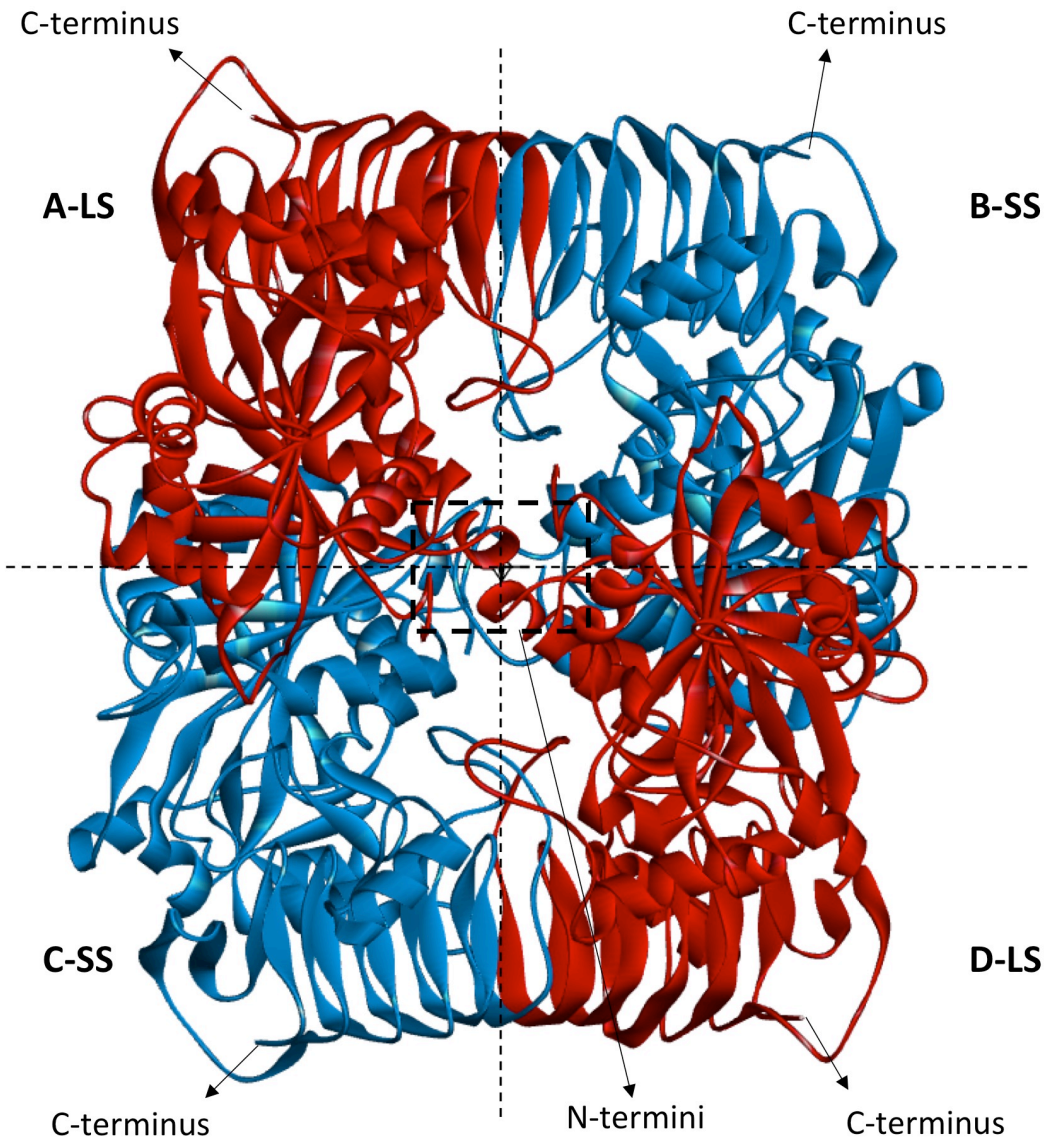

Figure 2 - 2 Homology modeled structure of the heteroterameric potato tuber AGPase. A nd D chains (red) indicate LSs; B and C chains (blue) indicated SSs. Structure was visualized by BIOVIA Discovery Studio. Adapted from [82].

Computational methods also facilitated to obtain more detailed pictures of the heterotetrameric enzyme. According to the homology-modeled structure of heterotetrameric potato AGPase, the most favorable heterotetramer is formed by side-by-side and up-down interaction of LS-SS monomers. Relative binding free energies indicates that first side-by-side LS-SS dimers form then up-down tetramerization takes place [82]. In a subsequent study, using molecular mechanics generalized born surface area (MM-GBSA) method on homology-modeled heterotetrameric potato AGPase, important residues mediating interactions between the LS and the SS were mainly identified and most of them were confirmed experimentally [86].

Together with computational studies, mutagenesis and experimental studies have identified essential motifs/residues required for subunit-subunit interaction of AGPase. One of the earlier studies have proved direct interaction of SH2 (LS) and BT2 (SS) subunits of maize AGPase [87]. Truncation of N or C-terminus of either subunits revealed that C-terminus of SH2 is significantly important for SH2-BT2 interactions. In a mutagenesis study, it has been found that a His-to-Tyr mutation at the posisiton of 333 in SH2 increased heat stability of maize AGPase [88].

The conserved QTCL motif on the SS of plastidial AGPases is both responsible for redox regulation and heat stability of enzyme. The Cys residue in QTCL motif increases heat stability of potato tuber AGPase at high temperatures by formation of covalent disulfide bond between the two small subunits [89]. Insertion of QTCL motif on heat labile maize endosperm AGPase, increased heat stability of the enzyme significantly [90]. In another study, recombinant expression of chimeric potato/maize small subunits in *E.coli* has led to the identification of a small motif within the SS, which is required for proper subunit interaction and functioning of AGPase [66].

Recent studies revealed that LS-SS interaction of AGPase is particularly crucial for the functioning of enzyme. Interacting residues on the subunit interface not only act for structural stability of AGPase but also affect its allosteric regulation. Boehlein et.al have shown that substrate and allosteric effector binding stabilize activity of maize endosperm AGPase to heat inactivation [91]. Specific amino acid residues both of the

LS and the SS of potato tuber AGPase located at subunit interaction interface have been identified in a study using both computational and experimental methods [86]. Later, a phylogenetic analysis of AGPase subunits showed how subunit interface amino acids are important for the allosteric properties of the enzyme [92].

To sum up, investigation of AGPase in terms of subunit interaction is a good example showing how an enzymes' structural information can affect its stability and functioning in a synchronized manner.

2.5 Manipulation of AGPase activity to increase starch yield in plants

Starch synthesis in crop plants essentially depends on source/sink relationship of plants. Therefore, much of the efforts have been directed to increase photosynthesis efficiency in source tissues (leaves). However, feedback mechanisms can limit photosynthesis. One of the most limiting feedback mechanisms inhibiting more photosynthesis is the inefficient conversion of triose phopshates into carbohydrates. Basically, conversion of triose phosphates recycles P_i that required for ATP synthesis via photophosphorylation. Therefore capacity of plants partitioning fixed carbon into carbohydrates releases P_i and allows further photosynthesis.

The reaction catalyzed by AGPase plays an important role in starch synthesis is not only being the first committed reaction step but also because it is extensively controlled allosterically by small effector molecules. Therefore, modulating the activity of this pivotal enzyme has a potential to increase starch yield in crop plants.

Allosteric regulation of AGPase is very important in apportioning of carbon between sucrose and starch. When sucrose synthesis is not enough for sink organs, P_i levels increase in chloroplast to induce more ATP synthesis. Reduced 3PGA/P_i ratio lowers AGPase activity and starch synthesis. On the other hand, when sucrose synthesis is saturated, 3PGA/Pi ratio increases as triose phosphate levels rise which activates AGPase more and directs carbon flow into starch synthesis instead of sucrose synthesis [93].

To increase starch yield of plants two strategies can be applied. One is to try increasing source strength and in turn, increasing photosynthetic capacity of the plant. The other one is to increase capacity of sink organs for better utilization of photosynthesis products.

The strategy of overexpressing AGPase in leaves to increase source strength relies on two principles. First, increased transitory starch levels would support vegetative and reproductive growth during night. Second, increased rate of starch synthesis would result in utilization of triose phosphates into carbohydrates, which would lessen feedback inhibition of photosynthesis [93]. Transforming *Arabidopsis* studies starch-deficient and starch-null mutants have shown importance of leaf starch on photosynthesis indicating the dependence of CO_2 assimilation rates, starch synthesis and plant growth [94, 95].

Introducing up-regulated AGPase LS gene into *Arabidopsis* ApL1 deficient TL46 plant line resulted in more leaf starch at the end of the day and enhanced turnover of transitory starch than wild-type plants [96]. They also showed higher photosynthetic capacity, increased starch levels and leaf biomass [97]. Similarly analysis of transforming wild-type rice plants with up-regulated potato AGPase LS genes under the control of Rubisco small subunit promoter improved capacity of plants for leaf starch synthesis [97].

Increasing photosynthate-utilizing capacity of sink organs is another approach to increase starch yield of plants. One of the earlier studies have shown that overexpression of AGPase in potato tubers led to an increase in starch content of tubers by 30-60% [98]. Studies with cereal plants for increasing sink capacity is useful to see how developing seeds can improve seed filling process through starch synthesis. Major isoform of AGPase in cereals is cytosolic and genetic studies indicate that cytosolic AGPase directs carbon flow to starch. Increase in seed weight was first shown in maize by introduction and over-expression of a P_i insensitive AGPase transgene [99]. Similarly, when bacterial mutant AGPase gene [100] or native maize AGPase genes,

sh2 and *bt2*, [101] were overexpressed under endosperm specific promoters, kernel weight increased around 10-20%.

Similar studies in rice where a bacterial triple mutant AGPase (glgC-TM) over-expressed have shown that seed weight increased up to 11% [102]. glgC-TM carries three mutations (R67K, P295D, G366D) which make the enzyme fully activated independent of activators and insensitive to the inhibitor P_i [103].

Interestingly, endosperm specific AGPase over-expression in maize, wheat and rice resulted in seed number and vegetative growth increase instead of increase in individual seed weight [104-107]. More recently, over-expression of cytosolic large subunit gene of wheat under the control of an endosperm specific promoter exhibited significant increase in AGPase activity, starch levels and grain number per spikelet [108]. A recent review discussed this phenomenon in detail in which authors proposed two possible explanations [93]. One of them points out that endosperm specific promoters may stimulate additional reproductive organs or improved starch accumulation in endosperm may prevent seed abortion. The other explanation is source limitation and/or inefficient nutrient transport into sink organs may inhibit increase of individual seed weight.

Collectively, transgenic plant studies have shown that besides its pivotal role in starch biosynthesis, AGPase enzyme seems to play a major role in plant development. Since AGPase is a complex enzyme in terms of structure and regulatory properties, a deeper understanding of structure-function relationship of AGPase *in vitro* and *in vivo* should be the basis of future studies. This dissertation examines plant AGPases in two different standpoints: (1) investigation of transcriptional regulation of AGPase in starch metabolism, (2) investigation of subunit-subunit interaction of AGPase to elucidate how heterotetrameric structure plays a role in enzyme's functioning and efficiency.

CHAPTER 3

Transcriptional Regulation of the ADP-Glucose Pyrophosphorylase Isoforms in the Leaf and the Stem under Long and Short Photoperiod in Lentil

3.1 Introduction

ADP-glucose pyrophosphorylase (AGPase) is a key regulatory allosteric enzyme involved in starch biosynthesis in higher plants. AGPase catalyzes a rate-limiting reversible reaction and controls carbon flux in the α-glucan pathway by converting glucose-1-phosphate and ATP to ADP-glucose and pyrophosphate using Mg^{2+} as a cofactor [1, 109-111]. The regulation of almost all AGPases in photosynthetic tissues depends on the ratio of 3-phosphoglyceric acid to inorganic phosphate (3-PGA/P_i); while 3-PGA functions as the main stimulator, P_i inhibits the activity of the enzyme [112, 113]. Plant AGPases consist of pairs of small (SS, or α) and large (LS, or β) subunits, thereby constituting a heterotetrameric structure ($\alpha_2\beta_2$). These two subunits are encoded by two distinct genes [114-116], and the sequence identity between the subunits is 40%-60%, suggesting a common ancestral gene [114, 116]. The molecular weights of tetrameric AGPases range from 200 to 240 kDa depending on the tissue and the plant species. Specifically, the molecular weights of the LS and SS in potato tuber AGPase are 51 and 50 kDa, respectively [115]. The SS and the LS have different roles in enzyme functionality [115]; the SS was shown to have both catalytic and regulatory functions, whereas the LS is mainly responsible for regulating the allosteric properties of SS [59, 64, 117]. These results were also supported by studies demonstrating that LS was incapable of assembling into a catalytically active oligomeric structure, whereas SS was able to form a homotetramer with catalytic properties [64, 118]. However, this SS

homotetramer was defective in terms of catalysis and regulation; it required higher concentrations of 3-PGA for activation and was more sensitive to P_i inhibition. These results suggested that the LS is essential for efficient enzyme function[61, 64, 109, 119]. Recent studies have indicated that the LS may bind to glucose 1-phosphate (G1-P) and ATP. The binding of the LS to these substrates may allow the LS to interact cooperatively with the catalytic SS in binding substrates and effectors and, in turn, influence net catalysis [68, 120, 121]. A recent study suggested that one of the AGPase LS isoforms from tomato exhibits catalytic activity as a monomer [69]. Additionally, specific regions from both the LS and the SS were found to be important for subunit association and enzyme stability [58, 62, 82, 86, 119].

The relationship between carbon assimilation and utilization has been studied in detail and greatly affects plant growth and yield. Studies using *Arabidopsis* subjected to either artificially extended or shortened day length indicated that plants respond globally to different light regimes and are able to adjust their carbon metabolism and growth by regulating enzymes that participate in both starch biosynthesis and turnover [35, 122]. This regulation occurs on both a transcriptional and a posttranslational level [123, 124]. When Arabidopsis was exposed to an artificially extended night period, plant growth decreased due to starch depletion [36]. Additionally, a similar experiment was performed using a mutant of *Arabidopsis* that cannot accumulate starch. This mutant exhibited a retarded growth phenotype under a normal night-dark cycle, and its transcriptional profile was altered compared with that of a wild-type plant [36, 125]. The aforementioned studies and other previous studies have revealed that AGPase is the key enzyme in starch biosynthesis, and AGPase activity is greatly reduced during an artificially extended night due to posttranslational modifications [36]. Additionally, a recent transcriptome analysis revealed that LS2 of *H. vulgare* AGPase is one of the enzymes that is differentially expressed during a 15-h light/9-h dark regime [126].

In this study, we explored the effect of photoperiod length on AGPase transcription; specifically, we examined the transcription of the LS and SS isoforms in a long-day plant, lentil. We analyzed the transcription profiles of isolated AGPases from lentil

growing under long-day (16-h light/8-h dark) and short-day (8-h light/16-h dark) conditions by qRT-PCR. Our results indicated that plants respond to the short photoperiod by decreasing LS1 AGPase transcription by approximately 65% in leaves, while LS2 transcription was increased by approximately 20-fold in leaves under a short-day regime. Additionally, transcription of lentil SS1 and SS2 increased by approximately 30% in leaves and stems, respectively, under a short-day regime. These results highlight the importance of photoperiod length on the differential regulation of AGPase isoforms in stems and leaves.

3.2 Materials and methods

3.2.1 Plant Material

Lentil (*Lens culinaris* Medik., cv. Firat87) seeds were obtained from the Southeastern Anatolia Agricultural Research Institute. The plants were grown in individual pots in a controlled climate chamber at 25 °C with supplementary humidity. Leaves, stems and roots were harvested from 24-day-old plants at 2-hour intervals. Tissues were used immediately or stored at -80 °C until use. For the expression profile analysis, seeds were harvested on the 15th day after flowering and stored at -80 °C until use.

3.2.2 Total RNA Extraction and First-strand cDNA Synthesis

Tissues were homogenized in liquid nitrogen with a mortar and pestle. Approximately 100 mg of powdered tissue was used for total RNA isolation. Total RNA was extracted from leaves, stems and roots using Trizol® reagent (Invitrogen, Carlsbad, California, USA) according to the manufacturer's protocol (phenol/guanidine isothiocyanate procedure). Total RNA was isolated from seeds using the method of Chang et al. [127] because of their high polysaccharide content. Seeds were frozen in liquid nitrogen and ground with a mortar and pestle. One ml of extraction buffer (2% CTAB, 2% PVP K30, 100 mM Tris–HCl, pH 8.0, 25 mM EDTA, pH 8.0, 0.5 g/L spermidine) including freshly added β-mercaptoethanol (2%) was used per 100 mg of powdered tissue. The

samples were extracted twice with chloroform followed by the addition of ¼ vol of 10 M LiCl to the aqueous phase. RNAs were precipitated at 4 °C overnight and centrifuged at 12000×*g* for 20 min at 4 °C. The resulting pellets were resuspended in 100 µl of DEPC-dH_2O. The quality and quantity of the total RNA were examined by agarose gel electrophoresis and an ND-1000 spectrophotometer (NanoDrop Technologies, Wilmington, Deleware, USA), respectively. Total RNA (1µg) was reverse transcribed using the First Strand cDNA Synthesis Kit™ (MBI Fermentas, Hanover, MD, Germany) with M-MLV reverse transcriptase and a random hexamer primer.

3.2.3 Degenerate and Gene-specific Primer Design

Degenerate and gene-specific primers (Table S3-1) were designed based on the most highly conserved regions according to a sequence alignment of homologous genes in other Leguminosae (*P. Sativum, P.vulgaris, C. arietinum, V. faba, and V. radiata*). After obtaining the desired fragment, gene-specific primers were designed. The BLAST algorithm (http://www.ncbi.nlm.nih.gov/blast) was used to ascertain the specificity of the gene-specific primers.

3.2.4 PCR Amplification of cDNAs

PCR was performed in a total volume of 25 µl containing 3 µl of cDNA, 2.5 mM $MgCl_2$, 0.2 mM dNTPs, 10-20 pmol of each primer, 2.5 µl of 10X buffer, and 1U of Dream Taq DNA polymerase (MBI Fermentas, Hanover, MD). The PCR program on the icycler™ thermal cycler (BioRad Laboratories, Hercules, CA) included an initial denaturation step at 94 ºC for 5 min followed by 35-45 cycles of 30 sec at 94 ºC, 45 sec at 45 ºC, 90 sec at 60 ºC, and a final extension step of 10 min at 60 ºC. A 15-µl aliquot of the reaction was electrophoresed on a 1% standard agarose gel at 100 V for 15 min. After staining with ethidium bromide, the fragments were visualized on a UV transilluminator. PCR products of the expected sizes were gel purified using the QIAquick Gel Extraction Kit (Qiagen, Valencia California, USA) according to the manufacturer's instructions. Approximately 100 ng of each purified PCR product was

ligated into the pGEM-T Easy vector (Promega, Madison, Wisconsin, USA) according to the manufacturer's instructions. Positive clones containing inserts of the correct sizes were sequenced (using T7 and SP6 primers) by the Burc Laboratory (Istanbul, Turkey). The resulting sequences were analyzed using BLASTN (http://www.ncbi.nlm.nih.gov/blast).

3.2.5 Phylogenetic Tree Analysis

The deduced amino acid sequences and alignments were analyzed using the BLAST search program (National Center for Biotechnology Information, NCBI). The conserved peptide domains were predicted using SDSC Biology Workbench/ClustalW. The phylogenetic tree was constructed using a neighbor-joining method with the MEGA4.1 program.

3.2.6 Quantitative Real-time qRT-PCR

Relative quantification of each gene expression was performed as follows: real time PCR was performed in a total volume of 20 µl containing 10 µl of 2X SYBR Green PCR Master Mix (TaKaRa, Japan), 10 pmol of each gene-specific primer, 1 µl of cDNA, and distilled water. The PCR protocol on the Light Cycler 1.5 (LC) (Roche Diagnostics, Mannheim, Germany) included an initial denaturation step (95 °C for 2 min) followed by amplification and quantification steps repeated for 30 cycles (95 °C for 5 sec, 58°C -60 °C for 10 sec, and 72 °C for 20 sec with a single fluorescence measurement at the end of the elongation step at 72 °C), a melting curve program (65°C –98 °C with a heating rate of 0.2 °C sec^{-1} and a continuous fluorescence measurement) and a final cooling step (40 °C). Each sample was amplified with gene-specific and reference gene primer pairs. The housekeeping gene Glyceraldehyde-3-phosphate dehydrogenase (GAPDH) was selected as an internal reference gene for normalization purposes because it is consistently expressed in all the tissues examined in this assay [128], which was also shown for *Cicer arientium* L. For comparative purposes, the mean expression value of each gene at the "0 hour" time point was arbitrarily set to 1,

and the mean at other time points was expressed as a ratio relative to the "0 hour" time point. Melting point analysis was conducted on all PCR products to ensure that nonspecific amplicons were not produced. To verify the specificity of each primer set, the amplicons were sequenced. All analyses were performed using the relative quantification method tool of the Light Cycler 1.5 analysis software (version 4.05). Each qRT-PCR was performed in triplicate for each tested sample.

Absolute quantification was carried out as follows: To obtain the mRNA copy number for each gene, pGEM-T Easy plasmids containing the gene of interest were used. Four serial dilutions were prepared from the stock solution containing 10^6 copies of the plasmid. Quantification was performed using the standard curve method. Within each PCR batch, four serial dilutions of plasmid DNA and sample cDNA were included to a construct a standard curve. The copy numbers of the genes in each sample were interpolated using these standard curves. All analyses were performed using the absolute quantification method (Fit Points Method) tool of the Light Cycler 1.5 analysis software (version 4.05). qRT-PCR was performed in triplicate for each gene.

3.2.7 Iodine Staining of Leaves from Lentil Grown under Long- and Short-Day Conditions

Leaf samples from plants grown under long- and short-day conditions were obtained during light exposure at 2-hour time intervals. Dark exposed samples were obtained at 18 hours and 16 hours from lentils grown under long- and short-day conditions, respectively. Leaf samples were first treated with 99.5% ethanol to remove pigments and then treated with iodine solution (0.06% I_2, 0.1% KI and 4 mM HCl) for staining [29].

3.2.8 Partial Purification and Immunoblot Analysis of Lentil AGPase

Four to 6 weeks after germination, young leaves (10 g) of lentils grown under short-and long-day conditions were frozen in liquid nitrogen, ground with a mortar and pestle and

subsequently homogenized in extraction buffer (50 mM Tris-HCl pH 8.0, 10% glycerol, 5 mM $MgCl_2$, 30 µl of protease inhibitor cocktail/g wet plant tissue). The supernatant was then subjected to 30%-65% ammonium sulfate fractionation, and the resulting precipitate was resuspended in 1 ml of extraction buffer and desalted by dialysis. The desalted sample was applied to a Macro-Prep DEAE weak anion exchange support previously equilibrated with extraction buffer. Enzymes were eluted from the column using a linear gradient of extraction buffer (60 ml, 0 to 0.5 M NaCl). Fractions containing enzyme activity were pooled and stored at -80°C after freezing in liquid nitrogen. Active fractions and crude extracts were analyzed on 10% SDS-polyacrylamide gels followed by immunoblot analysis with potato AGPase antibodies that recognize the LS and the SS as described previously [129]. The gel was transferred to a polyvinylidene difluoride membrane (Biotrace PVDF, Pall Corporation, FL, USA) with a transfer cell at 90 V for 1 h. After pre-blocking with BSA, the membrane was incubated with anti-LS or anti-SS (diluted 1:1000 in 0.01 % Tween-20/TBS) primary antibodies for 1 h and finally with an anti-rabbit HRP-conjugated secondary antibody (diluted 1:5000 in 0.01% Tween-20/TBS) for 1 h. Proteins were visualized using the ECL system.

3.2.9 Determination of the Kinetic Constants of Lentil AGPase

Kinetic characterization of partially purified extracts was performed in the forward direction [130]. The amount of PP_i produced was determined with a nonradioactive endpoint assay by monitoring the decrease in NADH concentration using PP_i reagent (P-7275 Sigma). The reaction mixture contained 50 mM HEPES pH 7.4, 15 mM $MgCl_2$, 4.0 mM ATP, 4 mM G1P and 5 mM DTT in a total volume of 200 µl. The assays were initiated by enzyme addition and the reactions were performed at 37°C for 10 min and terminated by boiling for 2 min. After the addition of 300 µl PP_i reagent, the NADH decrease was monitored at 340 nm. Blank samples were complete reaction mixtures without enzyme. PP_i production was determined from a standard curve using increasing amounts of PP_i in complete reaction mixtures without enzyme. K_m values were

determined in reaction mixtures in which one substrate or effectors were added in varying amounts and the other reaction components were saturated. The saturating amounts of G1P, ATP and 3-PGA were 4 mM, 4 mM and 5 mM, respectively. Into each reaction, 0.4 μg of partially purified enzyme was added. K_m and K_a values were obtained by nonlinear regression analysis using the Prism software program (Graph Pad, San Diego, CA). The K_i for P_i was determined in the presence of 5 mM 3-PGA by adding increasing amounts of P_i.

3.3 Results and Discussion

3.3.1 Isolation and Characterization of Lentil AGPases

To isolate cDNAs encoding both the LS and SS of lentil AGPases, degenerate primers were designed based on the conserved amino acid regions of both the LS and SS of AGPases from various legume plants [116]. Initially, degenerate primers (Table S3-1) for the LS (LS Deg F1 and LS Deg R3) and the SS (SS Deg F2 and SS Deg R2) were used to amplify cDNA obtained from lentil stems and leaves. Our BLAST analysis indicated that one specific lentil AGPase LS exhibited high homology with pea LS1, while another clone exhibited the highest homology with fava bean LS2. Additionally, one of the SS of lentil AGPase exhibited the highest homology with pea AGPase SS1, and the second clone exhibited high homology with both pea AGPase SS2 and fava bean SS. To obtain full-length mature sequences, degenerate primers (Table S3-1) from conserved regions of legume AGPases and gene specific primers for lentil AGPase LS1, SS1 and SS2 were prepared and cDNAs were obtained. The lentil LS1, SS1 and SS2 sequences (accession numbers GQ861440, GQ919066, and HM136613, respectively) were deposited in GenBank. The presence of multiple cDNAs that encode the LS and the SS of AGPases has been observed in many different plants including rice [131], chickpea [132], tomato [133], and *Arabidopsis* [129, 134].

A comparison of the deduced amino acid sequences of four lentil AGP isoforms (LS1, LS2, SS1, and SS2) is shown in Figure S3-1A and B. The homology between SS1 and

SS2 is 95%, while the homology between the full-length LS1 and partially isolated LS2 is 56%. Because lentil LS2 was only partially isolated and SS2 was isolated from mature sequences, it is not known whether either sequence encodes a transit peptide. Both the LS1 and SS1 isoforms appear to contain a transit peptide and are likely to be targeted to the plastid (Figure S3-1C). The leader sequence was also predicted by the neuralnetwork-based tool, ChloroP [135] and PSORT [136].

The degrees of identity between lentil amino acid sequences and isoforms of various plant AGPases are presented in Table S3-2. Unlike the AGPase SS, the AGPase LS are less conserved among evolutionarily related species. However, a comparison of the amino acid sequence of LS1 with various LS amino acid sequences revealed a surprising result: LS1 shares 94.7% identity with pea AGP-L1 (Figure S3-2). This is the first demonstration of two the LS originating from different plants exhibiting such a high homology. Additionally, phylogenetic analysis indicated that LS1 clustered together with both *Pisum sativum* and *Phaseolus vulgaris* LS (Figure S3-3). Taken together, these results indicate that lentil is evolutionarily similar to *Pisum sativum* in terms of the starch biosynthesis pathway. An analysis of the amino acid sequences of AGPase LS from various legume plants (Table S3-2) indicated that there is no such conservation among LS. This shows that both lentil an pea are genetically more closely related. In fact, other studies have revealeded that pea and lentil are closely related genetically. For example, Galasso et al. [137] performed a phylogenetic analysis of lectin sequences that revealed a high level of sequence similarity between pea and lentil.

3.3.2 Expression Patterns of AGP Isoforms in Various Tissues

To gain further insight into the expression pattern of AGPase isoforms, quantitative real-time PCR (qRT-PCR) analysis was used to identify the spatial and temporal expression pattern in stems, leaves, roots, and seeds. The oligonucleotide primer pairs used for quantitative measurements are listed in Table S3-1. To discriminate between the two transcripts (SS1 and SS2), the primer pairs were designed against variable regions of the genes. To verify the specificity of each primer set, their amplification

products were cloned and sequenced (data not shown). The melting curves of all the PCR products showed a single peak with an identical melting temperature (Tm), indicating that there was no non-specific amplification. The specificity of the real-time PCR was further confirmed by analysis of the PCR products on an agarose gel, which showed the expected amplification products in all experiments (data not shown).

Samples obtained from both stems and leaves were collected at 4 hours after light exposure for each condition. All the samples were subjected to qRT-PCR to determine the relative amount of each transcript. The housekeeping gene glyceraldehyde-3-phosphate dehydrogenase (GAPDH) was selected as an internal reference gene for normalization. In fact, a study performed with chickpea indicated that the expression level of the *GAPDH* gene is the most constant across various conditions [128]. Because both lentil and chickpea belong to the same family, we designed several primer pairs based on a sequence alignment of homologs in the family Leguminosae (*P. sativum, P. vulgaris, O. sativa, C. arietinum, V. faba, and V. radiata*). Primers were tested for specificity and sensitivity, and one pair of primers was used (Table S3-1).

SS1 was expressed strongly in leaves, moderately in seeds, and weakly in the stem (Figure 3-1A). Its leaf expression level was 2.8-, 11.6-, and 19.3-fold higher than its expression in the seeds, stem, and roots, respectively. In contrast to the expression pattern of SS1, SS2 was expressed strongly in stems, and its expression in the stem was 2.3-, 4-, and 12-fold higher than that in the leaves, seeds, and roots, respectively (Figure 3-1B). SS1 was weakly expressed in the root tissue. A similar analysis indicated that LS1 was expressed highly in seeds with weak expression in the leaves and very weak expression in the stem and roots (Figure 3-1C). LS2 was expressed strongly in leaves but very weakly in the stem and roots (Figure 3-1D). The copy number of LS2 in leaves was approximately 2000 copies/ng of total RNA, whereas the copy number of LS2 in both seeds and stems was approximately 200 copies/ng of total RNA. It is worth to note that the significant difference between LS1 and LS2 RNA copy numbers, indicating LS1 is the dominantly expressed isoform in all tissues. All these results indicate that the major regulatory subunit of AGPase in lentil is LS1 in all tissues. LS1 possibly forms a

heterotetrameric structure with either SS1 or SS2 depending the type of tissues and generates ADP-glucose for the starch biosynthesis. On the other hand, it is possible that LS2 plays a role during the seed or plant development. It has been shown that some of LS isoforms are just highly expressed during endosperm development to maximize the starch biosynthesis in storage organs in rice [138]. The availability of these different lentil large subunit gene sequences will enable us to determine whether such expression exists during the seed development of lentil.

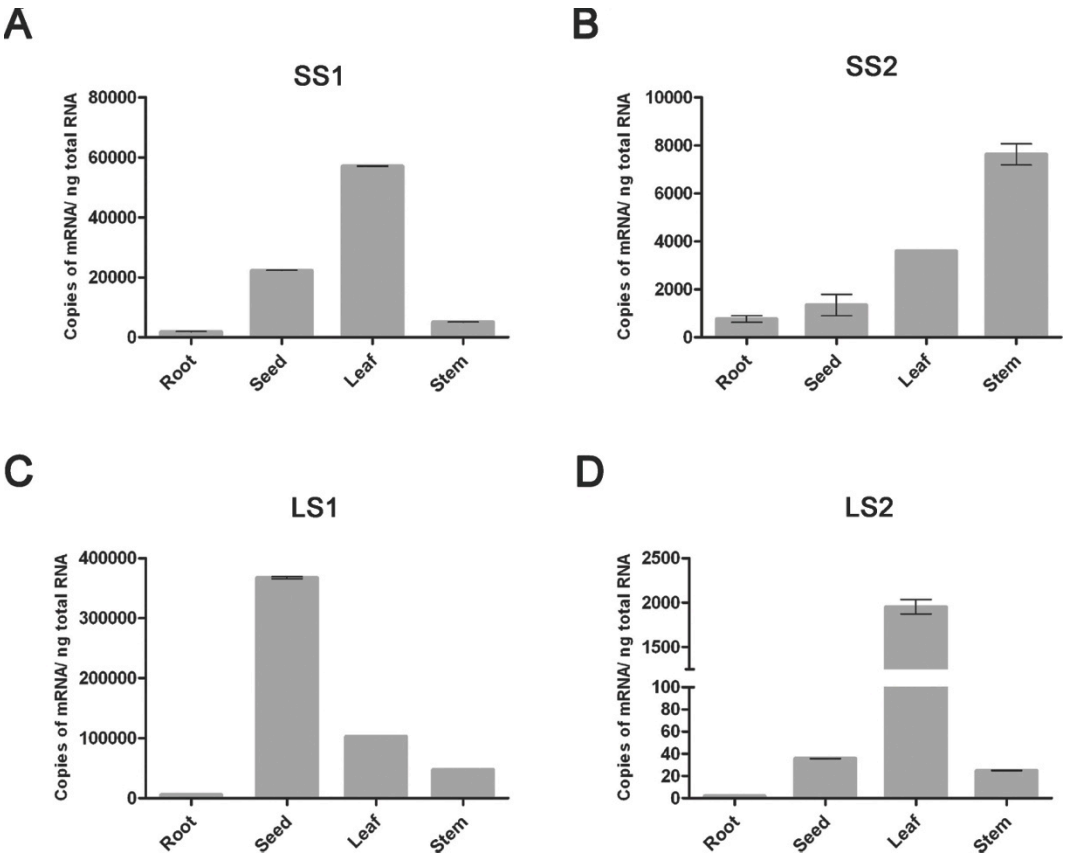

Figure 3 - 5 Quantitative analysis of the (A) SS1 (B) SS2 (C) LS1 and (D) LS2 by real time PCR. All values first normalized with GAPDH expression level and then quantified as described in materials and methods. Samples were taken 4 hours after illumination in long-day condition.

3.3.3 Transcription Patterns of Lentil AGPase Genes in Both Leaves and Stems under Long- and Short-Day Regimes

Although AGPase is one of the rate limiting enzymes of starch biosynthesis and is regulated by photoperiod, the effect of photoperiod length on the transcription of AGPase isoforms and, in turn, starch synthesis has not been studied in the legume family or in long day plants. Therefore, we chose to explore variations in the transcription pattern of lentil AGPase under different photoperiod conditions [36]. To examine AGPase transcription under different day lengths, we subjected lentil plants to 16-h/8-h light-dark and 8-h/16-h light-dark regimes. Leaf samples were collected at different time points and then total mRNA were isolated. The transcriptional levels of lentil AGPase isoforms were assessed by qRT-PCR on samples with specific primers designed against each gene, as indicated in Table S3-1. GAPDH was used as an internal reference gene for normalization purposes.

The LS1 transcription was peaked at 4 and 6 hours in leaves and in stems respectively and its expression levels were comparable in both stem and leaf tissues under long-day regimes (Figure 3-2A). Comparison of LS1 expression under two different light regimes revealed that photoperiod length affects the transcription level of LS1 in leaves. Peak to peak comparison the mRNA level revealed that the mRNA level of LS1 was approximately 105,000 molecules/ng total RNA under the long-day regime, while the mRNA level of LS1 was approximately 20,000 molecules/ng total RNA in leaves under the short-day regime (Figure 3-2A and B). On the other hand, photoperiod length had opposite effect on the transcription of the LS1 in stem. The transcriptional level of the LS1 in stem is slightly increased under short-photoperiod. The maximum expression level of LS1 in stem is around 90,000 molecules/ng total RNA under long-day regimes whereas the total transcript of the LS1 is 120,000 molecules/ng total RNA under short-day regime (Figure 3-2A and B).

LS2 is predominantly expressed in leaves and is very weakly expressed in stem tissue under both long- and short-day regimes (Figure 3-2C and D). The maximum expression

of LS2 in leaves and stems was observed at 6 h under long-day regime (Figure 3-2C**)**. However, when the plants were shifted to the short-day regime, the maximum expression level of LS2 was observed at 4h in stem while expression level of LS in leaf was observed at 10 h (Figure 3-2D**)**. The LS2 expression level in the stem was comparable; under both conditions, the mRNA copy number was approximately 50 copies/ng total RNA (Figure 3-2C and D). Although LS2 isoform has significantly less transcript levels relative to LS1, we observed that it is predominantly expressed in leaves under both long-day and short-day regimes. Besides, this expression level reduced from 3000 ng/total RNA to 1500 ng/total RNA under short-day regime. The transcript level of LS2, however, showed a 20 fold increase at particularly 10 h of short-day regime (Figure 3-2C and D).

The lentil SS1 was expressed at higher levels in leaves than in stems under both photoperiod regimes (Figure 3-2E and F). Its expression level peaked at between 4 and 8 h under the long-day regime in both tissues (Figure 3-2E). Under short-day conditions, the expression level of SS1 peaked at 4 h in stems, while the expression peak of SS1 was observed at 6 h in leaves (Figure 3-2E). The SS1 transcript levels were significantly increased in stem when plant was shifted to short-day regimes by approximately 3-folds (Figure 3-2E and F**)**. Similarly, the maximum expression level of SS1 in leaf was increased in plant subjected to the short-day conditions by 50% (Figure 3-2E and F**)**. SS2 was expressed dominantly in stems when compared with its expression level in leaf under both long- and short-day regimes. The maximum expression of the SS2 exhibited two peaks in both stem and leaf. In stem, SS2 peaks were observed at 6 h and 14 h under long-day regime (Figure 3-2G). Similarly, the SS2 was peaked at 4h and 14 h under long day conditions in leaf. However, the maximum expression level of SS2 was peaked only at 6 h under short-day regime (Figure 3-2G**)**.

All these analysis indicated that the major AGPase isoform in stem and leaf is the LS1 under short and long photoperiod conditions. On the other hand, SS1 and SS2 are the major form in leaf and stem under any conditions being tested, respectively. qRT-PCR analysis indicated that different photoperiod length greatly affects temporal and spatial

expression pattern of the all isoforms of lentil AGPases. Because the LS is the modulatory subunit in nature, this significant differential expression pattern of the LS isoforms may allow the plant to rapidly adjust to different light conditions. Additionally, we noted that the transcription level of all isoforms increased under short-day regime in stems. This result may be in accordance with the role of the stem as a sink-source balance during carbohydrate metabolism. Since leaves may not meet the carbon demand of stems in short photoperiod, it is reasonable to see such an increase in transcript levels of AGPase in stem to compensate the amount of carbohydrate being produced by whole plant. Furthermore, we noted that this type of transcriptional regulation takes place also in the leaves, which is supporting the role of the leaf as a source during carbohydrate metabolism.

LS1 and SS1 were highly expressed in leaf tissues, which strongly suggest that they are the main active isoforms in leaf tissues. It is likely that they form a heterotetrameric AGPase (2LS1-2SS1) that participates in the formation ADP-glucose and, in turn, transitory starch observed in leaf. On the other hand, LS1 and SS2 were comparably expressed in the stem tissue more than in leaves, and they may form a 2LS1-2SS2 heterotetrameric AGPase responsible for starch biosynthesis. The abundance of the different AGPase isoforms has been investigated in rice [131, 138, 139], where different isoforms of AGPases were thought to form heterotetramers based on an examination of gene expression patterns. The various AGPase isoforms in leaves and stems may aid in the synthesis of the various amounts of starch required in each tissue.

Additionally, it is worth to note that the degradation of mRNA transcripts occurs differently under long- and short-day conditions based on the qPCR results. In plants exposed to long-day conditions, AGPase mRNA is quite stable and requires at least 4 h to be completely degraded, whereas it takes 2 h or less to be completely degraded in plants exposed to short-day conditions (Figure 3-2). For example, the mRNA level of LS1 starts to decline after 6^{th} hours (Figure 3-2A), and this decay is likely to be completed by approximately 12^{th} hours in stem; however, the mRNA level of LS1 in plants exposed to short-day conditions abruptly decreases in 2 hour (Figure 3-2B).

The differential transcriptional regulation of these AGPase isoforms in different tissues in response to photoperiod length implies that the AGPase promoters are antagonistically regulated in lentil. In fact, several studies in various plant species have indicated that such regulation exists among the AGPase gene family [50, 140-142].

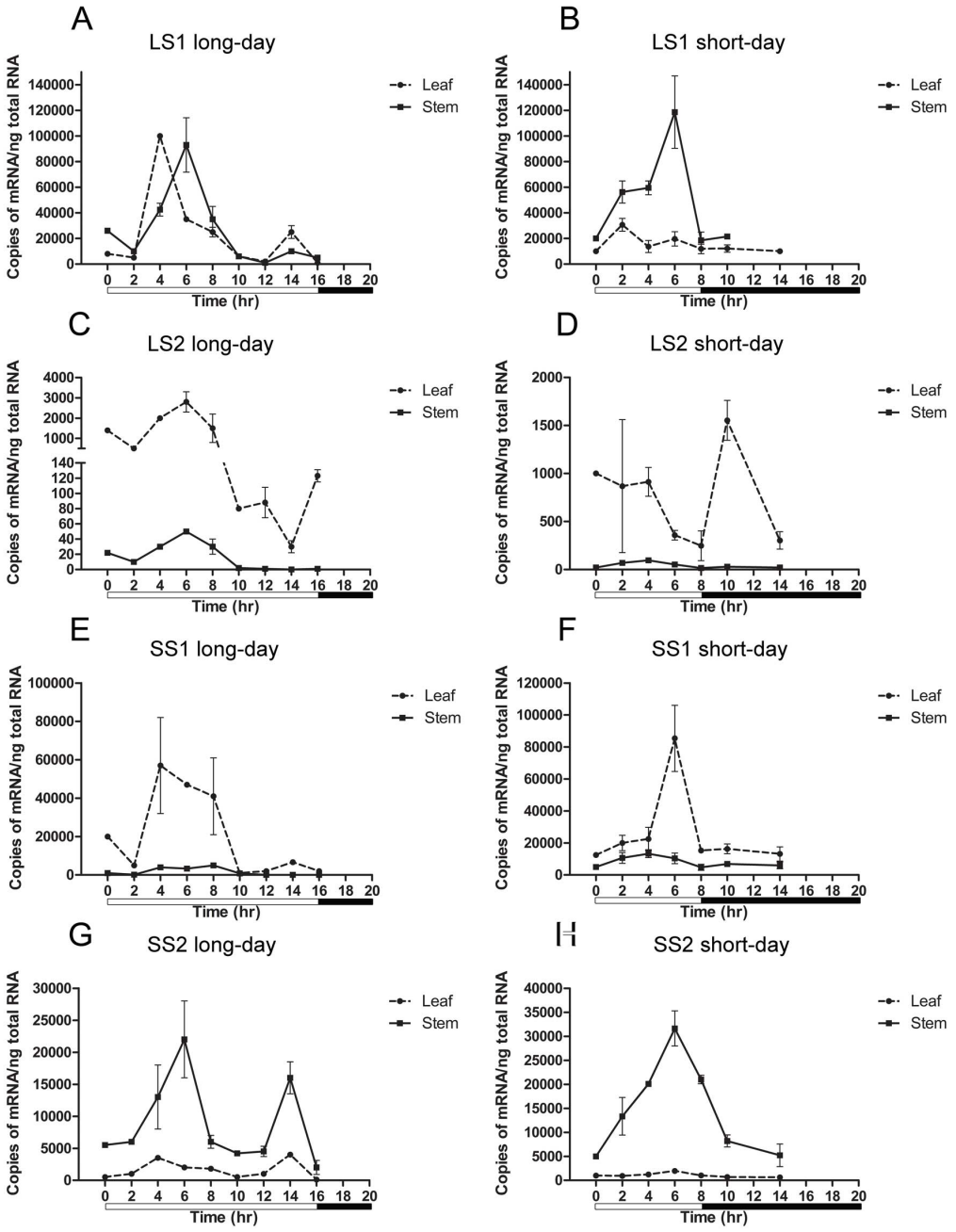

Figure 3 - 6 Comparison of transcript levels of the lentil AGPase isoforms under long-day and short-day regime. (A)LS1 long-day, (B) LS1 short-day, (C) LS2 long-day, (D) LS2 short-day, (E) SS1 long-day, (F) SS1 short-day, (G) SS2 long-day and (H) SS2 short-day. The numbers of transcripts were based on the quantitative RT-PCR explained in materials and methods.

3.3.4 Assessment of Starch Accumulation in Leaves via Iodine Staining

To examine the correlation between AGPase expression and starch accumulation in lentil leaves under different photoperiods, we stained the leaves with iodine and obtained samples every 2 hours after illumination. Figure 3-3 contains representative images of the stained leaves. In plants grown under long-day conditions, we detected a gradual increase in starch after 8 hours of light exposure and a decrease at 18 hours, which corresponded to the first 2 hours of night. This result can be correlated with the transcriptional profile of the LS1 and SS1 isoforms in leaf tissue from lentil plants grown under long-day conditions in which the mRNA expression profile displays two peaks at 4 and 14 hours. Nonetheless, in plants grown under short-day conditions, the starch amount began to increase after 4 hours, and its maximum amount was reached at 10 hours, which corresponds to the first two hours of night. This likely occurs because the breakdown of starch occurs more slowly under short- vs. long-day conditions. Indeed, several studies have indicated that transitory starch breaks down slowly in leaves under a short photoperiod and that this process is controlled by day length [34, 36, 143].

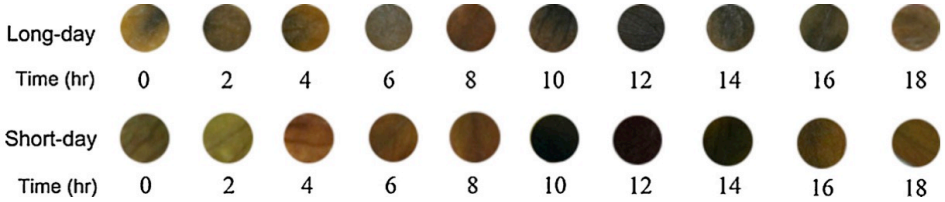

Figure 3 - 7 Iodine staining of leaves from long-day and short-day lentils. Upper panel shows representative stained samples from long day lentil taken at indicated hours. Lower panel shows iodine staining of leaf samples taken from short-day lentil every two hours during day time and at 10^{th} and 16^{th} hours of night time.

3.3.5 Kinetic Characterization of Lentil AGPase under Long- and Short-Day Regimes

Since the transcription of level of the LS1and SS1 is significantly higher than LS2 and SS2 in leaf, one would expect to see heterotetrameric AGPases that are enriched with LS1 and SS1 subunits in lentil leaf under different photoperiods. Therefore, we have partially purified the AGPases from the plant exposed to the different photoperiod conditions and performed kinetic studies to see whether there is a difference which may indicate an isoform shift in leaves under short-day regime. The presence of each subunit was detected using antibodies specific to the LS and SS of potato AGPase (Figure S3-6). Table 3-1 shows the K_m, K_a and K_i values of lentil AGPase obtained using assays in the forward direction. It was previously observed that AGPase activity in two samples (obtained from plants grown under short and long photoperiods) was very low when assayed in the absence of the 3-PGA. As the 3-PGA levels were increased in the reaction mixture, the amount of product increased significantly and achieved more than 20-fold activation. The K_a (amount of effector required for 50% activation) of native AGPase obtained from leaves exposed to long and short photoperiods was calculated as 0.25 mM and 0.33 mM, respectively (Figure S3-4A and Table 3-1). It appeared that AGPase obtained from lentil leaves exposed to a short photoperiod required a similar amount of 3-PGA for activation compared with AGPase obtained from lentil leaves exposed to a long photoperiod. The P_i sensitivity of the leaf AGPases under both conditions was measured in the presence of 5 mM 3-PGA. The K_i (amount of effector required for 50% inhibition) of the AGPase (short photoperiod) was estimated at 4.26 mM, and the K_i of the AGPase (long-photoperiod) was estimated at 3.95 mM (Figure S3-4B and Table 3-1). In the presence of a lesser amount of 3-PGA, we detected only a very low level of activity (data not shown), indicating that native lentil leaf AGPase is sensitive to P_i inhibition and requires 3-PGA to abolish this inhibitory effect. Additionally, P_i sensitivity and 3-PGA activation levels appear to be similar for AGPases under different photoperiod conditions. The K_m values for the substrates and co-factor (Mg^{2+}) of the native leaf AGPase are shown in Table 3-1. The assays were performed in the forward direction using a saturated amount of 3-PGA and Mg^{+2}. The

K_m values of ATP and G1P were 0.31 mM and 0.15 mM, respectively, for the AGPase obtained from plants exposed to the short photoperiods. The K_m values of ATP and G1P were 0.18 mM and 0.071 mM, respectively, for the AGPase obtained from plants exposed to the long-photoperiods (Figure S3-5 and Table 3-1). Additionally, the K_m values of the Mg^{2+} cofactor were determined as 3.0 mM for lentils grown under long-day conditions and 1.2 mM for lentils grown under short-day conditions. Then we would like to compare kinetic properties of native and recombinant lentil AGPases. Therefore, we cloned the cDNAs of the lentil LS1, SS1 and SS2 into bacterial expression plasmids. However, our attempt to obtain recombinant lentil AGPases failed due to inclusion body formation in the *E.coli* $glgC^-$ system. Although the proteins were expressed in large quantities, soluble and active proteins were not detectable by western blot or AGPase reverse assay (data not shown). Therefore, according to our kinetic analysis, native leaf samples did not show a significant difference in terms of their kinetic properties under either condition. We can conclude that the type of major isoforms do not change in response to photoperiod change, in lentil.

A comparison of the kinetic properties of lentil AGPase with the AGPases of other Leguminosae family members revealed that lentil AGPase has kinetic properties that are comparable with chickpea [144] AGPase but quite different from pea embryo [145] [52] and fava bean AGPases [54]. Pea and fava bean AGPases are insensitive to 3-PGA activation and P_i inhibition. This is in sharp contrast to the lentil enzymes tested, which displayed approximately 20–25-fold activation by 3-PGA and 15–20-fold inhibition by P_i. On the other hand chickpea AGPases displayed a similar sensitivity to 3-PGA activation and P_i inhibition compared to lentil AGPases.

Table 3 - 1 Substrate, activation and inhibition kinetic determinations of long-day and short-day lentil AGPases from leaf. Saturating activator and/or substrate concentrations were used for the enzymatic assays. K_i determination was performed at activator concentration shown in parentheses. Each assay performed for 2-3 times, average values and standard deviation values were indicated.

	ATP K_m (mM)	G1P K_m (mM)	3-PGA K_a(mM)	Mg^{2+} K_m (mM)	P_i K_i (mM)
Long-day	0.18 ± 0.028	0.071 ± 0.012	0.25 ± 0.09	3.0 ± 1.3	4.26 (5 mM 3-PGA)
Short-day	0.31 ± 0.078	0.15 ± 0.04	0.33 ± 0.061	1.2 ± 0.6	3.95 (5 mM 3-PGA)

3.4 Concluding Remarks

The allosteric regulatory behavior of AGPase is required in leaves and is important for the diurnal oscillation of leaf starch metabolism and for directing carbon into sucrose synthesis until this process becomes saturated. These allosteric regulatory properties would result in a decrease in catalytic activity to a level much lower than the maximum rate. Therefore, the AGPase reaction responsible for seed starch and transient leaf starch production is a prime target for genetic engineering as a means to increase the yields of important food crop. Additionally, several studies have indicated that the manipulation AGPase in various tissues leads not only to an increase in starch production but also to an increase in plant yield through enhanced photosynthesis [96-98, 146, 147]. Therefore, it appears that the seed AGPase could be a likely target for metabolic engineering, and recent studies in *Arabidopsis* have shown that targeting the leaf is another potential way to increase productivity [95-97, 148]. Indeed, *Arabidopsis* plants with a greater capacity to synthesize starch exhibited greater photosynthetic capacities due to an increased ability to utilize triose phosphates, resulting in an increase in growth and biomass [97]. There are studies shows that there is a correlation between the starch metabolism and circadian clock. These studies indicated that circadian clock regulates several genes in starch biosynthesis and degradation [9, 149, 150]. Therefore, in this study we explored whether shortened light and extended dark cycle affects transcriptional levels of AGPase isoforms in a long-day plant lentil. In this study we have shown that shortened light cycle has effect on the transcription of the AGPase isoform and in turn starch biosynthesis. Specifically, we have reached following conclusions. First, AGPase isoforms transcriptions showed spatial and temporal changes under different photoperiod regimes. Artificially shortened day length affect on the transcription of AGPase isoforms, which is possibly due to the circadian clock regulations. Second, our kinetic analysis of the leaf AGPase indicated that lentil leaf AGPase are subjected to the 3-PGA/P_i regulation similar to the chickpea AGPase. Third, our analyses indicated that one of the large subunits, LS1 AGPase, shares significant homology (94.7%) with the pea LS1 AGPase. This is the first study shown

that such LS genes are highly homologous between two different species. Thus, this study highlights the importance of the transcriptional regulation of AGPase under different photoperiods in lentil.

CHAPTER 4

Enhanced Heterotetrameric Assembly of Potato ADP-glucose Pyrophosphorylase Using Reverse Genetics

4.1 Introduction

Starch is the predominant carbohydrate reserve in many plants and is observed in both photosynthetic and non-photosynthetic tissues. Starch is a staple in the diet of much of the world's population and is also widely used in different industries as a raw material [110, 154]. ADP-glucose pyrophosphorylase is one of the key enzymes for plant starch biosynthesis. The enzyme controls the carbon flux in the α-glucan pathway by converting glucose-1-phosphate (G1P) and ATP to ADP-glucose and pyrophosphate [25, 110, 155, 156]. The activity of AGPase is allosterically regulated by small effectors. Plant AGPase is activated by 3-phosphoglycereate (3PGA) and inhibited by inorganic orthophosphate (P_i). Plant AGPases are heterotetrameric ($\alpha_2\beta_2$) enzymes consisting of two subunits called the large subunit (LS) and small subunit (SS), which are encoded by two different genes [63, 157]. The molecular weights of tetrameric AGPases range from 200 to 240 kDa, depending on the tissue and plant species. Specifically, the molecular weights of the LS and SS in the potato tuber AGPase are 51 kDa and 50 kDa, respectively [157]. Recent studies have demonstrated that both subunits contribute to the activity and allosteric regulation of the heterotetrameric enzyme [66, 67, 92, 117, 129, 158-160]. Evidence indicates that the LS may bind to the substrates G1P and ATP. The binding of the LS to its substrates may allow the LS to cooperatively interact with the SS for binding substrates and effectors, which, in turn, influences net catalysis [68, 117, 161, 162]. Furthermore, specific regions from both the LS and SS were found to be important for subunit association and enzyme stability [82,

86, 88, 154]. Using chimeric maize/potato small subunits, Cross et al. [66] found a 55-amino acid polymorphic motif in the SS that directly interacts with the LS and significantly contributes to the overall enzyme stability.

The heat stability properties of AGPase have also been shown to be considerably related with the interaction between subunits and the allosteric properties of the enzyme [87, 90, 91]. It is known that the heat stability of AGPase is because of strong interactions between subunits. In a study by Greene and Hannah et al. (1998), yeast two hybrid experiments revealed heat stable mutants displaying enhanced interaction between the LS and SS of maize endosperm AGPase. Most plant AGPases are stable because of the cysteine residues in the SS, which form disulfide bridges with the corresponding SS [74, 163]. The placement of cysteine, including the N-terminal motif of the potato AGPase in the maize endosperm AGPase, significantly increased the heat stability of the enzyme without affecting its affinity for substrates and allosteric regulators [90]. Later, it was found that in maize AGPase, heat stability increases when the active and allosteric sites are occupied by substrates and activators/inhibitors, respectively, indicating a relationship between allosteric regulation and the heat stability of the enzyme [91]. Current knowledge about AGPase suggests there is a strong relationship between subunit interaction, allosteric regulation and heat stability of the enzyme.

Recent studies have suggested that subunit interaction is not only required for an active heterotetramer but also has a significant role in the allosteric regulation of the enzyme [67, 91, 92]. It has been demonstrated that by comparing the allosteric properties of the combinations of up-regulated variants of the SS and LS, the enzyme requires both subunits for allosteric regulation [67]. In addition, a phylogenetic analysis revealed the importance of the subunit interface residues for allosteric regulation of the enzyme [92]. Although the crystal structure of heterotetrameric AGPase is not currently available, the subunit interaction dynamics and residues contributing to the interaction were mainly identified through a heterotetrameric model of potato AGPase by Tuncel et al. [82] and confirmed using computational and experimental studies (Figure 4-1A) [86]. According to the model, energetically, the most favorable heterotetramer occurs via longitudinal

and lateral interaction between the LS and SS. Because the lateral interaction is more stable because of its rich hydrophobic interactions, it was presumed that the lateral dimers form first, and then, the longitudinal dimers combine with the lateral dimers to form the heterotetrameric enzyme [82]. The model indicates that the interaction between longitudinal LS-SS dimers is thermodynamically much weaker than the interaction between lateral LS-SS dimers. In fact, experimental observation supports the model because the co-expression of the LS and SS AGPase in *E.coli glg*C$^-$ followed by native gel analysis indicated that there are free monomers (SS and LS) and dimers (LS-SS) in addition to the heterotetrameric AGPase in the cell free extract.

In this study, we enhanced heterotetrameric assembly between dimers and monomers of AGPase using the reverse genetics approach. The AGPase LS^{R88A} hotspot mutant for the interaction of longitudinal LS-SS dimers [86] was subjected to error-prone PCR mutagenesis to identify second site revertants. Revertants were co-expressed with wild-type SS, whereupon the cells were then screened for their capacity to form an enzyme restoring glycogen production in glycogen-deficient *E.coli glgC*$^-$ with iodine vapor. Several second-site revertants were identified. Characterization of the mutants enabled the identification of two groups of mutants: mutants (LS^{I90V} and LS^{Y378C}) displaying a significant increase in heterotetramer formation due to both enhanced monomer-monomer and dimer-dimer interaction and a mutant (LS^{D410G}) with increased heterotetramer formation because of enhanced dimer-dimer interaction with modified allosteric properties. Our study not only clearly demonstrates the increased heterotetramer formation on AGPase but also highlights the importance of subunit interaction for the proper functioning and stability of the enzyme.

4.2 Materials and Methods

4.2.1 PCR mutagenesis, screening and selection

Thirty femtomoles of potato AGPase LS^{R88A} in the pML7 plasmid was amplified using the primers LSDS1 and LSDS2 (Table S5-1). The PCR mixture contained 1× mutagenic

buffer (3 mM $MgCl_2$, 0.5 mM $MgSO_4$, 50 mM KCl and 10 mM Tris-HCl, pH 8.3), 1 mM dGTP, 1 mM dATP, 0.2 mM dCTP, 0.2 mM dTTP, 30 pmol of each primer, and 5 units of Taq polymerase. PCR was performed using a Biorad T-100 robocycler for 15 cycles under the following conditions: 30 s at 94°C, 30 s at 50°C, and 2 min 72°C. The PCR products were purified using a PCR clean-up kit. The amplified products were digested with NcoI and HindIII, cloned into the corresponding sites of the pML7 vector, and transformed into glgC$^-$ E. coli, carrying the SS expression plasmid pML10. Revertants were identified by their ability to complement the glgC$^-$ phenotype, thereby restoring glycogen production, which was readily scored using iodine staining of the bacterial colonies on Kornberg medium enriched with 2% glucose.

4.2.2 Site-directed mutagenesis

Mutations were introduced into potato AGPase LS using PCR, as described in [164]. The PCR reaction was performed in a total volume of 50 µl containing 50-100 ng of template plasmid pML7, 20 pmol of each appropriate primer (Table S3-1), 0.2 mM dNTPs, and 2.5 units of PfuTurbo DNA polymerase. The PCR was performed for 14 cycles under the following conditions: 95°C for 30 s, 50°C for 30 s and 68°C for 14 min. The PCR products were digested with DpnI to remove template plasmid DNA and transformed into E. coli DH5α. The presence of the site-directed mutations was confirmed by DNA sequencing using the Macrogen sequencing facility (Netherlands).

4.2.3 Protein expression and blue native gel analysis

The wild-type and various LS mutants were expressed in *E.coli* AC70R1–504 (*glg*C$^-$) cells containing pML7 grown in LB medium. Expression of both the LS and SS was induced with 10 mg/L of nalidixic acid and 200 mM isopropyl- b-D-thiogalactopyranoside (IPTG) at room temperature for 20 h. Cells were harvested by centrifugation when the culture OD_{600} reached 1–1.2. The cells were disrupted by sonication in lysis buffer [Tris-buffered saline (TBS), 200 mg/ml lysozyme, 5 mg/ml protease inhibitor (Sigma), and 1 mM phenylmethylsulfonyl fluoride (PMSF) (Roche)]. The crude homogenate was centrifuged at 14,000 × *g* for 15 min. The resulting

supernatant was used in PAGE and western blotting analysis. Protein levels were determined using the Bradford assay according to the manufacturer's (Bio-Rad) instructions. All native gel and western blot analysis were carried out under the identical conditions using identical reagents and solutions. Results are average of the at least three independent experiments.

Native-PAGE was performed using a Bio-Rad Mini-PROTEAN III electrophoresis cell. Cell lysates, containing the indicated amounts of total protein, were mixed with Laemmli's sample loading buffer without any reducing or denaturing agent. Samples were then electrophoresed using a 3–13% polyacrylamide gradient gel with 1× running buffer (192 mM Glycine, 25 mM Tris, pH 7.0) containing 0.002% Coomassie Blue G at 100 V for 20 min at 4°C, and the blue buffer was then exchanged with a buffer that did not contain Coomassie Blue G. The gels were run at 180 V until the dye front migrated to the bottom of the gel. The observed position of the protein complexes was compared with the BSA oligomer running pattern. After native-PAGE, the gels were transferred to polyvinylidene difluoride membranes (Biotrace PVDF, Pall Corporation, FL, USA) using a semi-dry transfer unit. After blocking with 5% BSA dissolved in TBS-Tween20 (0.15%), the membranes were incubated with anti-LS or anti-SS primary antibodies and a HRP-conjugated secondary anti-rabbit IgG antibody. Proteins were detected with ECL reagents.

SDS–PAGE was performed using a Bio-Rad Mini-PROTEAN III electrophoresis unit. Cell lysates or partially purified proteins were electrophoresed on a 10% separating gel. Gels were run at 150 V for 1.5 h. The gels were subjected to western blotting as previously described.

Quantification of the western blots was performed using the ImageJ software.

4.2.4 Heat stability

The wild-type and mutant AGPases were expressed, and the cells were harvested as previously described [165]. Cells were dissolved in 50 mM HEPES pH 7.5, 5 mM KPO_4, 5 mM $MgCl_2$, and 10% glycerol. Aliquots of cell-free extracts of the wild-type

and mutant AGPases were exposed to temperatures of 50°C and 60°C for 5 min, were cooled on ice and were then harvested by centrifugation at 4°C at maximum speed for 15 min. The supernatants were transferred into the eppendorf tubes, and the AGPase activity was determined using the reverse direction assay in the presence of saturated substrate and 3PGA concentration by monitoring G1P production. Duplicate samples were left on ice and their activity was taken to be 100% which was calculated around 0.3-0.4 nmol G1P/min for each sample. The time-point heat exposure was applied at 65°C for 5, 10 and 15 mins.

4.2.5 Reverse direction assay

A nonradioactive endpoint assay was used to determine the amount of G1P produced by coupling its formation to NADPH production using phosphoglucomutase and Glc-6-P dehydrogenase [166]. The standard reaction mixture contained 100 mM HEPES (pH 7.4), 4 mM DTT, 5 mM 3PGA, 5 mM $MgCl_2$ 1 mM NaPPi, 1 mM ADP-Glucose, and 0.4 mg/ml BSA in a 100-µl reaction volume. Reactions were initiated by the addition of enzyme, incubated at 37°C for 10 min and stopped by boiling for 2 min. After termination, to detect the produced G1P, a development mixture containing 100 mM HEPES, 7 mM $MgCl_2$, 0.6 mM NAD^+, 0.5 U Glc-6-P dehydrogenase and 0.5 U phosphoglucomutase was added. After 15 min of incubation at room temperature, the mixture was separated by 5 min of centrifugation. The absorbance was recorded at 340 nm. The amount of G1P produced was determined from a standard curve using freshly prepared G1P in complete reaction mixtures and omitting enzyme. The specific activity was defined as unit/mg protein, whereby 1 unit was defined as 1 µmol/min.

4.2.6 Partial purification

E. coli AC70R1–504 (*glg*C$^-$) cells were grown in 1 L of LB medium and then induced as previously described. Harvested cells were resuspended in cold lysis buffer (50 mM Tris pH 8.0, 5 mM $MgCl_2$, 5 mM EDTA, 10% glycerol) supplemented with protease inhibitors. The cells were disrupted by sonication, and crude cell extracts were obtained by centrifugation at 14000 × *g* for 20 min. The supernatant was then subjected to 30%-

65% ammonium sulfate fractionation, and the resulting precipitate was resuspended in 1-2 ml of extraction buffer. Dissolved samples were subjected to heat shock at 55°C for 5 min with gentle mixing and centrifuged at 14000 rpm for 40 min. The supernatant was then desalted using dialysis and the desalted sample was applied to a Macro-Prep DEAE weak anion exchange support that was previously equilibrated with extraction buffer. Enzymes were eluted from the column using a linear gradient of extraction buffer (60 ml, 0 to 0.5 M NaCl). Fractions containing enzyme activity were pooled and stored at -80°C after freezing in liquid nitrogen.

4.2.7 Kinetic characterization

Kinetic characterization of partially purified extracts was performed in the forward direction [130, 167]. The amount of PP_i produced was determined using a nonradioactive endpoint assay by monitoring the decrease in NADH concentration using the PP_i reagent (P-7275 Sigma). The reaction mixture contained 50 mM HEPES pH 7.4, 15 mM $MgCl_2$, 4.0 mM ATP, 4 mM G1P and 5 mM DTT in a total volume of 200 µl. The assays were initiated by addition of the enzyme and the reactions were performed at 37°C for 10 min and terminated by boiling for 2 min. After addition of 300 µl PP_i reagent, the NADH decrease was monitored at 340 nm. Blank samples were complete reaction mixtures without enzyme. PP_i production was determined from a standard curve using increasing amounts of PP_i in complete reaction mixtures without enzyme. The K_m values were determined in reaction mixtures in which one substrate or effectors were added in varying amounts and the other reaction components were saturated. The saturating amounts of G1P, ATP and 3PGA were 4 mM, 4 mM and 5 mM, respectively. To each reaction, 0.4 µg of partially purified enzyme was added. The K_m and $A_{0.5}$ values were obtained by nonlinear regression analysis using the Prism software (Graph Pad, San Diego, CA). The $I_{0.5}$ for P_i was determined in the presence of 5 mM 3PGA by adding increasing amounts of P_i.

4.2.8 Reducing and nonreducing conditions for AGPase

Cell free extracts were prepared as described previously. For reducing condition samples were heated at 95^{o}C for 5 min with Laemmli sample buffer containing 4 mM of DTT. For non-reducing condition Laemmli sample buffer without any reducing agent was used. Same 10% SDS polyacrylamide gels were used for both conditions. Western blotting and detection were performed as described previously.

For activity measurements, samples were incubated in 100 mM Hepes, pH 8.0 and 3 mM DTT for 30 min at room temperature. This condition was referred to as the reducing condition. In the control, samples were incubated similarly without DTT.

4.3 Results

4.3.1 Identification of second-site revertants of the potato LS AGPase

Previous work identified several interface amino acid residues in the LS AGPase play role in the interaction with the SS AGPase [86]. Among those interface amino acids, it has been demonstrated that Arg at the position of 88 in the LS plays an important role in the heterotetrameric formation of the AGPase. Further characterization of the LS^{R88A} mutant indicated that it is unable to interact with the SS to form heterotetrameric AGPase as assessed by yeast two-hybrid assays, bacterial complementation and native gel analyses [86]. To gain a better understanding of subunit-subunit interaction between the LS and SS and also identify the LS mutant(s) with enhanced heterotetramer assembly, we employed an error-prone PCR random mutagenesis approach using the LS^{A88} AGPase cDNA as template to select second-site LS suppressors that could reverse the iodine staining deficiency of the *E.coli glg*C^{-} cells containing wild-type SS AGPase cDNA. Any colonies stained by iodine vapor were assumed to contain second site mutation(s) in the LS^{A88} that restored AGPase activity and, in turn, substantial quantities of glycogen. Approximately 2x10^{4} colonies were examined by iodine staining, and of these colonies, 14 colonies that restored glycogen production were identified. Fourteen plasmids containing mutant LS cDNAs were then purified and

subjected to site-directed mutagenesis by PCR to convert the primary mutation Ala-88 back to the corresponding wild-type amino acid residue (Arg). The LS cDNAs containing only the secondary mutations were then co-expressed with the wild-type SS in *E.coli glg*C$^-$, and their activity was assessed by iodine staining. The results indicated that only the cells containing RM2 LS and wild-type SS accumulated more glycogen with respect to the cells containing the wild-type LS and the SS (Figure S4-1). Cells that contain eight revertants LSs (RM6, RM7, RM10, RM11, RM13, RM20, RM22 and RM28) together with wild-type SS stained as dark as cells that contained wild-type cDNAs of the LS and SS, whereas the cells with five revertant LSs (RM4, RM5, RM25, RM27, and RM29) displayed low levels of the iodine-staining phenotype compared with cells containing the wild-type LS and SS AGPase (Figure S4-1).

DNA sequence analysis of the 14 LS mutants indicated that they fell into different mutation classes (Table 4-1). To classify these mutants based on their location in the homology-modeled heterotetrameric AGPase [82], position of each mutation was determined on the modeled structure. The result indicated that several mutations (in RM2, RM7, RM10 and RM27) were both located on or near the lateral and longitudinal subunit interfaces (Figure 4-1B). We previously reported that lateral interaction of the LS-SS is much stronger than the longitudinal interaction, which is mainly mediated by hydrophobic interactions (Figure 4-1A) [82, 86]. Considering that the longitudinal LS-SS interaction is critical, as revealed in the LS^{R88A} mutant, we focused on the mutations located in the region of the longitudinal LS-SS interface. Therefore, RM2, RM7, RM10 and RM27 were selected for further analysis (Table 4-1, Figure 4-1C). Sequence analysis of these selected LS revertants indicated that both RM2 and RM7 contained two amino acids changes. Ile-90 and Tyr-378 were changed into Val and Cys in RM2, whereas Tyr-378 and Asp-410 were replaced with His and Gly in RM7, respectively (Table 4-1). Unlike RM2 and RM7, RM10 contained a single amino acid substitution, where Asp-410 is replaced with Gly in the LS of AGPase. Observed common mutations, such as Tyr-378 and Asp-410, in different revertants indicated the importance of these residues in longitudinal LS-SS interactions. Another mutant, RM27, contained seven mutations (Table 4-1). Among these mutations, only two amino acid

changes, A91T and F101L, were located on the longitudinal LS-SS interfaces (Figure 4-1C). To assess the effect of the individual amino acid changes in RM2, RM7, and RM27 on heterotetrameric AGPase assembly, Ile-90, Ala-91, and Phe-101 were changed into the Thr, Val, and Leu in the wild-type LS AGPases by site-directed mutagenesis. Similarly, Tyr was replaced with both Cys and His at the position of 378 in wild-type LS AGPase for further analysis.

Table 4 - 2 Amino acid replacements in 14 revertants as identified in sequence analysis [168]

Clone	Wild-type Residues	Position	Revertant residues	Clone	Wild-type Residues	Position	Revertant residues
RM2	Ile	90	Val	**RM13**	Val	202	Ala
	Tyr	378	Cys				
RM4	Ile	62	Val	**RM20**	Val	223	Ala
	Asn	418	Ser		Ile	236	Asn
RM5	Asp	219	Val	**RM22**	Arg	200	Glu
	Thr	291	Ala		Val	419	Ala
					Arg	200	Glu
RM6	Pro	395	Leu	**RM25**	Val	419	Ala
					Ile	90	Val
					Ala	91	Thr
RM7	Tyr	378	His		Phe	101	Leu
	Asp	410	Gly	**RM27**	Ile	330	Thr
					Asn	332	Lys
					Asn	401	Asp
					Asp	410	Gly
RM10	Asp	410	Gly	**RM28**	Phe	345	Ser
					Met	373	Val
RM11	Glu	138	Gly	**RM29**	Phe	95	Leu

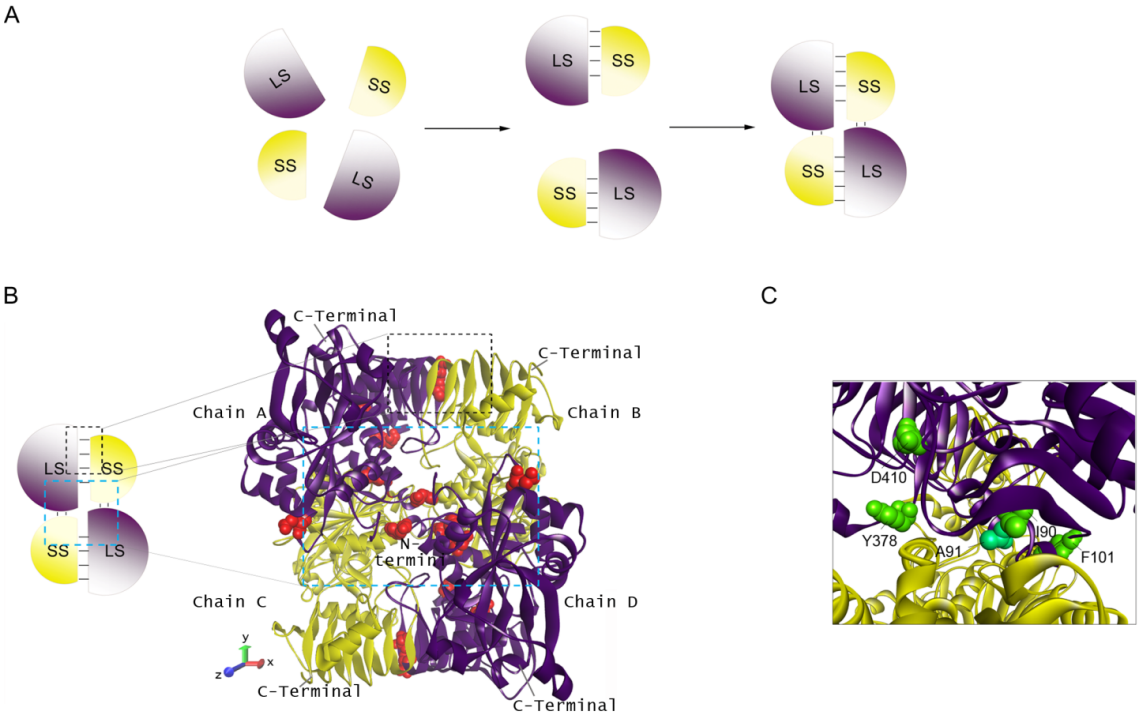

Figure 4 - 1 (A) Order of tetramer formation in AGPase. First LS and SS form a lateral dimer, and then longitudinal tetramerization takes place. Lateral interaction of subunits is much stronger than the longitudinal interaction due to hydrophobic interactions. (B) Location of the mutated interface residues on homology modeled AGPase in which the LS and the SS are depicted by violet and yellow colors, respectively. Residues (red) located at both longitudinal and lateral interfaces. Coordinates of the model were set to define the lateral and longitudinal interaction regions in which strong hydrophobic interaction between LS-SS (A to B and C to D) are designated as lateral interactions, and the relatively weaker interaction of the dimers (AB to CD) are designated as longitudinal interactions. (C) Location of the residues (green) selected for further characterization in the region of longitudinal interface (I90, A91, F101, Y378, and D410)

4.3.2 Native-PAGE analysis of the mutants for the formation of heterotetramers

The heterotetrameric assembly properties of the LS mutant AGPases (RM2, RM7, RM10, LS^{I90V}, LS^{A91T}, LS^{F101L}, LS^{Y378C}, and LS^{Y378H}) with wild-type SS were investigated using 3-13% gradient native polyacrylamide gels followed by Western blot using potato anti-LS and anti-SS. First, these mutants were co-expressed with the wild-type SS in *E.coli glg*C^- in the presence of the IPTG and nalidixic acid. Then, integrity and expression level of both subunits in all samples were assessed by 10% SDS-PAGE followed by western blot analysis using anti-LS and anti-SS antibodies. As expected, the LS mutants and SS proteins in all cell-free extract were detected with molecular weight of approximately 50 kDa, and their expression levels were found to be comparable with the wild-type AGPase (data not shown). Then, variable amounts of the samples were subjected to a gradient native gel electrophoresis (Figure 4-2A). The wild-type AGPase Western blot results revealed three major bands. One band corresponded to approximately 200 kDa, which indicated the presence of tetramers. The second band was detected at approximately 100 kDa, which indicated dimers. The third band was identified at approximately 50 kDa, demonstrating the presence of monomers (Figure 4-2A). To ensure that an equal amount of AGPase in the total protein was loaded, the intensity of the each band was calculated, and the total band intensities were found to be comparable (data not shown). In the wild-type AGPase, heterotetramers comprised 35% of the total band intensity, whereas dimers and monomers comprised 24% and 41% of the total band intensity, respectively (Figure 4-2B). On the other hand, the band intensities of heterotetramers, dimers and monomers in the RM2 AGPase corresponded to 83%, 3% and 17%, respectively (Figure 4-2B). The disappearance of monomers and dimers in RM2 AGPase indicate that they were most probably assembled with the wild-type SS and formed more heterotetrameric AGPase as evidenced by the >2-fold increased heterotetramer amount compared with the wild-type AGPase (Figure 4-2A). To see whether the wild-type SS were assembled with the RM2 LS, we decided to probe the same blot with anti-SS and then quantify the amount of the SS in monomers, dimers, and heterotetramers. The results indicated that, in fact, the amount of the SS is the limiting factor for the heterotetrameric assembly of the RM2 LS AGPase. As seen in

Figure 4-2A, there were no detectable free monomers and dimers of the wild-type SS in RM2 samples, and they were all detected in heterotetramer form with RM2 LS compared to wild-type AGPase where 48% of the SS were in the form of dimer and monomers.

As RM2 has two amino acid changes, Ile and Tyr at the positions of 90 and 378 were separately replaced with Val and Cys in the wild-type LS using site-directed mutagenesis to describe the effects of these two mutations independently on heterotetrameric assembly (Figure 4-2A). The results of Western blots of the native gel indicated that both mutants had enhanced heterotetrameric assembly, in which 75% and 80% of the $LS^{I90V}SS^{WT}$ and the $LS^{Y378C}SS^{WT}$ AGPases were in the form of heterotetramers, respectively (Figure 4-2B). As expected, the majority of the wild-type SS in mutant AGPases (>94%) were also detected in the heterotetramers (Figure 4-2B). These results indicated that the individual or combined effect of the LS^{I90V} and the LS^{Y378C} mutations had a similar effect on the heterotetrameric assembly of the potato AGPase with wild-type SS (Figure 4-2A and B).

A similar analysis was performed with RM7 (Y378H and D410G) and RM10 (D410G) to assess the effect of the mutations on heterotetrameric AGPase assembly. Western blot analyses of the native gel indicated that mutations in the revertants caused the disappearance of the dimers rather than monomers (Figure 4-2A). The amount of disappeared dimers correlated with the amount of increased tetramers (Figure 4-2B). The amount of dimers decreased by approximately 40 to 60% in both RM7 and RM10, whereas the amounts of tetramers increased by similar ratios. The detection of a decrease only in dimers indicated an enhanced interaction between dimers but not monomers. Next, the $LS^{Y378H}SS^{WT}$ AGPase was examined to determine the independent contribution of this mutation for the heterotetrameric formation. The Tyr change into His at the position of 378 in LS did not cause any changes in the heterotetramer formation with wild-type SS of the AGPase (Figure 4-2B). Comparison of the $LS^{Y378C}SS^{WT}$ and $LS^{Y378H}SS^{WT}$ mutants for the heterotetrameric assembly indicated the importance of the hydrophobic residue, Cys, for the subunit interaction of the enzyme at

this identical position. Hydrophobic amino acid residues possibly increase rigidity of the interface and enable better interaction of the subunits.

The effects of longitudinal interface mutations of RM27, LS^{A91T} and LS^{F101L} were analyzed using native PAGE. However, the results indicated that both mutants had a very similar ratio of the heterotetramer, dimer and monomer compared with wild-type AGPase (Figure S4-2).

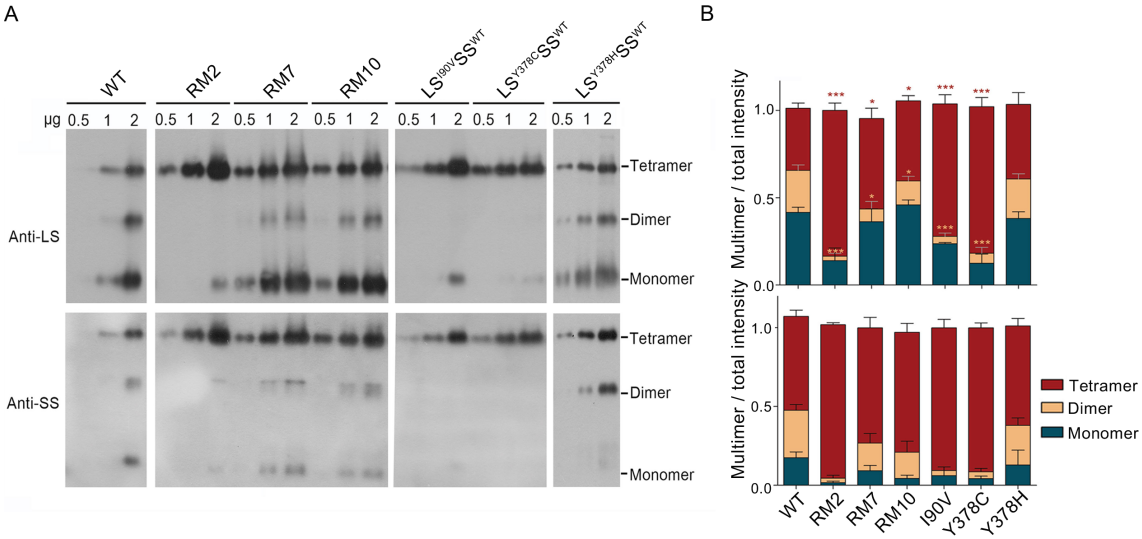

Figure 4 - 2 Native-PAGE and western blot analysis. (A) Crude extract samples of the wild-type LS and LS mutants named RM2 (I90V-Y378C), RM7 (Y378H-D410G), RM10 (D410G), I90V, Y378C and Y378H coexpressed with the wild-type SS were loaded in equal amount in an increasing manner with 0.5, 1 and 2 µg of total protein. In addition, 3 to 13% native gradient gels were used to separate monomeric and oligomeric forms of AGPase followed by western blot using anti-LS and anti-SS antibodies. (B) Stacked column graph showing the ratio of monomer, dimer and tetramer to total band intensity, respectively. Average values with standard error for more than 6 independent experiments were compared with Student's t test compared with wild-type; *** p<0.0001, * p<0.05.

4.3.3 Heat stability of the mutants

The native potato tuber and recombinant AGPase retained major activity after 5 min of incubation between 60°C and 70°C, depending on the presence of P_i [169]. It has been demonstrated that the heat stability of the AGPase is dependent on the intermolecular disulfide bridge located between Cys12 of the small subunits [89]. However, other studies have demonstrated that mutations in the subunit-subunit interfaces or mutations in the allosteric sites increased the temperature stability of the AGPase [91]. Thus, we investigated the heat stability of the mutant AGPases to determine whether the mutation(s) had an effect on the enzyme's structural stability. The heat stability of the mutants was examined by incubating the enzymes at 60°C for 5 min. The remaining activity of each sample was measured at saturated concentrations of substrates and 3PGA with the reverse direction assay. At 60°C, there were no significant difference in heat stability of the RM7, $LS^{I90V}SS^{WT}$, LS^{D410G} SS^{WT} and LS^{Y378H} SS^{WT} AGPases compared with wild-type AGPase, in which they had 65 and 75% of the remaining activities (Figure 4-3). However, RM2 and $LS^{Y378C}SS^{WT}$ AGPases were heat stable under the identical assay conditions compared with the activity of the wild-type AGPases. The remaining activities of RM2 and $LS^{Y378C}SS^{WT}$ AGPases were 92% and 85%, respectively (Figure 4-3). It is interesting to note that Cys at the position of 378 in the LS played a significant role for the heat stability properties of the LS^{Y378C} SS^{WT} AGPase.

We next investigated importance of Cys at the position of 378 of the LS AGPase in heat stability in a time dependent manner at 65 °C. The $LS^{Y378C}SS^{WT}$ AGPase was subjected to the 65°C along with wild-type and LS^{Y378H} SS^{WT} AGPases in a time-dependent manner. The remaining activities of the wild-type and $LS^{Y378H}SS^{WT}$ AGPases were measured as 30% and 20% at 65 °C for 5 min, respectively. On the other hand, under identical conditions, the remaining activity of the $LS^{Y378C}SS^{WT}$ was measured as 50%, which is two-fold higher than the wild-type AGPase (Figure 4-4A). A very similar heat stability trend was observed with the experiment performed at 65 °C for 15 min (Figure 4-4A). Both wild-type and $LS^{Y378H}SS^{WT}$ AGPases had approximately 10% remaining

enzymatic activities, whereas $LS^{Y378C}SS^{WT}$ AGPase had 22% remaining activity, which is again two-fold higher than the wild-type AGPase (Figure 4-4A). To see how such activity correlates with the amount of the heterotetrameric AGPase, the samples were subjected to native-PAGE analysis. The results clearly indicated that the $LS^{Y378C}SS^{WT}$ mutant contained more heterotetrameric enzyme compared with the wild-type and $LS^{Y378H}SS^{WT}$ AGPases at the end of 5 and 15 min (Figure 4-4B). To explore the possibility of the Cys-378 residue in the LS AGPase makes an additional disulfide bond in the interface region, $LS^{Y378C}SS^{WT}$ AGPase was subjected to the non-reducing SDS-PAGE electrophoresis followed by Western blot. The results indicated that both wild-type and $LS^{Y378C}SS^{WT}$ AGPases had all LS subunits as monomers, which indicates there was no disulfide bond formation through the Cys residue (Figure S4-3). In addition, heat stability analysis was performed with and without DTT to see if Cys-378 involved in a stabilizing disulfide bridge. $LS^{C378}SS^{WT}$ and the wild-type AGPase had similar responses (Data not shown).

All these results indicate that the presence of Cys at the position of 378 in the LS not only enhances the heterotetrameric assembly but also enhances the heat stability of the AGPase.

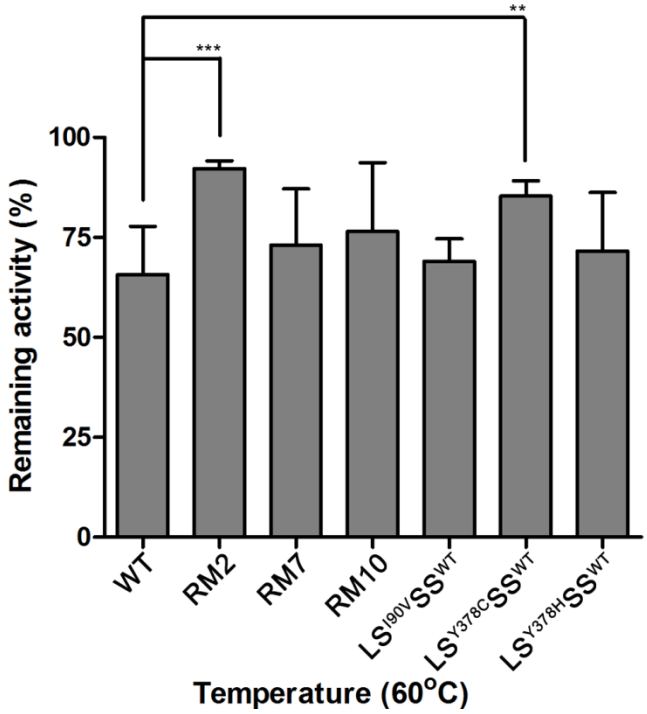

Figure 4 - 3 Comparing the heat stability of mutants with the wild-type. Remaining AGPase activity was demonstrated after heat treatment at 50 and 60°C for 5 min. % heat stability is the activity remaining after heat treatment divided by activity before heating. Duplicate samples were left on ice and their activity was taken to be 100% which was calculated around 0.3-0.4 nmol/min for each sample. Activity measurements were performed by the reverse direction assay in the presence of saturated substrate and 3PGA concentration. Results are the average of 4-6 independent sample preparations with the standard error compared with Student's t test with regard to wild-type; ** $p<0.01$, * $p<0.05$.

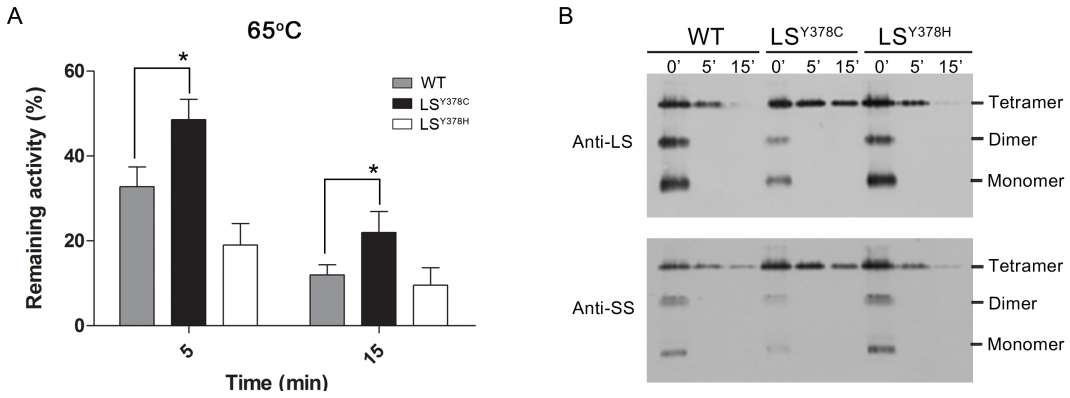

Figure 4 - 4 Heat stability profiles of the $LS^{WT}SS^{WT}$, $LS^{Y378C}SS^{WT}$ and $LS^{Y378H}SS^{WT}$ at 65°C. (A) Remaining activities of the samples were measured after 5 and 15 min heat treatment at 65°C. Duplicate samples were left on ice, and their activity was taken to be 100%. Activity measurements were accomplished using the reverse direction assay in the presence of saturated substrate and 3PGA concentration. (B) Native-PAGE analysis of heat treated samples for 5 and 15 min at 65°C. Same amount and same volume of total protein was loaded to 3 to 13% native gradient gel and proteins were detected with the anti-LS and the anti-SS antibodies.

4.3.4 Kinetic and allosteric properties of the mutants

To determine the catalytic and allosteric properties of the mutant AGPases displaying enhanced heterotetrameric assembly, each mutant enzyme was partially purified using ammonium sulfate fractionation and Macro-Prep DEAE weak anion exchange chromatography with a final purity of 20 to 30%. Because degraded AGPase exhibits altered kinetic behavior [119], all mutant enzymes were subjected to SDS-PAGE and a subsequent Western blot analysis using potato anti-LS and anti-SS antibodies. No apparent degradation was observed for any of the mutant enzymes that were analyzed (Figure S4-4). The K_m values of all mutants for the substrates (ATP, G1P) and the cofactor (Mg^{2+}) were determined in the presence of 3PGA and were comparable with wild-type values (Table 4-2). Allosteric analysis revealed that RM2, $LS^{I90V}SS^{WT}$, $LS^{Y378C}SS^{WT}$ and $LS^{Y378H}SS^{WT}$ AGPases did not display a significant change in sensitivity towards 3PGA/P_i compared with the wild-type AGPase (Table 4-2). However, RM7 and RM10 AGPases exhibited altered allosteric behavior compared with the wild-type. $A_{0.5}$ values were calculated as 0.84 and 1.9 mM for RM7 and RM10, respectively (Table 4-2, Figure S4-5). Both RM7 and RM10 required 4- to 8- fold more 3-PGA than the wild-type enzyme AGPase, which required 0.2 mM of 3PGA to reach $A_{0.5}$. Both revertants contained an Asp change at the 410 position into Gly. This residue was previously identified by as an important residue for the allosteric function of the AGPase [60], as replacing Asp410 to Ala generated an AGPase mutant that requires 6- to 10-fold higher levels of 3PGA and is inhibited by lower levels of P_i than the wild-type enzyme. Similarly, kinetic analysis indicated that both RM7 and RM10 AGPases were more sensitive to the P_i inhibition than the wild-type AGPase (Figure S4-5). To obtain a measurable activity, P_i inhibition curves were obtained in the presence of 1 mM 3PGA (Figure S4-5). Whereas wild-type AGPase required 0.4 mM P_i for 50% inhibition, the amount of P_i required to inhibit 50% of the enzyme's activity was 0.095 mM and 0.070 mM for RM7 and RM10 AGPases, respectively (Table 4-2).

Analysis of the locations of the selected mutations in homology-modeled potato AGPase indicated that these mutations (LS^{I90V}, LS^{Y378C}, LS^{Y378H} and LS^{D410G}) in the LS

were not randomly distributed but were clustered close to the LS-SS interface (Figure 4-1C). To determine the degree of the conservation of these residues, multiple alignments from the mature AGPase sequences were performed using CLUSTALW2 (Figure 4-5). Conservation analysis revealed that the Ile residue at the position of the 90 in LS is highly conserved in different plant species of the LS AGPases, but *Arabidopsis* LS and potato SS have Leu instead of Ile. The amino acid of Tyr at the position of the 378 in the LS is conserved in *Arabidopsis*, lentil, and the potato SS. However, *E. coli* AGPase lacks this residue, rice LS has Ile and maize LS has an uncharged polar Thr residue at this location. Our conservation analysis revealed that LS^{D410} residue is highly conserved among different species, including *E. coli*.

Table 4 - 3 Kinetic and allosteric parameters of the wild-type and mutant AGPases; RM2 ($LS^{I90V-Y378C}SS^{WT}$), RM7 ($LS^{Y378H-D410G}SS^{WT}$), RM10 ($LS^{D410G}SS^{WT}$), $LS^{I90V}SS^{WT}$, $LS^{Y378C}SS^{WT}$ and $LS^{Y378H}SS^{WT}$. Kinetic and regulatory properties were determined in the ADP glucose synthesis direction. All values are in mM. K_m and $A_{0.5}$ for substrates/cofactor and 3PGA, respectively, correspond to the concentration of these molecules required for the enzyme activity to attain 50% of maximal activity. $I_{0.5}$ is the amount of P_i required to inhibit the enzyme activity by 50% of maximal activity. Depicted are the mean values with standard error of at least two independent experiments.

	K_m (mM)			$A_{0.5}$ (mM)	$I_{0.5}$ (mM) for P_i
	ATP	G1P	Mg^{+2}	3PGA	at 1 mM 3PGA
$LS^{WT}SS^{WT}$	0.11 ± 0.05	0.073 ± 0.018	3.57 ± 0.2	0.22 ± 0.05	0.387 ± 0.036
RM2	0.14 ± 0.017	0.11 ± 0.035	3.52 ± 0.5	0.13 ± 0.045	0.482 ± 0.16
RM7	0.14 ± 0.026	0.029 ± 0.013	3.9 ± 0.4	0.84 ± 0.27	0.095 ± 0.022
RM10	0.34 ± 0.1	0.26 ± 0.12	3.3	1.9 ± 0.36	0.070 ± 0.005
$LS^{I90V}SS^{WT}$	0.38 ± 0.013	0.071 ± 0.03	4.36	0.25 ± 0.086	0.385 ± 0.16
LS^{Y378C}SSWT	0.20 ± 0.0058	0.22 ± 0.018	4.97	0.11 ± 0.068	0.395 ± 0.22
$LS^{Y378H}SS^{WT}$	0.17 ± 0.095	0.081 ± 0.019	4.84	0.15 ± 0.058	0.35 ± 0.032

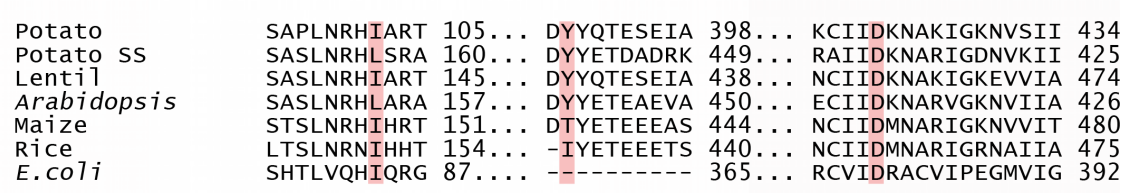

Figure 4 - 5 Primary sequence alignments. Potato LS (Q00081.1) and SS (AAA66057.1), Lentil LS1 (ACW82825.1), *Arabidopsis* LS (CAA51779.2), Maize LS (P55241.1), Rice LS (AAB38781.1) and *E.coli* (A8A5P0.1) were aligned with ClustalW2. Red highlights indicate the amino acids analyzed in this study (I90, Y378 and D410).

4.4 Discussion

AGPase is one of the key regulatory enzymes of the starch biosynthetic pathway. Plant AGPases are structurally complex and consist of two large and two small subunits. Because of the lack of a crystal structure of the native heterotetrameric AGPase, mutagenesis studies have come into prominence to describe the structure-function relationship of the enzyme. A bacterial expression system has facilitated the understanding of plant AGPase function because random mutagenesis and the rapid screening of activity in *E. coli* are feasible. Detailed analyses have identified sites important for the kinetic and allosteric properties and heat stability of the enzyme [87, 91, 117, 159, 164, 165].

Although there is evidence suggesting that the involvement of the interface amino acids contributes to both the lateral and longitudinal interaction between LS-SS, there is currently no information pertaining to specific amino acid changes that may enhance the longitudinal LS-SS interaction and, in turn, increase heterotetrameric assembly of AGPase. A previous study of maize endosperm AGPase revealed heat stable mutants that display enhanced interaction between the LS and SS [87]. In this study, we applied a second-site genetic reversion approach to identify peptide region(s) and amino acids that may comprise a portion of the longitudinal LS-SS interaction in AGPase. Using this approach, the LS^{R88A} mutant, which contributes to the longitudinal interaction, was subjected to error-prone PCR to generate second-site mutations. The mutated LSs were then co-expressed with the wild-type SS and screened for the restoration of AGPase activity. Two general types of second site mutations were expected. The first type included suppressor mutations that functioned in conjunction to counteract the down-regulatory phenotype of the primary mutation. The second type consisted of dominant mutations that acted independently of the primary mutation. Of the initial positive clones obtained, the clones containing dominant mutations were identified by "rescuing" the primary defect and were re-screened for glycogen production after eliminating the primary mutation. Although several of the lines, *e.g.,* clones RM2, RM7 and RM10, share identical amino acid replacements (Table 4-1), they were

independently derived because they also contained other unique mutations. The generation of multiple independent mutants of the same class suggested that our mutagenesis and screening procedure was close to saturation.

Native gel analysis indicated that LS AGPase mutants have altered heterotetrameric assembly. Among the mutants $LS^{I90V}SS^{WT}$ and $LS^{Y378C}SS^{WT}$ AGPases were predominantly in heterotetrameric form compared with the wild-type AGPase. Interestingly, $LS^{Y378C}SS^{WT}$ AGPase is also exhibited increased heat stability relative to the wild-type enzyme. The underlying reason for enhanced heterotetrameric formation and strong stability, for example, in $LS^{Y378C}SS^{WT}$ AGPase may be the location of this residue, which is notably close to the both small subunits within a range of 4 - 5 Å according to the heterotetrameric model [82]. Tyr-378 on the D chain of the LS, for example, is 4.6 Å close to the Glu-124, 4.9 Å close to the Thr-126 residues in B chain of the SS and 4.6 Å close to the Arg-298 residue in the C chain of the SS (Figure S4-6A). Moreover, substitution of Tyr-378 to Cys in the LS reduced the 4.6 Å distance to 3.2 Å between $LS_D{}^{C378}$ and $SS_B{}^{E124}$ and it appears to generate a new hydrogen bond between the side chains of LS^{C378} and SS^{E124} residues (Figure S4-6B). In addition, it is possible that mutations in the LS (at positions of the 90 and 378) may increase the rigidity of the interface and therefore enable better interactions between the subunits. However, to elucidate the exact role of these residues in subunit-subunit interactions, the crystal structure of the heterotetrameric plant AGPase is essential. We next investigated the effect of the mutations obtained in this study on heat stability properties of the AGPase. Heat stability analysis indicated that only $LS^{Y378C}SS^{WT}$ AGPase was heat stable compared with other mutants and wild-type AGPases. Tyr378 of the LS possibly generates new H-bonds, which is not only the result of enhanced heterotetrameric interaction between the subunits but also the increasing heat tolerance of the AGPase. Other possibly is that having a specific hydrophobic amino acids residues at the indicated position in the LS subunit interface results in increasing the rigidity and, in turn, enhancing subunit-subunit interaction and heat stability.

Kinetic analysis revealed that only $LS^{D410G}SS^{WT}$ AGPase has distinct allosteric properties (Table 4-2, Figure S4-5). These results are consistent with the Asp residue at position 410 of the LS, which has been previously demonstrated to be crucial for the normal allosteric behavior of the potato AGPase and spinach AGPase [56, 60]. Although the Asp at the position of 410 in the LS was not demonstrated to be positioned directly at the subunit interface, its location on the model was close to the subunit interface (Figure 4-1C). Previous studies have indicated the relation between allosteric properties and subunit interaction of the AGPase [92, 170]. Homologous residue of potato LS^{R88} in maize SH2 (R146) was demonstrated to be involved in P_i binding. $SH2^{R146A}$ mutation altered the 3PGA and P_i affinity of the enzyme in a down-regulatory manner [170]. In addition, a potato LS^{R88A} mutant has been demonstrated to be defective in the heterotetramer formation as stated previously [86]. These studies suggest that subunit interaction and allosteric properties of the AGPase are closely related with each other.

In this study, we identified a novel amino acid on the LS AGPase interface important for the heterotetrameric assembly and heat stability of the AGPase. The novel mutations, LS^{I90V} and LS^{Y378C}, were identified and characterized as significantly enhancing the LS-SS interaction and, in turn, increasing heterotetrameric assembly of the enzyme without affecting the kinetic and allosteric properties. In addition, we also identified the amino acid residue that moderately enhanced heterotetrameric assembly with altered kinetic properties.

CHAPTER 5

Investigation of the Effect of Better Assembling Heterotetrameric AGPases in Transgenic Rice Plants

5.1 Introduction

Cereals are one of the most important essential food sources for humans. Due to their high starch content, cereals have also been utilized for the production of biofuels environmentally friendly biopolymers and for many various industrial processes. Cereal seeds such as rice, maize, barley and wheat supply the majority of starch production with an overall yield of 2 billion tons annually. 75 million tons of starch is used for industrial purposes according to 2012 data published by the International Starch Institute*. From both nutritional and industrial perspectives, improving the starch yield in cereal plants is crucial due to increasing population and industrial demand.

As described in Chapter 1, starch biosynthesis in plants depends on the relation between the rate and also duration of photosynthesis in source tissues and the capacity of sink tissues to assimilate carbon. Therefore, two strategies can be applied to increase the starch yield of plants. One possible method is to try increasing the source strength, which will in turn increase the photosynthetic capacity of the plant. The second method is to enhance the capacity of sink organs for better utilization of photosynthesis products. In terms of improving starch production of cereals, modulating starch synthesis in endosperms can be targeted. When photosynthesis is not limiting, better variants of AGPase, pivotal enzyme of starch biosynthesis, can be used to increase sink strength and in turn, better utilization of photosynthesis products.

* http://www.starch.dk

Plant AGPases are heterotetrameric ($\alpha_2\beta_2$) enzymes consisting of two subunits called the large subunit (LS) and the small subunit (SS), which are encoded by two different genes [63, 115]. AGPase is allosterically activated by 3-phosphoglycereate (3PGA) and inhibited by inorganic orthophosphate (P_i). Recent studies have demonstrated that both subunits contribute to the activity and allosteric regulation of the heterotetrameric enzyme [66, 67, 117, 129, 158-160]. Furthermore, specific regions from both the LS and the SS are important for subunit association and enzyme stability [82, 86, 88]. Recent studies have suggested that subunit interaction is not only required for an active heterotetramer but also needed for the allosteric regulation of the enzyme [67, 91, 92]. Most transgenic studies have focused on modulating allosteric regulatory properties of AGPase to increase the starch yield in cereals. For example, using allosterically insensitive *E.coli* mutant AGPase resulted in increased seed weight up to 11% in rice endosperm [102]. More recently, transgenic maize plants expressing a form of the AGPase with enhanced heat stability and reduced phosphate inhibition showed an improvement in the yield up to 64% by increasing seed number [107]. In another study an improvement in rice seed number was observed by overexpressing potato LS upreg1 gene under the control of the rice glutelin promoter [171].

As indicated in Chapter 3, point mutations by the conversion of Ile90 to Val or Tyr378 to Cys on the LS of the potato AGPase produced heterotetrameric enzymes with enhanced subunit-subunit interaction [172]. In this chapter, we address how subunit-subunit interaction affects functioning of AGPase *in vivo* using rice plants from a structure-function point of view based on the data obtained from *in vitro* recombinant studies of the potato tuber AGPase [172].

Rice AGPase has considerably weak structure compared to the potato AGPase. Even under mild tempreratures heterotetrameric structure dissociates and this causes yield loss. In addition, rice plant is an important cereal throughout the world. Rice is one of the most widely consumed staple foods as it has third-highest worldwide cultivated area and second-highest grain production according to data of FAOSTAT 2013 [173].

Nonetheless, it is an ideal model organism for the investigation of starch metabolism, as 80% of its endosperm is comprised of starch [174].

Rice AGPase has two isoforms for the small subunit: OsAGPS1 and OsAGPS2. OsAGPS1 gene encodes for the plastidial isoform of endosperm. OsAGPS2 gene encodes two different transcript, OsAGPS2a and 2b. OsAGPS2a is the plastidial isoform in leaves and OsAGPS2b is the cytosolic isoform in endosperms [175, 176]. There are four different isoforms for the LS of AGPase in rice, OsAGPL1 to L4. OsAGPL2 is the cytosolic isoform in endosperm [175-177]. The major AGPase form in rice endosperm is located in the cytoplasm, where newly synthesized ADP-glucose is subsequently imported to the amyloplast for starch synthesis. OsAGPS2b and OsAGPL2 isoforms form the heterotetrameric, cytoplasmic-localized AGPase in rice endosperm.

The aim of this work is to study the physiological effects of better assembling variants of AGPase in rice. First, identical replacements of the residues found on the LS of potato AGPase have been generated in the LS of rice endosperm (OsAGPL2) in order to analyze *in vitro* enzymatic and structural properties of recombinant AGPases. *In vivo* analysis revealed that rice endosperm AGPases carrying I150V and Q438C mutations on OsAGPL2 subunit showed significantly increased iodine staining in AGPase deficient *E.coli*. Plant expression vectors carrying mutant LSs of rice endosperm AGPase were generated for *Agrobacterium* mediated transformation of rice. In order to investigate the effects of the mutant AGPases independently from their wild-type form, LS mutant EM541 rice [178] which contains a null mutation in OsAGPL2, was used for transformation studies. Preliminary analysis indicated that Q348C mutation on OsAGPL2 subunit has a great impact on tillering of transgenic rice plants.

5.2 Materials and Methods

5.2.1 Plant material

Oryza sativa cv Kinmaze EM541 mutant was used for the transformation which has a nonsense mutation in the coding region of OsAGPL2 gene and lacks detectable levels of endosperm cytosolic isoform of LS [178].

5.2.2 Site directed mutagenesis

Mutations were introduced into the LS cDNAs using PCR by using mutagenic primers listed on Table 1. The PCR was performed in a total volume 50 ul containing 50-100 ng of template plasmid pUC58 (Genbank: AF253496) containing wild type OsAGPL2 cDNA. PCR conditions were 18 cycles at 95^{o}C for 50 sec, 60^{o}C for 50 sec and 68^{o}C for 8 minutes. Following the reaction, products were digested with DpnI and transformed into the XL10 competent cells. Plasmids were isolated from selected colonies and presence of the mutations was confirmed by DNA sequencing (Eurofins MWG Operon)

5.2.3 Construction of bacterial expression vectors

Mutated L2 genes on pUC58 vector were subcloned into pSH476 [68] a 6x-His tag carrying expression plasmid which was derived from pQE30 (Qiagen) for bacterial expression.

5.2.4 Iodine staining for bacterial glycogen production

The wild type and mutant LSs were co-expressed in the presence of wild type S2b in glgC-deficient *E.coli* strain AC70R1-504 (Ballicora 1995) and/or in *E. coli* EA345 cells which contain a mull mutation in the AGPase gene glgC [68].

Single bacterial colonies were streaked on Kornberg's media (2.2% K2HPO4, 0.85% KH2PO4, 0.6 % yeast extract, 1.5 % agar, 200 mg/L penicillin G and 50 mg/L

kanamycin) supplemented with 1% glucose. The overnight grown cells were exposed to iodine vapor to detect and compare glycogen production levels.

5.2.5 Expression of OsAGPL2 (LS) and OsAGPS2b (SS) cDNAs in EA345 cells

Three colonies of EA345 cells carrying wild type recombinant rice endosperm SS were inoculated into 25 ml of LB containing 0.4% glucose, 200 mg/L penicillin G and 50 mg/L kanamycin. Overnight grown cells at 37^{o}C were used to inoculate 1 L of NZCYM liquid medium containing 200 mg/L penicillin and 50 mg/L kanamycin. Cells were grown at room temperature until OD600 reached 1-1.2, then expression of both LS and SS were induced by addition of IPTG at a final concentration of 100 μM. Induction was performed for 18 h at room temperature with rigorous shaking.

5.2.6 Purification

Induced cells were harvested by centrifugation and resuspended in 25 ml of cold lysis buffer (25mM HEPES-NaOH, pH 8.0, 10% glycerol, 0.5 mg/ml lysozyme, 1mM PMSF and 1 ug/ml each of leupeptin and pepstatin A). Cells were disrupted by sonication and crude cell extracts were obtained by centrifugation at 12000 rpm for 20 min at 4^{o}C. Cell free extracts were loaded on a DEAE-Sepharose Fast Flow (Amersham) column pre equilibrated with buffer A (25 mM HEPES-NaOH, pH 8.0, 10% glycerol). After washing column with 4-5 bed volumes of buffer A, AGPase enzyme activity was eluted with buffer A containing 0.3 M NaCl. Elute was passed through immobilized metal affinity column (TALON Superflow, Clontech) for further purification using a Bio Logic DuoFlow Chromatography system (BioRad). The column was pre-equilibrated with buffer B (25 mM HEPES-NaOH, pH 8.0, 10% glycerol, 0.3 M NaCl) prior to loading of the elute, then extensively washed with 5 mM imidazole in buffer B. AGPase was then eluted with 100 mM imidazole in buffer B and fractions containing the highest AGPase activity were pooled and concentrated using a 30kDa cut-off ultrafiltration membrane (Millipore). The concentrated enzymes were divided into small aliquots and stored at -80^{o}C.

5.2.7 Kinetic characterization

AGPase activities were measured in the ADP-glucose synthesis (forward) direction for kinetic characterization. The amount of PP_i produced was determined using a nonradioactive endpoint assay by monitoring inorganic phosphate amount at 650 nm using pyrophosphatase and coupling reagent containing 1 part of 12% ascorbic acid in 1M H_2SO_4 and 2 parts of 20 mM ammonium molybdate in 1.4 M H_2SO_4. Unless indicated, the complete reaction mixture contained 50 mM Hepes-NaOH, pH 7.5, 10 mM $MgCl_2$, 5 mM DTT, 4 mM ATP, 4 mM G1P, 10 mM 0.15 U pyrophosphatase in a total volume of 100 µl. Reactions were initiated by addition of the reaction mixture on the enzymes, which were added formerly on the 96 well plate, and were performed at room temperature for 15 min following additional 5 min incubation with 100 µl coupling reagent. Reactions were terminated by addition of 100 µl of 0.5 M citric acid. Blank samples were complete reaction mixtures without enzyme. Absorbances were read at 650 nm using a plate reader. P_i production was determined from a standard curve using increasing amounts of P_i in complete reaction mixtures without enzyme. The K_m values were determined in reaction mixtures in which one substrate or effectors were added in varying amounts and the other reaction components were saturated. The saturating amounts of G1P, ATP and 3PGA were 4 mM, 4 mM and 10 mM, respectively. To each reaction, 2 µg of partially purified enzyme was added. The K_m and $A_{0.5}$ values were obtained by nonlinear regression analysis using the Prism software (Graph Pad, San Diego, CA). The $I_{0.5}$ for P_i was determined in the presence of 1 mM 3PGA by adding increasing amounts of P_i.

5.2.8 Construction of plant expression vectors

The wild type and mutant LS genes were cloned into between OsAGPL2 promoter and terminator sequences in NcoI-SalI sites of the pSH719 vector (Appendix 1). Then LS genes with promoter and terminator sequences were cloned into the HindIII-BamHI sites of pCAMBIA 1303 binary vector (Genbank: AF234299, Appendix 1) for plant transformation.

5.2.9 Plant transformation

Main steps of the *Agrobacterium* mediated transformation of rice were illustrated on Figure 5-1.

5.2.9.1 Callus induction:

Glumes were removed from mature EM541 seeds using forceps. Seeds were sterilized with 100% bleach for 3 minutes and rinsed four times with sterile water. Excess water was removed by blotting seeds on sterile filter paper. Sterilized seeds were placed on N6D medium and incubated at 28^{o}C in dark for 7-9 days where. Small embryogenic calli were formed. The plates were then transferred to continuous light condition for 3-4 weeks for secondary calli formation. Secondary calli were transferred into fresh N6D medium three days before *Agrobacterium* transformation.

5.2.9.2Agrobacterium infection:

pCAMBIA constructs carrying wild-type and mutant LSs were transformed into AGL1 strain of *Agrobacterium* and incubated for 3 days at 28^{o}C. Grown AGL1 cells were scraped from plate and resuspended in *Agrobacterium* resuspension medium containing 10 mg/L Acetosyringone. Embryogenic calli were incubated with *Agrobacterium* suspension for 3 minutes. Excess suspension was removed by blotting on filter paper. Then *Agrobacterium* suspended calli were placed onto solid co-culture medium and incubated for 3 days at 28^{o}C in dark.

After three days calli were washed with sterile water with a final wash containing the antibiotic timentin (250 mg/L) to inhibit further *Agrobacterium* growth.

5.2.9.3 Selection:

Washed calli were transferred onto selection medium. 3 rounds of hygromycin selection, each for 14 days, was performed by transferring healthy hygromycin resistant calli to fresh selection plates.

5.2.9.4 Regeneration and rooting

Surviving hygromycin resistant embryogenic calli were transferred to regeneration medium to induce shoot and root formation under continuous light at 30^{o}C for up to 20 days.

Green embrioids were transferred to rooting medium and cultured under long day conditions at 30^{o}C for 4 weeks until healthy plants are ready for transfer to soil for further plants growth and seed harvesting.

5.2.10 Genomic DNA isolation and detection of transgenes in T0 plants with PCR

To confirm the presence of transgenes in putative transgenic T0 plants we conducted a rapid genomic DNA isolation procedure followed by PCR. 15-30 mg of fresh leaves of 30 days grown plants were used for genomic DNA extraction. Leaf samples were put into 1.5 ml tubes and liquid nitrogen was poured onto each tube. Frozen leaf tissue was crushed into fine powder with plastic tissue grinder pestles fitting 1.5 ml tubes. Each ground sample was mixed well with 400 µl of CTAB buffer containing 2% (w/v) CTAB, 1.4 M NaCl, 100 mM Tris-HCl, pH 8.0, 50 mM EDTA, pH 8.0, 1% (w/v) PVP-40, 0.5% (w/v) sodium bisulfate. 1% (v/v) β-mercaptoethanol was added freshly before use. Powdered tissue and buffer suspension was incubated for 20 min at 65^{o}C with occasional mixing. Suspension was centrifuged for 5 min at 12000 rpm, at room temperature. Supernatant was transferred to clean microfuge tube and 400 µl of chloroform:isoamyl alcohol (24:1) was added and vortexed vigorously for 10 sec. After mixing samples were centrifuged at 12000 rpm for 10 min. Nucleic acid containing top layer was carefully transferred to clean microfuge tubes and precipitated for 5 min with an equal volume of ice-cold isopropanol at maximum speed. DNA pellets were washed with 1 ml 70% ethanol and centrifuged for 1 min at maximum speed. Then pellet was dried with SpeedVac and resuspended in sterile water containing 50 µg/ml RNase A.

PCRs were performed in a total volume of 25 µl consisting of 1X Taq polymerase buffer, 200 µM dNTP mixture, 0.5 µM of gene specific forward and reverse primers,

1% DMSO, 1 U Taq polymerase and 100-200 ng of genomic DNA under following conditions: denaturation at 95°C for 5 min followed by 35 cycles of 95°C for 40 sec, 55°C for 40 sec, 72°C for 2 min with a final extension step of 72°C for 5 min.

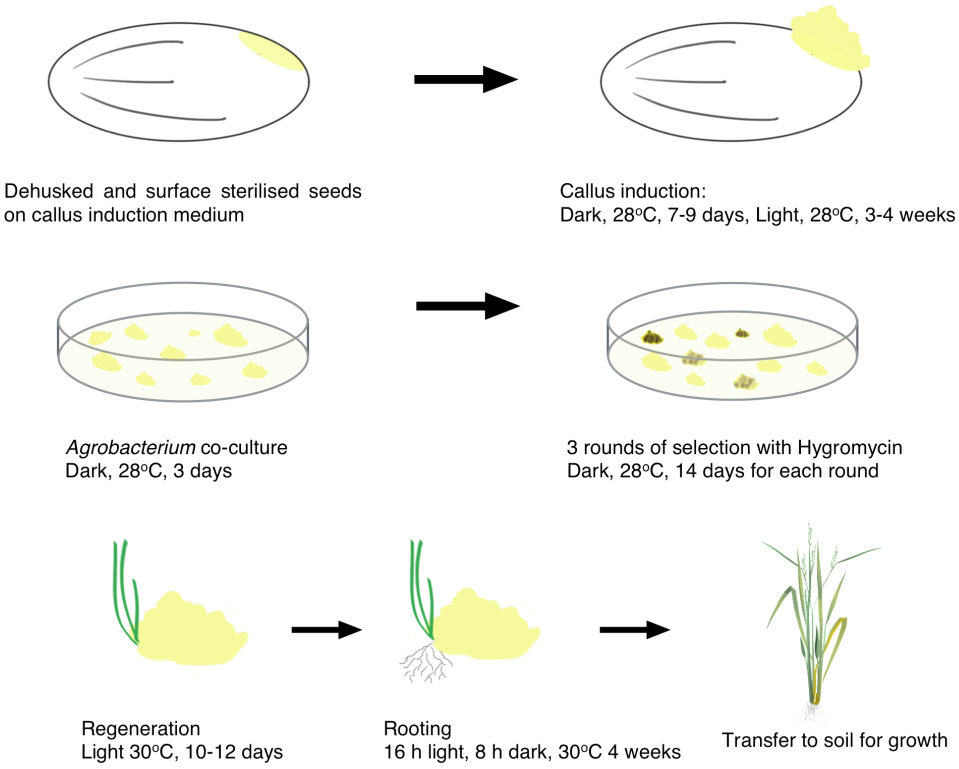

Figure 5 - 1 Illustration of steps in *Agrobacterium*-mediated transformation of rice

5.3 Results

5.3.1 Site directed mutagenesis and construction of bacterial expression vectors

Comparison of the LS sequences from potato AGPase with rice OsAGPL2 shows 78% similarity at the protein level. The rice and potato LSs share a conserved Ile90 of the potato. At the position of Tyr378 for the potato enzyme, the rice endosperm LS has a glutamine (Figure 5-2). To generate identical replacement of the corresponding residues, Ile150 and Gln438 in the rice endosperm AGPase LS, primer sets were designed for site directed mutagenesis PCR (Table S5-1).

I150V (IV) and Q438C (QC) mutations were introduced into LS of the rice endosperm cDNA on pUC58 vector by site directed mutagenesis PCR method (Figure 5-3A). Presence of the mutations was confirmed by sequencing (Figure 5-4). Double amino acid substitutions (IVQC) were performed using IV construct as template and QC primers (Figure 5-3B).

To construct bacterial expression vectors, mutated cDNAs were subcloned onto OsAGPL2 expression vector pSH476. Presence of the inserts was verified with restriction digest test (Figure S5-1).

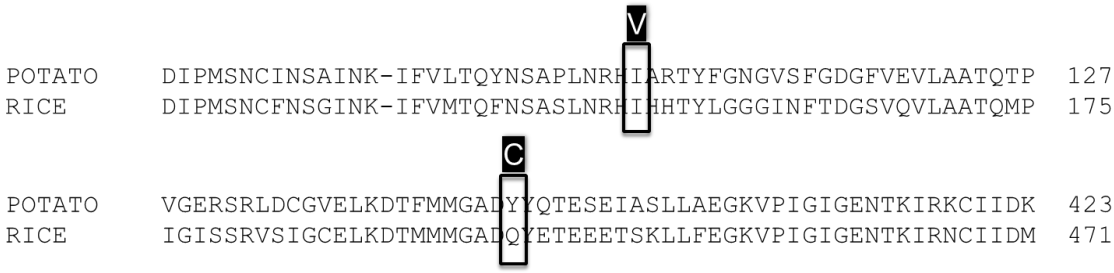

Figure 5 - 2 Seqeunce alignment of potato and rice endosperm AGPase LSs. Genbank accesison numbers: Potato LS, Q00081, Rice OsAGPL2, BAG92523

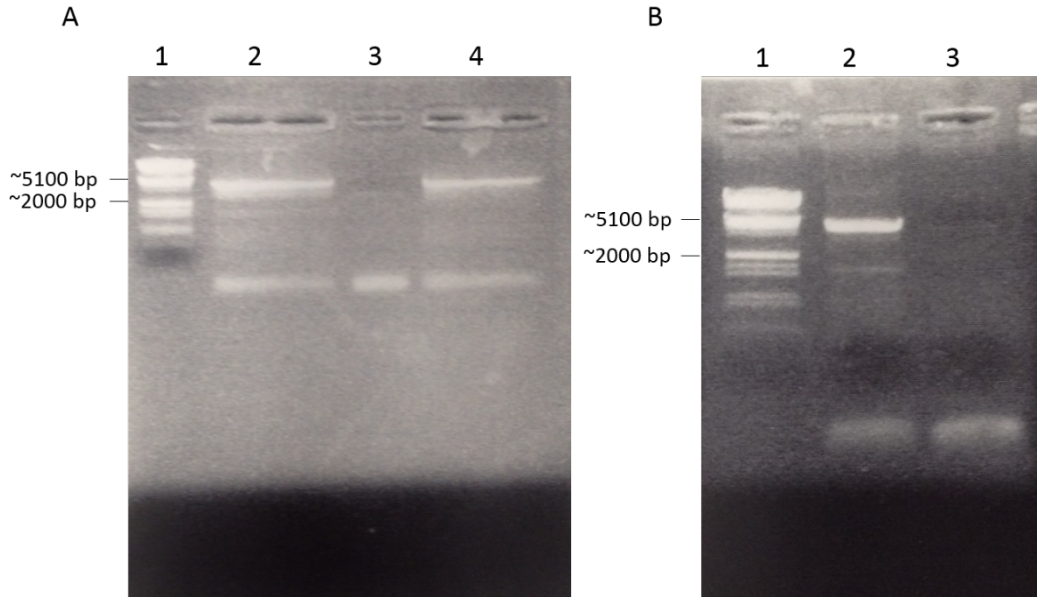

Figure 5 - 3 Site directed mutagenesis PCR results run on 1% agarose gels. First lanes show lambda DNA marker HindIII-EcoRI digest A) Lane 2: PCR product of IV mutagenesis, Lane:3 control PCR without enzyme addition, Lane 4: PCR product of QC mutagenesis B) Lane 2: Site directed mutagenesis PCR result of the construct carrying both of the mutations in which IV template was amplified with QC primers

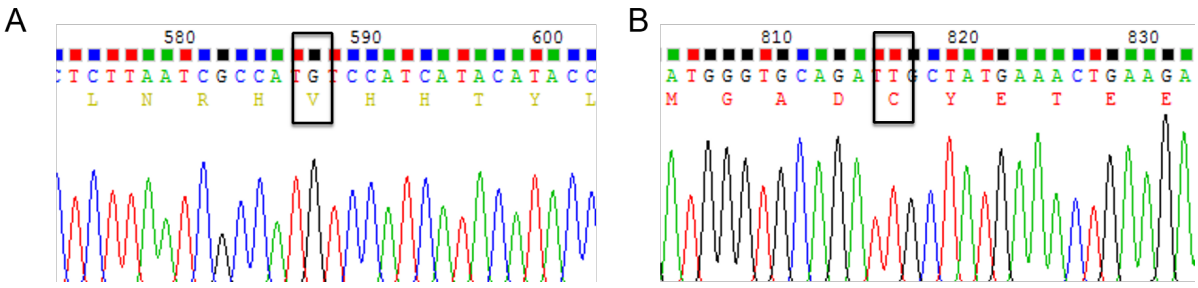

Figure 5 - 4 Sequence analysis to confirm presence of the incorporated mutations with site directed mutagenesis. A and B show Leucine to Valine change, Glutamine to Cysteine change, respectively. No other additional mutations were detected.

5.3.2 Bacterial complementation analysis of AGPases by iodine staining

Effects of the IV, QC and IVQC mutations were examined by measuring the level of glycogen accumulation in the glgC deficient *E.coli* strains using iodine staining. Each recombinant AGPase large subunit was co-expressed with the wild-type rice endosperm small subunit in an glgC-deficient *E.coli* strain (AC70R1-504) and/or in another *E.coli* strain harboring a glgC null mutation on glgCAP operon (EA345). Functional AGPase encoded by the plasmids complements the glgC deficient/mutant *E.coli*, resulting in glycogen production which is easily detected by staining of colonies when exposed to iodine vapor. As seen in Figure 5-5 higher glycogen accumulation is easily observable with significantly dark staining of cells carrying $LS^{QC}SS^{WT}$ and $LS^{IVQC}SS^{WT}$ constructs compared to cells carrying WT rice endosperm AGPase. Note that, mutant AGPase carrying LS^{IVQC} mutations is slightly darker than AGPase carrying LS^{QC} mutation. Stained cells expressing $LS^{IV}SS^{WT}$ construct showed slightly increased staining relative to wild-type AGPase.

5.3.3 Expression and purification of the recombinant AGPases

To determine the effects of the mutations on enzyme activity recombinant wild-type and mutant AGPases were purified as described in the methodology part. SDS-PAGE and western blot analysis were performed to see the purity levels and integrity of the purified proteins, respectively. Comparing cell free extracts with purified proteins showed that purity level is up to 70-80% and both subunits were present at stoichiometric amounts (Figure 5-6). The size of the small subunit (OsAGPS2b) is approximately 53 kDa and the size of the LS (OsAGPL2) together with the 6xHis tag is around 59 kDa. Western blot analysis of the purified enzymes using the anti-LS and anti-SS antibodies confirmed that protein bands observed in the Coomassie blue stained SDS-PAGE correspond to the AGPase LS and SS with no significant degradation (Figure 5-7). Then we decided to further characterize these mutants to see any alterations in their kinetics.

Figure 5 - 5 Iodine staining of the *E.coli* AC70 (A) and EA345 (B) cells expressing the rice endosperm recombinant wild type and mutant AGPases. The wild type and mutant AGPase forms were streaked onto Kornberg media containing 2% glucose.

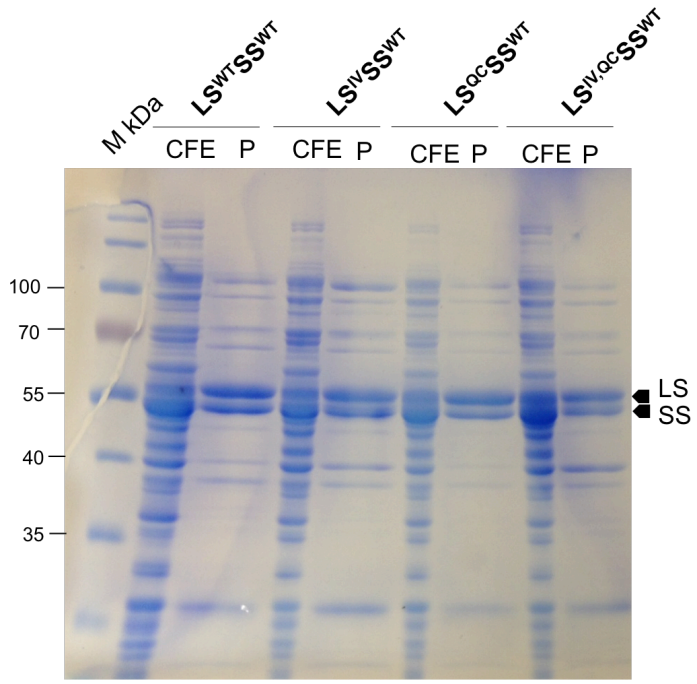

Figure 5 - 6 SDS-PAGE analysis of the recombinant partially purified AGPases. Lanes labelled with CFE indicates cell free extracts prior to purification steps, lanes labelled with P indicates purified protein after DEAE anion exchange and IMAC purification steps

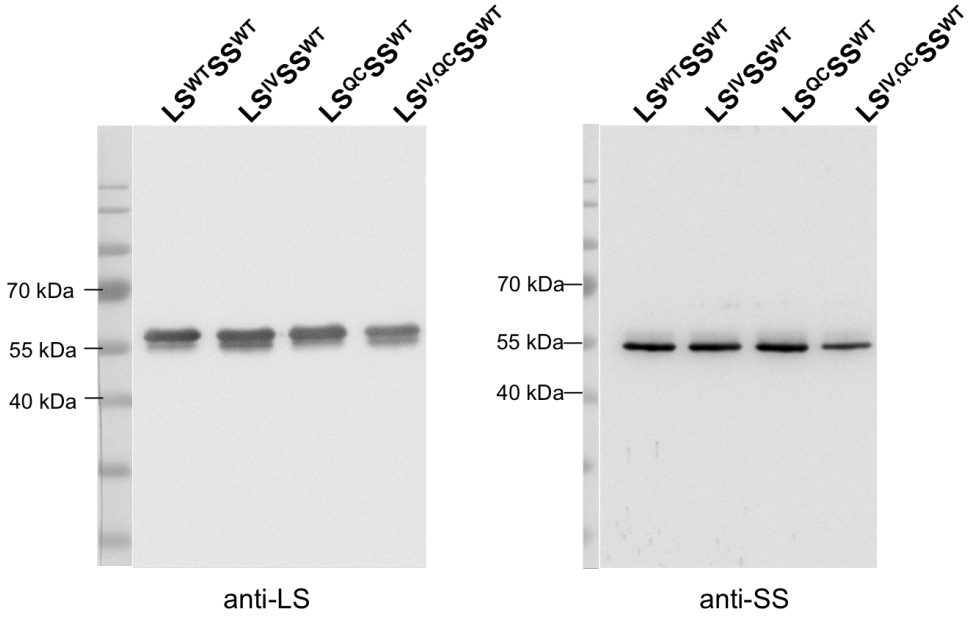

Figure 5 - 7 Western blot analysis of purified wild-type and mutant rice endosperm AGPases After purification, samples subjected to SDS–PAGE followed by western blot analysis with rice specific anti-LS and potato specific anti-SS antibodies showed no apparent degradation of AGPase.

5.3.4 Kinetic characterization

The purified recombinant wild-type and mutant AGPases were assayed to determine the effects of mutations on enzyme activity. The kinetic parameters of the wild-type and mutants are shown in Table 5-1. Analyses of the substrate binding affinities of the AGPases revealed that there were no significant differences in ATP and G1P $S_{0.5}$ values between the wild-type and mutant enzymes (Figure 5-8). The $S_{0.5}$ for ATP and G1P of all enzymes ranged from 0.2 to 0.36 and 0.2 to 0.3, respectively.

The 3PGA affinities of the mutants and wild-type were also similar (Figure 5-9A). The $A_{0.5}$ values for 3PGA of all enzymes ranges from 0.42 to 0.5.

In addition to substrate and activator analyses, effects of the inhibitor, P_i, were also investigated. In the presence of 1 mM 3PGA all the mutants and wild-type AGPases exhibited similar inhibition profile (Figure 5-9B).

Collectively, these results show that IV and QC mutations on the LS did not change any substrate binding or allosteric properties of rice endosperm AGPase significantly.

Table 5 - 1 Kinetic parameters of the recombinant wild-type and mutant AGPases. Assays were performed in the ADP glucose synthesis direction. All values are in mM. $S_{0.5}$ and $A_{0.5}$ for substrates and 3PGA, respectively, correspond to the concentration of these molecules required for the enzyme activity to attain 50% of maximal activity. $I_{0.5}$ is the amount of P_i required to inhibit the enzyme activity by 50% of maximal activity. Depicted are the mean values with standard error of at least two independent experiments.

	$S_{0.5}$ (mM)		$A_{0.5}$ (mM)	$I_{0.5}$ (mM) for P_i
	ATP	G1P	3PGA	at 1 mM 3PGA
$LS^{WT}SS^{WT}$	0.36 ± 0.05	0.21 ± 0.03	0.45 ± 0.08	0.27
$LS^{IV}SS^{WT}$	0.34 ± 0.04	0.3 ± 0.02	0.42 ± 0.2	0.4
$LS^{QC}SS^{WT}$	0.29 ± 0.04	0.22 ± 0.02	0.5 ± 0.11	0.23
$LS^{IV,QC}SS^{WT}$	0.2 ± 0.01	0.19 ± 0.02	0.45 ± 0.09	0.4

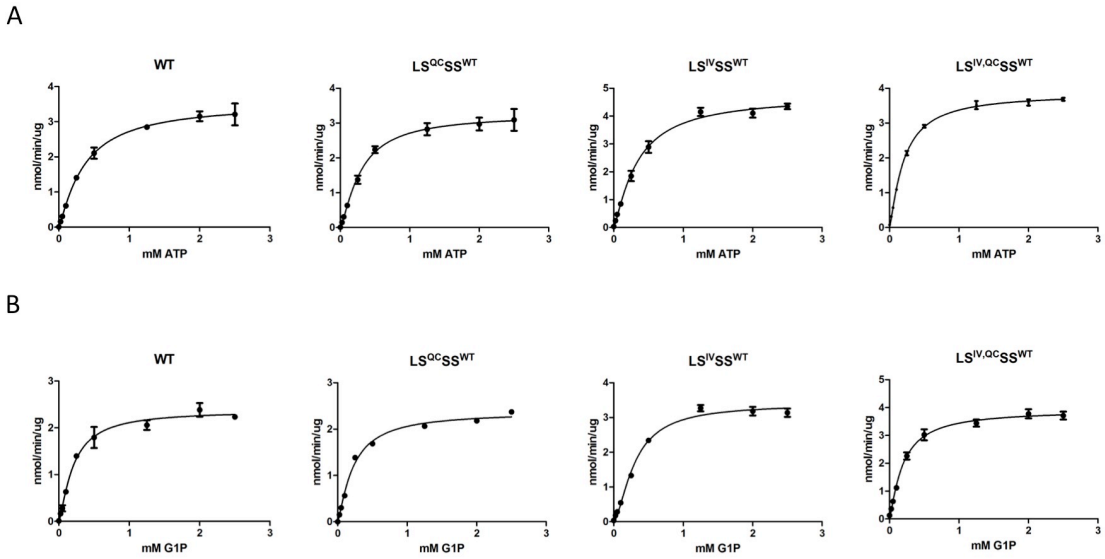

Figure 5 - 8 (A) Velocity versus ATP concentration graphs of of the wild-type AGPase and $LS^{QC}SS^{WT}$, $LS^{IV}SS^{WT}$, $LS^{IV,QC}SS^{WT}$ mutant AGPases in the presence of 5 mM 3PGA. (B) Velocity versus G1P concentration graphs of of the wild-type AGPase and $LS^{QC}SS^{WT}$, $LS^{IV}SS^{WT}$, $LS^{IV,QC}SS^{WT}$ mutant AGPases in the presence of 5 mM 3PGA.

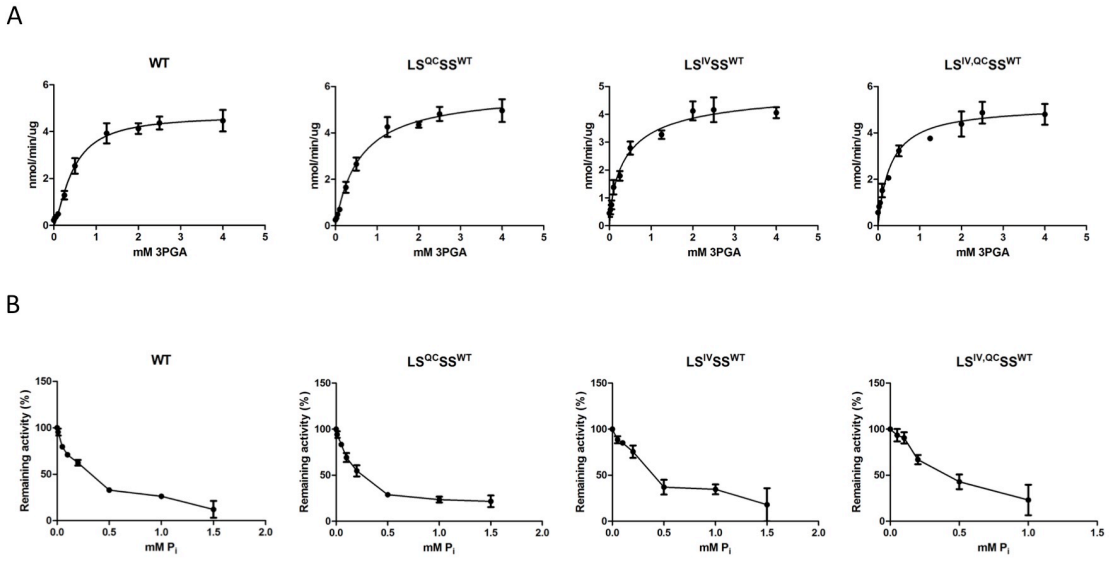

Figure 5 - 9 3PGA activation (A) and P_i inhibition (B) profiles of the wild-type AGPase and $LS^{IV}SS^{WT}$, $LS^{QC}SS^{WT}$, $LS^{IV,QC}SS^{WT}$ mutant AGPases. (A) Reactions were performed in the forward direction under saturating substrate conditions and with varying amounts of 3-PGA. (B) Reactions were performed in the forward direction under saturating substrate conditions and with 1 mM 3PGA.

5.3.5 Construction of plant expression vectors and Agrobacterium mediated transformation of EM541 rice

To assess the effect of the LS mutants *in vivo*, we decided to transfer the rice LS AGPase mutants to the rice plants which do not possess a functional LS AGPase gene.

First, mutant AGPase LS cDNAs were cloned into the pSH719 vector between the native promoter and terminator sequences of the rice endosperm LS (OsAGPL2) with NcoI-SalI restriction enzymes (Figure S5-2). Then fragments containing promoter-OsAGPL2 cDNA-terminator (~4500 bp) sequences were cloned into the HindIII-BamHI sites of the pCAMBIA1303 binary vector (Figure S5-3).

For the *Agrobacterium* mediated transformation, AGPase constructs in the binary vector were transformed into the AGL1 strain of the *Agrobacterium tumefaciens*.

To investigate the physiological effect of mutant AGPases, seeds of EM541 mutant rice, which contains a null endosperm AGPase LS subunit, was used for the transformation. The idea is to complement mutant EM541 rice with wild-type or three mutant AGPase constructs (IV, QC and IVQC) and see their effect on growth, seed production and amount of the starch.

Rice transformation was started by culturing mature seeds of EM541 for the formation of embryogenic calli (Figure 5-10A-B). For each construct at least 40-50 seeds were required. Figure 5-10 shows representative progress of callus induction and rice transformation procedure.

Once healthy small embryogenic calli were obtained by incubating the plates in the dark, plates were transferred to continuous light condition to induce secondary calli formation (Figure 5-10C). Whole calli induction process requires at least one month. Once healthy secondary calli were obtained, *Agrobacterium* cultures were prepared by streaking AGL1 cells containing constructs and growing them for 3 days at 28^{o}C. Grown AGL1 cells were scraped from the plates and resuspended in the medium containing 10 mg/L of acetosyringone which is the key component for plant-pathogen recognition. Calli and agrobacterium suspension were incubated together for 3 min.

After removal of excess *Agrobacterium*, the suspension calli were placed on to solid medium containing 10mg/L acetosyringone (Figure 5-10D). After incubation on this medium, the calli were transferred to the selection medium containing 35 mg/L hygromycin for the selection of plasmid and 150 mg/L timentin for the inhibition of further *Agrobacterium* growth. Transformed and non-transformed calli can easily be distinguished from each other based on their color on the selection medium (Figure 5-10 E-F). While transformed ones stay yellow and show further growth, non-transformed ones become dark brown and do not grow to form secondary calli. Healthy resistant calli were subjected to three rounds of selection to obtain real transformants.

After selection calli were transferred to the regeneration medium to induce plant growth. Approximately one week later green embryoids appeared on the calli, which are the regeneration initiation sites of shoots and roots (Figure 5-11A). Regenerating calli were grown on the same media for another 12-15 days. Then, green embryoids were transferred to rooting medium, which is a basic Murashige and Skoog medium containing B5 vitamins and sucrose together with hygromycin and timentin antibiotics for selection and inhibiting possible *Agrobacterium* contamination, respectively. Within 2-3 weeks healthy shoot and root formation were observed. Once growing plantlets reached to a reasonable size, they were transferred to peat pellets prior transferring to bigger pots (Figure 5-11B).

5.3.6 PCR screen of transformants

Preliminary screening of putative transformants was performed by PCR amplification of the transgene. Leaf samples were collected from each plant and their genomic DNAs were isolated for PCR analysis. Gene specific primers, which give an expected band size around 900 bp due to the amplification of cDNA of OsAGPL2, were used for the PCR analysis. Results of the PCR screening were shown in Figure 5-12. Among 10 plants of putative transformants carrying LS^{WT} constructs, 8 plants gave positive result. 11 out of 13 plants with LS^{QC} construct, resulted in the amplification of expected 900 bp product. Similar analysis for putative transformants with LS^{IV} and LS^{IVQC} constructs

showed that 8 and 6 out of 10 plants carry the transgene, respectively. This PCR analysis was performed for a rapid and initial screening of putative transformants. Since EM541 plants lack protein product of OsAGPL2, western blot analysis of endosperm tissue carrying the transgene would provide more accurate analysis of transgenic plants which will be conducted in future as plants grow until grain filling stage.

5.3.7 Comparing tiller and leaf number of T0 plants

As potted T0 transgenic rice plants were growing in the growth chamber in 12-hour light, 12-hour dark condition, their growth was followed regularly. Even at the vegetative stage, plants harboring LS^{QC} and LS^{IVQC} transgenes showed a noticeable increase in tiller and leaf number relative to the plants with LS^{WT} construct. Therefore, tiller and leaf number per plant were counted for a quantitative comparison. 1-month-old plants, carrying LS^{QC} construct, have visibly more tiller and leaf number than the plants carrying LS^{WT} constructs. Plants carrying LS^{IV} and LS^{IVQC} constructs were planted approximately 10 days after plants carrying LS^{WT} and LS^{QC} constructs. Therefore, a direct comparison between plants carrying either LS^{IV} or LS^{IVQC} constructs and plants carrying LS^{WT} construct was not feasible. Just to have an insight, tiller and leaf numbers of LS^{IV} and LS^{IVQC} carrying plants were also counted and results were plotted (Figure 5-14). Plants having LS^{IVQC} construct had more leaf and tiller number compared to the plants carrying LS^{IV} constructs. Even EM541-LS^{IVQC} plants were 10-15 days younger than the plants carrying LS^{WT} construct, tiller and leaf numbers were higher in the plants carrying LS^{IVQC} mutant transgene. Since tiller number determines panicle number of the plant, it is regarded to be a key component of the grain yield [179]. Therefore, observing an increase in the tiller number of plants carrying mutant LSs with Q438C mutation, which also significantly increased glycogen synthesis levels in the bacterial complementation analysis, encourages us to expect an increase in the starch yield of the plants.

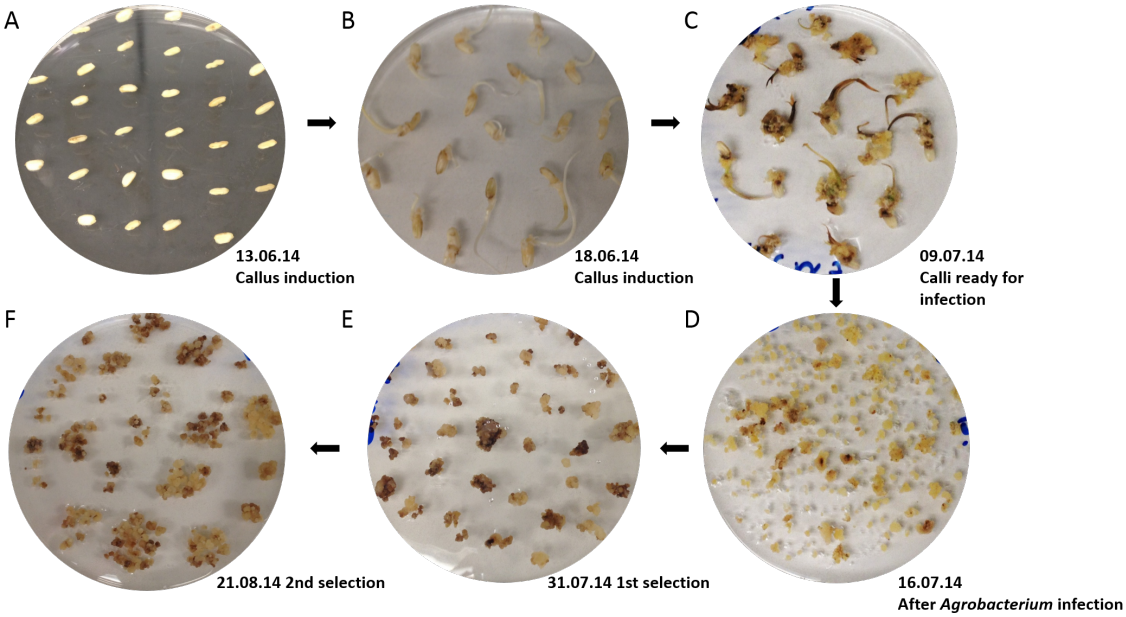

Figure 5 - 10 Representative images showing progress of callus induction and selection steps in EM541 seeds

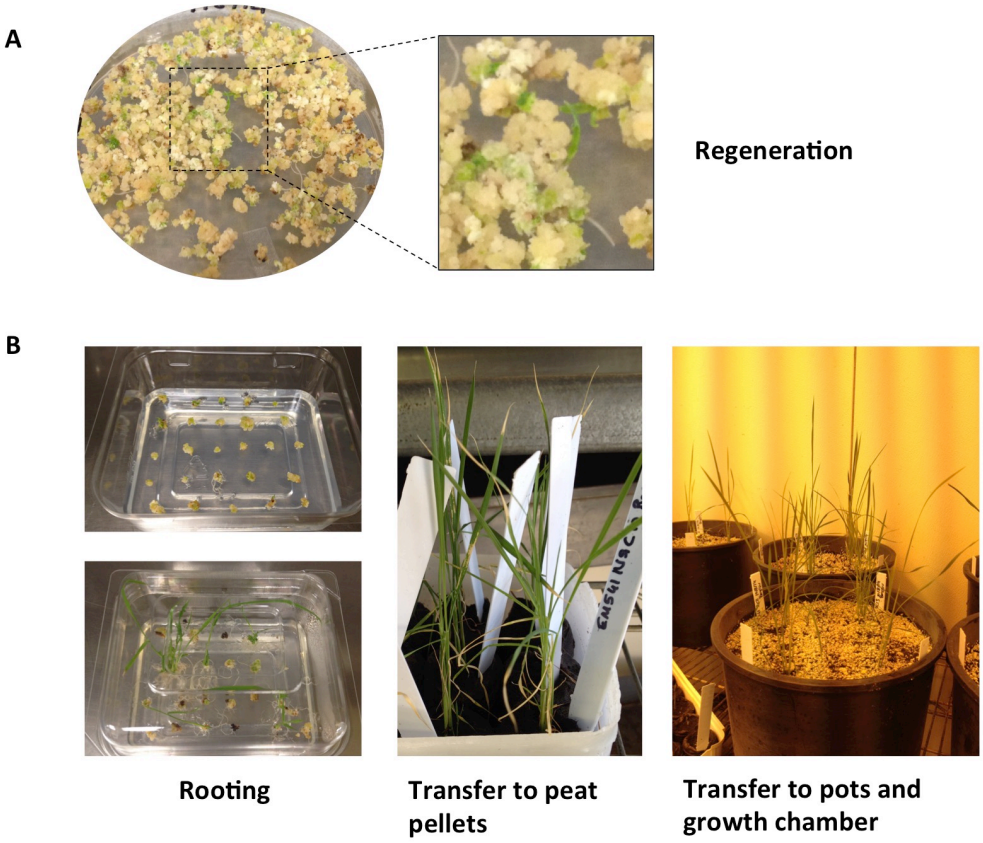

Figure 5 - 11 Representative images showing (A) regeneration (B) rooting and pot conditions of putative transgenic rice plants containing the mutant and wild-type AGPase constructs.

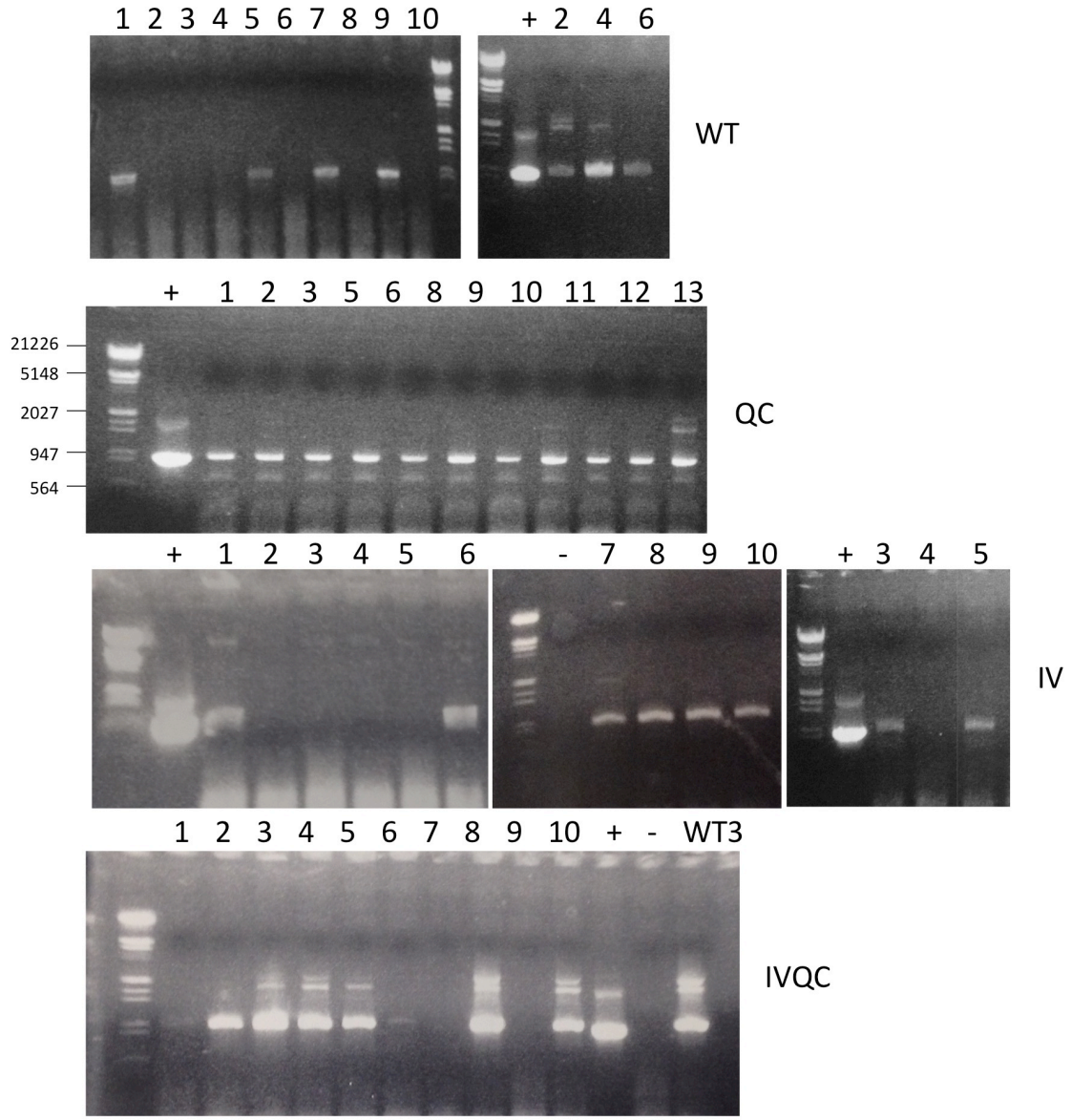

Figure 5 - 12 PCR results of EM541-LS^{WT}, EM541-LS^{QC}, EM541-LS^{IV}, EM541-LS^{IVQC} T0 plants to verify the presence of the wild-type/mutant OsAGPL2 transgene. Lanes with the numbers specify the plant used. Lanes labeled with "+" are the positive control for PCR in which pCAMBIA1303 vector containing gene of interest was used as template DNA. Lanes labeled with "-" are the negative control for PCR in which genomic DNA extracts of wild-type taichung rice plants. On the each gel Lambda DNA/EcoR+HindIII marker was used.

Figure 5 - 13 A) Phenotypes of 30 days old EM541 plants carrying LS^{WT} and LS^{QC} constructs. B) Phenotypes of 20 days old EM541 plants carrying LS^{IV} and LS^{IVQC} constructs

(a) same pots were used

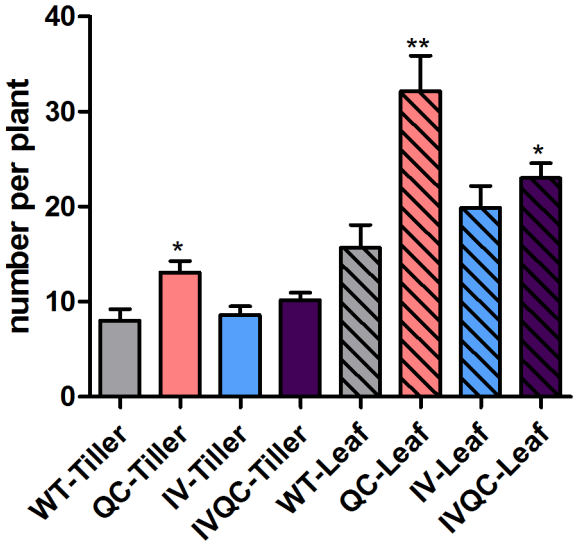

Figure 5 - 14 Graph showing tiller and leaf number of plants carrying LS^{WT} (n=10), LS^{QC} (n=12), LS^{IV} (n=10) and LS^{IVQC} transgenes; students t-test was perfomed to see any significant difference. Tiller numbers were compared to the WT-Tiller results and Leaf numbers were compared to the WT-Leaf results ** p<0.01, * p<0.05

5.4 Discussion and future prospects

The relation between the productivity of source and sink tissues of plants determines the crop yield. Since approximately 80% of rice endosperm is composed of starch, carbon flux leading to starch production has a big impact on sink strength in rice endosperm. AGPase catalyzes a key regulatory step in starch biosynthesis in developing rice seeds and hence modulation of the structure-function relationship of AGPase can be a feasible way to increase sink strength.

We have shown thatmutations, Ile90 to Val or Tyr378 to Cys, in the LS of the potato AGPase lead to more stable heterotetrameric AGPase [172]. Next, we decided to study the effects of these mutant AGPase variants in vivo by transferring them to rice plant.

To this end, mutations were introduced into the corresponding residues in the LS of rice endosperm by site directed mutagenesis. To assess the effects of mutations in rice endosperm AGPase on glycogen production in *E.coli*, iodine-staining assay was perfomed. Results indicated that cells carrying the LS^{Q438C} mutant plasmid along with the wild-type SS plasmid had elevated levels of glycogen production compared to cells carrying both of the wild-type LS and SS plasmids. This indicates that the Q438C mutation on the rice endosperm LS seems indeed advantageous for the functioning of enzyme. The LS^{I150V} mutation also increased glycogen synthesis compared to the wild-type AGPase although it's effect was not as high as the LS^{Q438C} mutation. Besides, kinetic and allosteric characterization showed no significant difference between the wild-type and the mutant AGPases. Observing significantly higher glycogen production despite seeing no change in the kinetic and allosteric properties of the enzyme indicates that I150V and Q438C mutations probably provide prolonged stability for the enzyme. Since rice AGPase is much more weaker than potato AGPase, in terms of structural stability and subunit-subunit interaction, it can be speculated that prolonged stability leads to the high levels of glycogen in the bacterial complementation assay in the presence of mutant AGPases.

Observing a significantly enhanced phenotype in bacterial complementation assay encouraged us to transfer those mutants and see the physiological effects of them in rice

plant. To this end, plant expression vectors, which contain native promoter and terminator sequences of OsAGPL2, were prepared and transferred to the EM541 mutant rice via *Agrobacterium tumefaciens*. The EM541 mutant rice [178] contains a null mutation leading to early stop codon in OsAGPL2 translation. The idea was to complement the mutant EM541 rice with the wild-type or three mutant AGPase constructs (LS^{IV}, LS^{QC} and LS^{IVQC}) and see their effect on starch production during seed development.

Transgenic T0 plants, carrying LS^{WT}, LS^{QC}, LS^{IV} and $LS^{IV,QC}$ constructs under the control of OsAGPL2 promoter, were obtained successfully at the end of two rounds of selection with appropriate antibiotics. At least 10 T0 plants for each construct were transferred to bigger pots for further growth and seed collection. As plants growing in controlled growth chambers in 12 h day-12 h night condition, a notable phenotypic difference was observed between plants carrying LS^{WT} and LS^{QC}, LS^{IVQC} constructs. Plants expressing LS^{QC} and LS^{IVQC} constructs seem to have more tiller and leaf number per plant compared to the plants expressing LS^{WT} (Figures 4-13 and 14). Since tiller number determines panicle number of the plant, it is regarded to be a key component of the grain yield [179]. Therefore, observing an increase in the tiller number of plants carrying mutant LSs with Q438C mutation, which also significantly increased glycogen synthesis levels in the bacterial complementation analysis, encourages us to expect an increase in the starch yield of the plants.

Most of the previous studies, which were mentioned in the introduction part, have focused on using AGPase variants with altered allosteric properties to improve crop yield in cereals such as maize and rice. Most of these studies obtained moderate increases in seed number and plant biomass [93]. Hannah et al obtained one of the most significant increases in seed number using a heat stable variant of AGPase together with decreased P_i sensitivity in maize. This transgenic maize plant resulted in 64% increase in the number of seeds [107]. In that study, the increase in seed number was related to the expression of the transgene not only in the endosperm but also in maternal tissues. Therefore expression of AGPase subunits, which are mainly thought as endosperm

specific, may also be expressed in maternal/vegetative tissues. Our complementation study in which we used OsAGPL2 null EM541 mutant rice for *Agrobacterium* mediated transformation of the wild-type and the mutant OsAGPL2 constructs under the control of its native promoter will also provide to see tissue specific expression patterns of OsAGPL2 subunit and its role in that tissues. Using native promoter and terminator sequences of OsAGPL2, the expression of transgenes in natural locations within the plant is provided. The transcriptome data from Rice Genome Annotation Project (ref) suggests that OsAGPL2 is not only expressed in rice endosperm but also in leaves, roots and pollens. An unpublished data of Okita laboratory indicates that the most prominent GUS expression, under the control of L2 promoter, is seen in endosperm. L2 promoter also seems to induce GUS expression in somatic tissues such as leaves, stems and roots and reproductive tissues such as anthers and pollen grains. Although experimental evidence coming from OsAGPL2 lacking plants [178] indicates that OsAGPL2 subunuit is the dominant isoform in rice endosperm, expression studies imply that it may also involve in the vegetative and reproductive parts of rice plant. Expression of OsAGPL2 not only in endosperm but also in somatic tissues, as indicated above, supports our preliminary data where we observed increased tiller and leaf number in plants carrying LS transgene with the Q438C mutation. Most probably prolonged stability of the AGPase resulted in increased AGPase activity in vegetative tissues of the plant. In other words, according to our preliminary data increased AGPase stability/activity can lead to better utilization of photosynthesis products for starch synthesis, which may stimulate setting of additional tillers and leaves, as transitory starch is used for the growth and development of plants [24].

In future, seeds collected from T0 plants will be used for the generation and growth of homozygous stable T2 or T3 lines of the transgenic plants which were complemented with LS^{WT}, LS^{QC}, LS^{IV} and $LS^{IV,QC}$ constructs. More detailed physiological analysis including seed number/weight determination and enzymatic analysis of the AGPase enzyme from rice endosperm will be performed to gain insight about the effect of those mutant AGPases.

CHAPTER 6

CONCLUSION

Starch is the primary energy reserve of plants. This carbohydrate is one of the major components of human and livestock diet and also has various important industrial applications. This is why, understanding starch biosynthesis in plants would open new ways to improve crop yield of plants. AGPase enzyme plays a pivotal role in the starch biosynthesis as it catalyzes the rate limiting step. Therefore, the structure-function relationship of plant AGPases including lentil, potato and rice was studied to gain further insight to improve the functioning of AGPase in this dissertation.

This PhD dissertation encompasses the role of AGPase in starch synthesis in two main topics. First one sought to answer this question: does day-length affect the transcription level of AGPase isoforms in a long-day plant lentil? The study which is described in Chapter 2 was conducted to answer this question. The results showed that shortened light cycle affected the transcription of the AGPase isoforms and, in turn, the starch biosynthesis. For this purpose, cDNA clones of two LS isoforms and two SS isoforms were isolated from plants grown under long-day and short-day conditions and their RNA expression level was determined with quantitative real time PCR. In addition, kinetic and allosteric properties of the native lentil AGPase were determined for the first time.

Second topic addresses ways to improve potato and rice AGPases based on the structure-function relationship properties of the enzyme. Chapter 3 describes how heterotetrameric assembly of potato AGPase was enhanced using the reverse genetics approach. Using this approach, the LS^{R88A} mutant, which contributes to the longitudinal interaction, was subjected to error-prone PCR to generate second-site mutations. Biochemical characterization showed a significant increase in heterotetramer formation of LS^{I90V} and LS^{Y378C} mutant LSs through interacting with the wild-type SS due to both enhanced monomer-monomer and dimer-dimer interaction. Another mutation on the

LS, D410G, increased heterotetramer formation moderately together with a change in the allosteric properties of enzyme. To elucidate the exact role of these residues in subunit-subunit interactions the crystal structure of the heterotetrameric plant AGPase is essential. Besides, here we clearly demonstrated the importance of subunit interactions for proper functioning and stability of the enzyme.

In chapter 4 of this dissertation, considering the weak stability of rice AGPase and economical/agricultural importance of rice plants, we aimed to investigate the effect of the mutations which enhanced the heterotetrameric assembly of potato AGPase, in the rice enzyme. Therefore, I150V and Q438C mutations were introduced into the LS of rice endosperm AGPase, OsAGPL2. According to iodine staining experiment cells expressing AGPase with LS^{QC} and $LS^{IV,QC}$ mutants exhibited much darker staining than those expressing the wild-type AGPase. The kinetic characterization results showed that darker staining phenotype did not stem from any kinetic or allosteric changes. To further understand the effect of these mutations at physiological level in rice plant, we transferred the wild-type and the mutant LSs into OsAGPL2 null mutant EM541 rice under the control of its native promoter. As a result transgenic plants were successfully obtained. Our preliminary data suggested that plants carrying LS^{QC} and LS^{IVQC} transgenes had more tiller and leaf number, which may indicate a potential crop yield increase. The effect of these mutations should be investigated in the stable homozygous transgenic plants in future.

There have been significant efforts to improve crop yield of plants by modulating the activity of key enzymes involved in carbohydrate metabolism. AGPase is one of the target enzymes with its critical role in starch biosynthesis. In this regard, this dissertation contributes to understanding and functioning of plant AGPases in different ways. In Chapter 2 it was shown that lentil AGPase responds to the daytime length change with a change in transcriptional levels of different isoforms of the enzyme. Moreover, in Chapter 3 and 4, it was revealed that changes in the subunit interface residues are critical for the subunit-subunit interaction and functioning of both potato and rice AGPases.

VITA

Ayşe Bengisu Seferoğlu was born in Isparta, Turkey, on July 8, 1986. She received her B.Sc. Degree in Molecular Biology and Genetics from Istanbul Technical University, Istanbul, Turkey, in 2009. Later she joined the MSc. program in Chemical and Biological Engineering at Koç University with full scholarship from TUBITAK-2210 where she studied "Identification of important residues for modulation of allosteric properties of potato ADP glucose pyrophosphorylase" under the supervision of Assoc. Prof. Dr. I. Halil Kavaklı. After she received her MSc. Degree in 2011, she continued with the same group as a Ph.D. candidate in Chemical and Biological Engineering at Koç University with full scholarship from TUBITAK-2211. She conducted a part of her research in Institute of Biological Chemisrty in Washington State University with TUBITAK 2214A scholarship. During her PhD she worked on structure function relationship of plant ADP glucose pyrophosphorylases. She also worked as a teaching assistant during her MSc and PhD years.

Appendix 1

Supplementary Data – Chapter 3

Table S3 - 1 Primers that have been used for the isolation lentil AGPase isoforms and used for the quantitative RT-PCR

LS and SS PCR Primers	Nucleotide Sequence
LS ORF F1	5'-ATGGCTTCTNNTTNTGTRANCTTG-3'
LS ORF R2	5'-TTANATNACNGTNCCNTCRTCNATNGTNGCRTT-3'
SS ORF F1	5'-ATGGCYTCAATGGCNGCGATCGGTG-3'
SS ORF R2	5'-TTANATNACNGTNCCNCTNGGYATNAANGCNTCRTT-3'
LS Deg F1	5'-GCXAXRCCTGCBGTKCCNRT-3'
LS Deg R3	5'-CCDATRTCYTCCCARTARTC-3'
SS Deg F2	5'-GRGCGAARCCWGCWGTKCC-3'
SS Deg R2	5'-GCAGCYTCYTGVACRTTRTC-3'
LS 5'RACE	5'CTGTCAATGTGTCTCTGCACAAGATCCATG-3'
LS 3' RACE	5'-CAAACATTGATAATGTGATAATCTTGGC-3'
SS 5'RACE	5'-GCTTGTATAAATCTCTCATAATCCATTCGATAC-3'
SS 3'RACE	5'-GAAGCACGTGCCACTGCATTCGGTCTGATG-3'
Real Time PCR Primers	
L1-RT-F	5'-GGTTTGTGGAGGTTCTGGCGGCG-3'
L1-RT-R	5'-ATGCACGGTTGCCACCGACAGCA-3'
L2-RT-F	5'-GATACCTAGAGTTTCTTGCGGCT-3'
L2-RT-R	5'-ATGCGCGGCTGTCACCAACAGCG-3'
S1-RT-F	5'-GTGAAGTTATTCCTGGTGCGACCGA-3'
S1-RT-R	5'-ATCGCAGTCCAACAACAGAATGGTG-3'
S2-RT-F	5'-GTGAAGTGATTCCTGGTGCTACTTC-3'
S2-RT-R	5'-ATCGCAGCCCGACCACAGAATGGAA-3'
GAPDH-F	5'-ACCACCAACTGCCTTGCCTTGCHCCACTTGCN-3'
GAPDH-R	5'-TTGCCRACAGCCTTWGCAGCTCCN-3'

Table S3 - 2 Comparison of mature lentil ADPG-PPase sequences to other mature ADPG-PPase sequences.

	SS1	**SS2**	**LS1**	**LS2**
	% identity	**% identity**	**% identity**	**% identity**
	aa	**aa**	**aa**	**aa**
Small Subunit				
Pisum sativum Psagps1	97,3	94,4	46	51
Pisum sativum Psagps2	89	98	46	50
Vicia faba VfAgPC	88,2	98	46	51
Vicia faba VfAgPP	96,3	94,4	45	51
Cicer arietinum Cagps1	93,8	96	46	50
Cicer arietinum Cagps2	87,8	94,4	46	51
Phaseolus vulgaris Pvagps1	88,5	93,3	45	50
Solanum tuberosum	86,1	92,7	45	51
Solanum lycopersicum	85,7	92,2	45	47
Hordeum vulgare	82,4	90,9	46	53
Large Subunit				
Pisum sativum Psagpl1	48	53	94,7	70
Cicer arietinum Cagpl1	51	57	60,4	58
Cicer arietinum Cagpl2	49	55	64,6	60
Phaseolus vulgaris Pvagpl1	45	52	79,8	69
Solanum tuberosum	46	53	76	65
Solanum lycopersicum	50	52	71	59
Hordeum vulgare	41	47	67,7	55

A

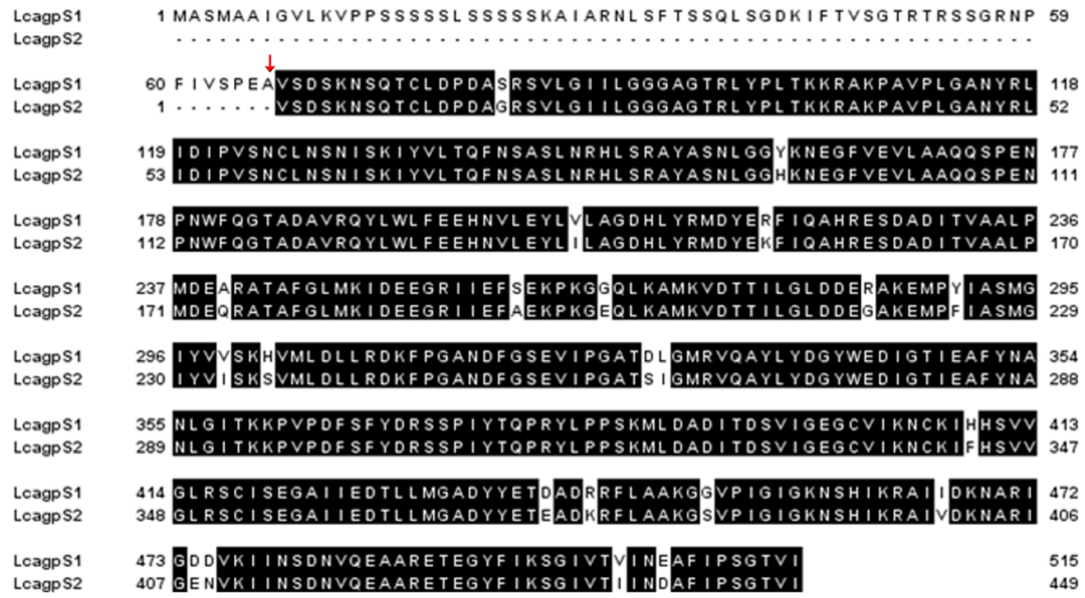

B

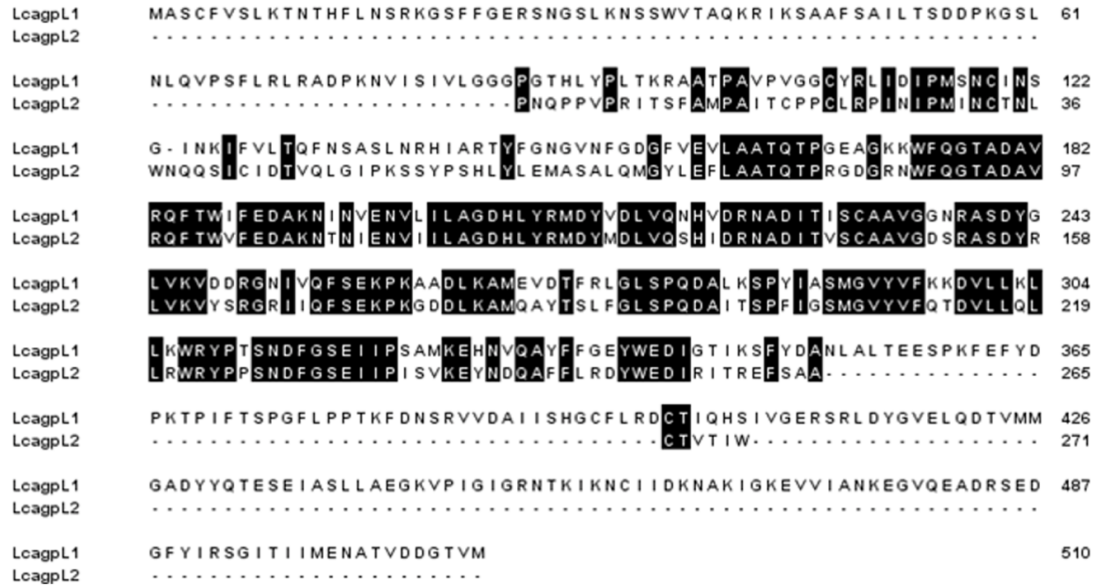

C

```
SagpL       ISV-TADNASETKVREIGQ--EK
PagpL       ASVITT-ENDTQTVFVDMPRLER
TagpL3      ASVITT-ENDTETVFVDMPRLER
LcagpL1     AAILTS-DDPKGSLNLQVPSFLR
CagpL2      ASVLTSGINDFEESMTFHEGPYF
```

Figure S3 - 1 Comparison of the deduced amino acid sequences of cDNA clones encoding lentil (A) SS. Arrow indicates the beginning of the mature amino acid sequences when compared with spinach mature SS mature sequence. (B) Large subunits. (C) Comparison of the derived N-terminal sequences of LS1, tomato LS, potato LS, and spinach mature LS amino acids of AGPases. Blue color indicates fully conserved residues, green shows conservation of strong groups, and indigo blue indicates weak conservation.

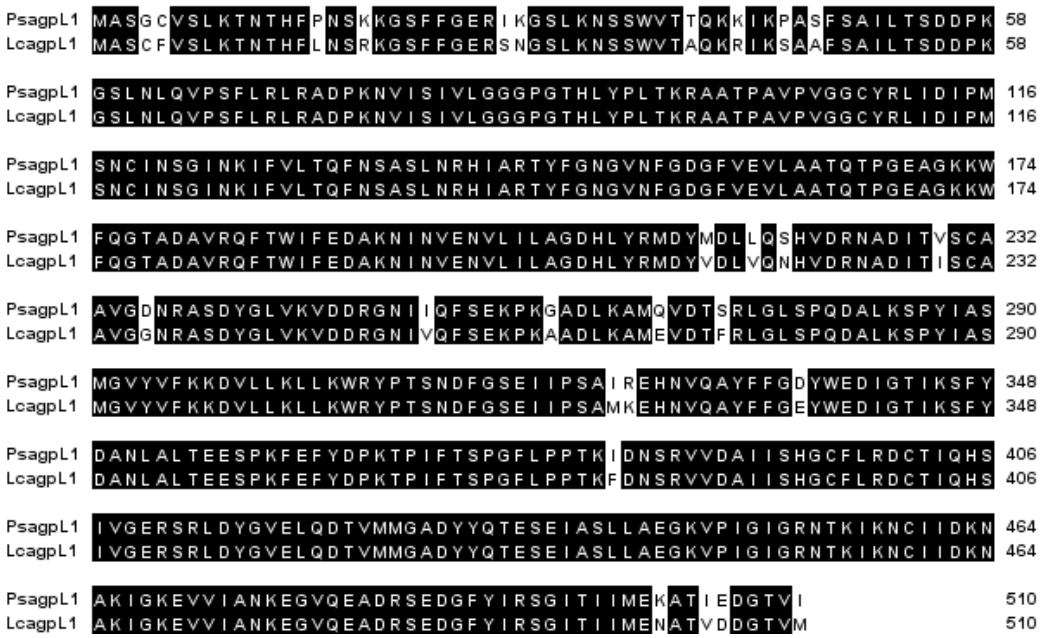

Figure S3 - 2 Comparison of the deduced amino acid sequences of both LS1 and pea agpL1.

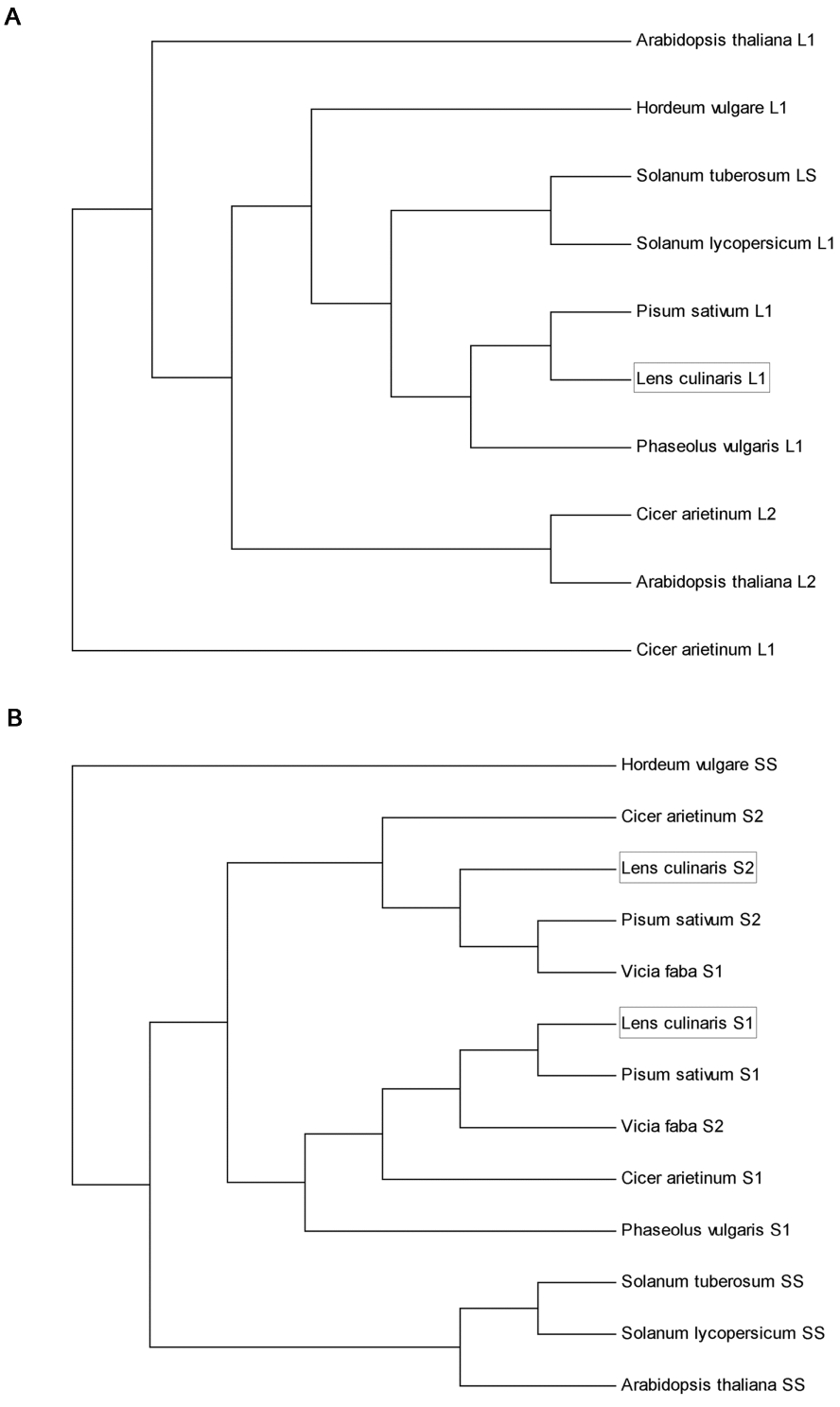
A
Arabidopsis thaliana L1
Hordeum vulgare L1
Solanum tuberosum LS
Solanum lycopersicum L1
Pisum sativum L1
Lens culinaris L1
Phaseolus vulgaris L1
Cicer arietinum L2
Arabidopsis thaliana L2
Cicer arietinum L1
B
Hordeum vulgare SS
Cicer arietinum S2
Lens culinaris S2
Pisum sativum S2
Vicia faba S1
Lens culinaris S1
Pisum sativum S1
Vicia faba S2
Cicer arietinum S1
Phaseolus vulgaris S1
Solanum tuberosum SS
Solanum lycopersicum SS
Arabidopsis thaliana SS

Figure S3 - 3 A dendogram for AGPase (A) large and (B) SS proteins from diverse sources was generated by Biology WorkBench software program. Sequence data are from the following sources with the accession numbers, *Pisum sativum* [151], Psagps1 (CAA65539.1) , Psagps2 (CAA65540.1), Psagpl1 (CAA65541.1), *Vicia faba* [152], VFAgPC (P52417.1), VfAgPP (P52416.1), *Cicer arietinum* [132], Cagps1 (AAK27720.1), Cagps2 (AAK27721.2), Cagpl1 (AAK27718.1), Cagpl2 (AAK27719.1), *Phaseolus vulgaris*, Pvagps1(BAC66693.1), Pvagpl1 (BAC66692.1), *Solanum tuberosum* [114], SS(P23509.2), LS(Q00081.1), *Solanum lycopersicum* SS (NP_001234696.1, [69]), LS (AAC49941.1, [133]), *Hordeum vulgare*, SS (ABX72229.1), LS (P30524.2, [153]), *Lens culinaris* LS1(ACW82825.1), SS1(ACX48912.1), SS2 (ADI99791.1).

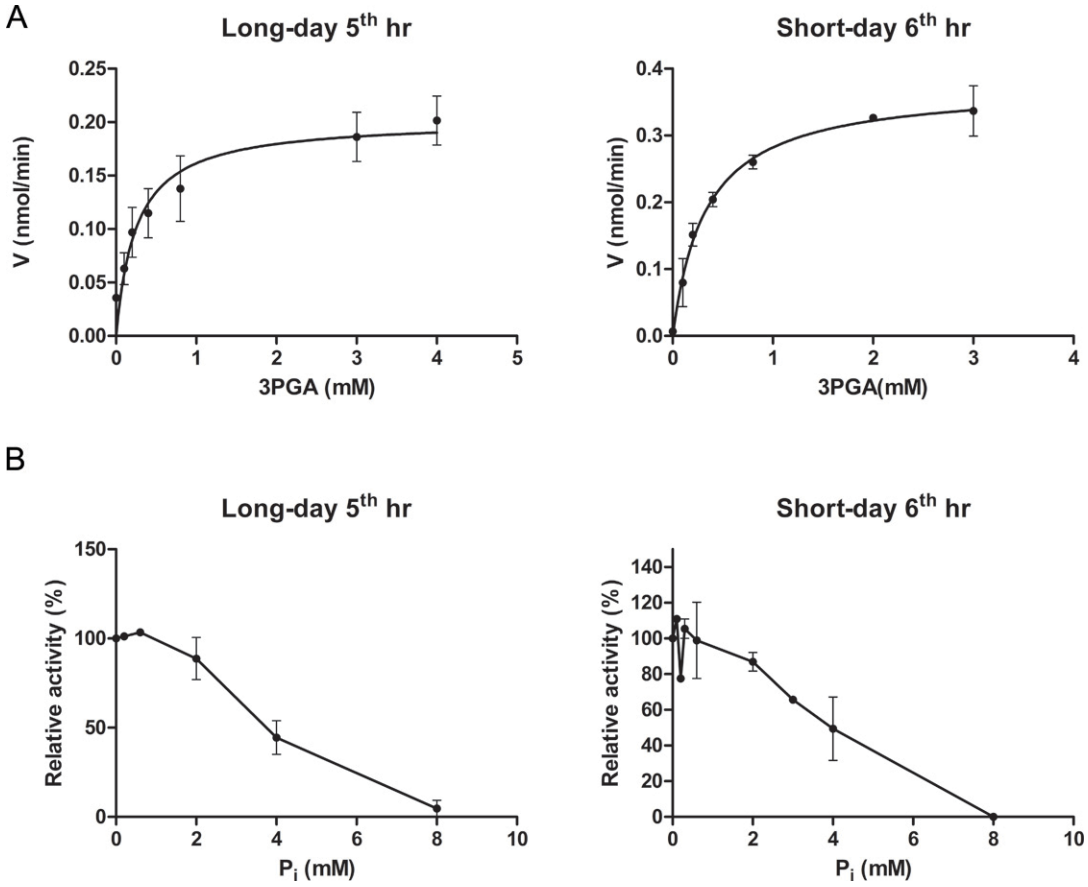

Figure S3 - 4 (A) 3-PGA activation graphs of long-day and short-day lentils, (B) Phosphate inhibition graphs of indicated long-day and short-day lentils under 5 mM 3-PGA concentration. Long-day samples and short-day samples were taken at 5 hours and 6 hours after illumination, respectively.

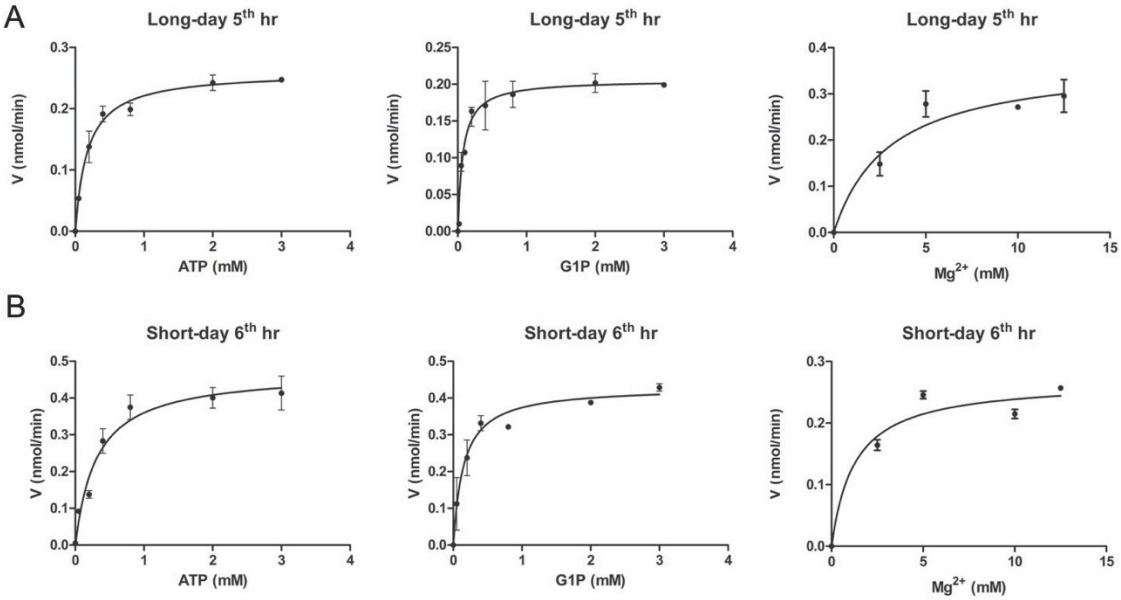

Figure S3 - 5 (A) Velocity vs substrate/cofactor concentration graphs for long-day grown lentil and (B) Velocity vs substrate/cofactor concentration graphs for short day grown lentil for K_m calculations. Long-day samples and short-day samples were taken at 5 hours and 6 hours after illumination, respectively.

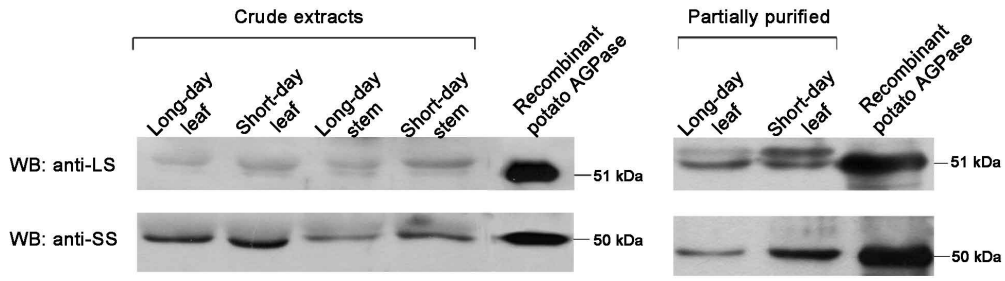

Figure S3 - 6 Western blot analysis of crude extracts from leaf and stem and partially purified samples of long-day and short day lentil. Samples for long-day and short-day exposed plants were taken at 5th hour and 6th hour of day time, respectively. For detection potato AGPase large and small subunit specific antibodies were used. Upper panel and lower panel show blots detected with anti-LS and anti-SS antibodies, respectively. For crude extratcs 5 µg protein, for partially purified samples 1 µg protein loaded to the each lane.

Supplementary Data – Chapter 4

Table S4 - 1 Primer sequences used in this study for cloning and site-directed mutagenesis

Cloning primers	LSDS1	F 5'ACGTGCATCTTATCCATGGTGATCACTACTGAAAATGAC3'
	LSDS2	R 5'GAGGGCGCATAAGCTTTCATATGACTGTTCCATCTCTAATTG3'
	A88R	F 5'CTGCTCCCCTGAATCGTCACATTGCTCGAAC3'
		R 5'GTTCGAGCAATGTGACGATTCAGGGGAGCAG3'
	I90V	F 5' CTCCCCTGAATCGTCACGTTGCTCGAACATATTTTG 3'
		R 5' CAAAATATGTTCGAGCAACGTGACGATTCAGGGGAG 3'
SDM primers	Y378C	F 5' GATGGGAGCAGACTGCTACCAAACAGAATC 3'
		R 5' GATTCTGTTTGGTAGCAGTCTGCTCCCATC 3'
	Y378H	F 5' CATGATGGGAGCAGACCACTACCAAACAGAATC 3'
		R 5' GATTCTGTTTGGTAGTGGTCTGCTCCCATCATG 3'
	A91T	F 5' CCTGAATCGTCACATTACTCGGACATATTTTGG 3'
		R 5' CCAAAATATGTCCGAGTAATGTGACGATTCAGG 3'
	F101L	F 5' GCAATGGTGTGAGCCTTGGAGATGGATTTG 3'
		R 5' CAAATCCATCTCCAAGGCTCACACCATTGC 3'

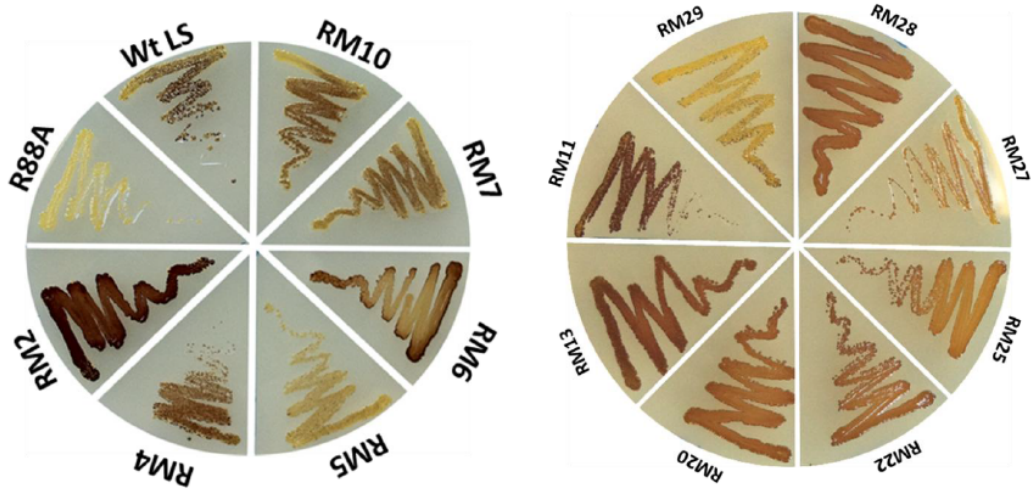

Figure S4 - 1 Bacterial complementation assay using various mutants of the LS and the wild-type SS. Iodine staining comparison for the primary screening of the obtained random mutants without R88A mutation. Wild-type and mutant LSs were co-expressed with the wild-type SS in *E.coli* glgC$^-$ lacking endogenous AGPase activity. The plate was streaked from a single colony of each strain onto a Kornberg's 2% glucose enriched plate and incubated overnight at 37^{0}C [168]

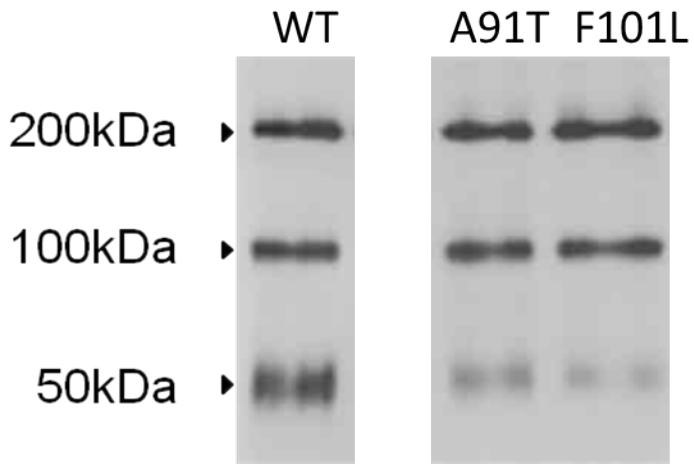

Figure S4 - 2 Native-PAGE and western blot analysis of crude extract samples of the wild-type LS and LS^{A91T} and LS^{F101L} mutants co-expressed with the wild-type SS were loaded in equal amount (1 µg of total protein). 3 to 13 % native gradient gel was used in order to separate monomeric and oligomeric forms of AGPase followed by western blot using anti-LS antibody.

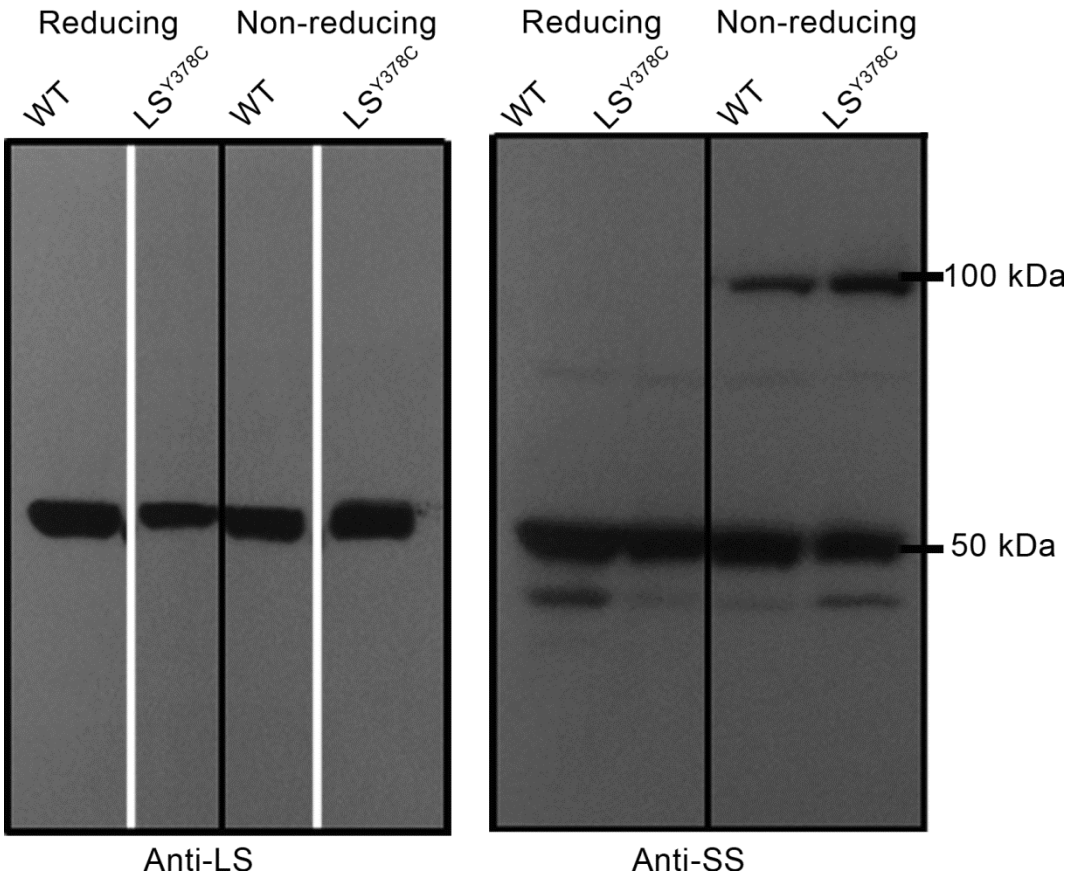

Figure S4 - 3 Comparison of reducing and non-reducing SDS-PAGE western blot analysis of the wild-type and Y378C mutant. A non-reducing 10% SDS-PAGE gel followed by western blot with potato specific anti-LS and anti-SS antibodies was performed to investigate the formation of the disulfide bridge. Only anti-SS probed blot showed dimers in both the wild-type and LS^{Y378C} AGPase. Anti-LS probed blot showed only monomers in both reducing and non-reducing conditions indicating the absence of the disulfide bonds.

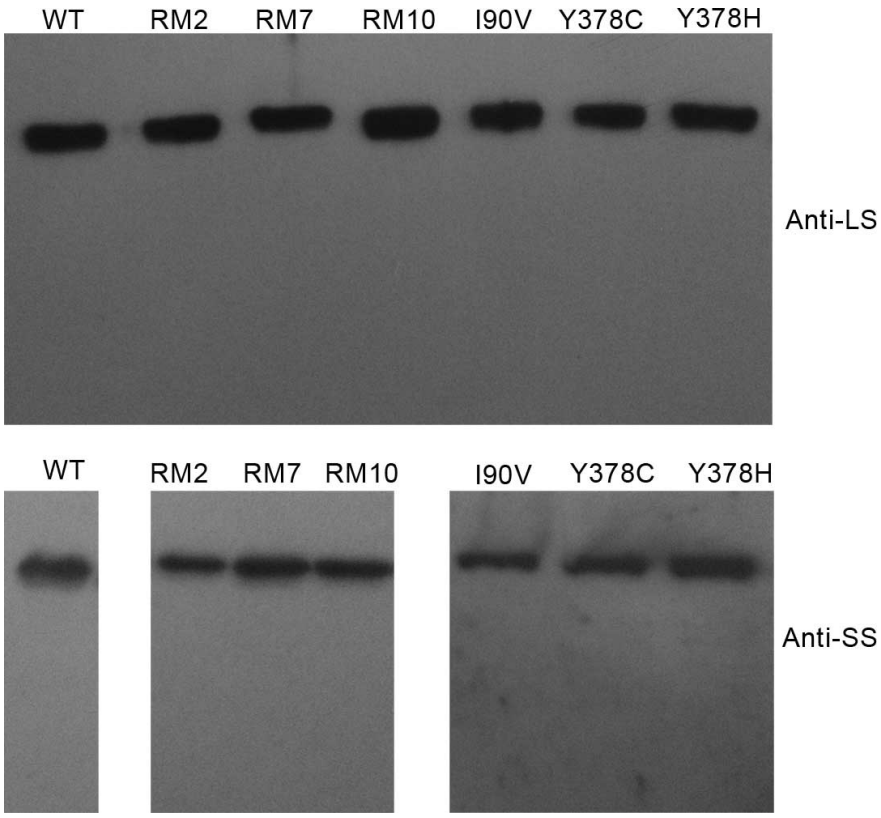

Figure S4 - 4 Western blot of partially purified wild-type and mutant AGPases. After partial purification, samples subjected to SDS–PAGE followed by western blot analysis with anti-LS and anti-SS antibodies showed no apparent degradation of AGPase.

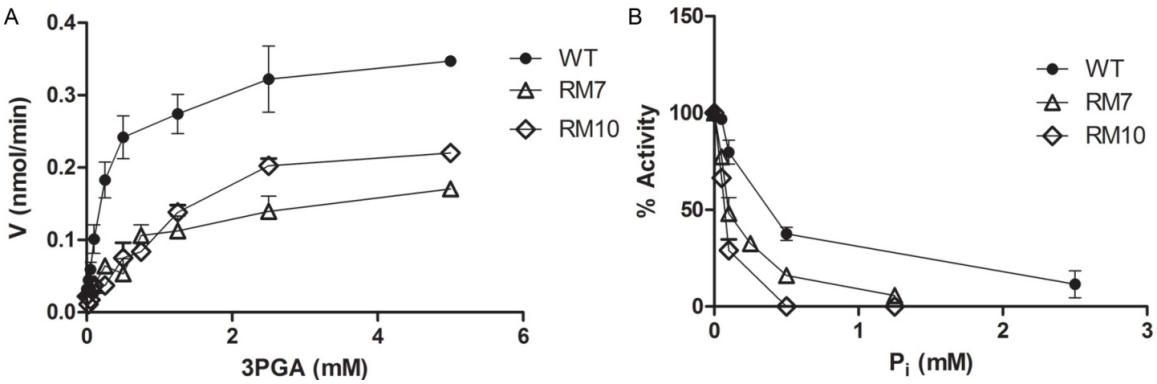

Figure S4 - 5 3PGA activation and P_i inhibition profiles of the wild-type AGPase(●), RM7(Δ) and RM10(◊) mutants. (A) Reactions were performed in the forward direction under saturating substrate conditions and with varying amounts of 3-PGA. (B) Reactions were performed in the forward direction under saturating substrate conditions and with 1 mM 3PGA.

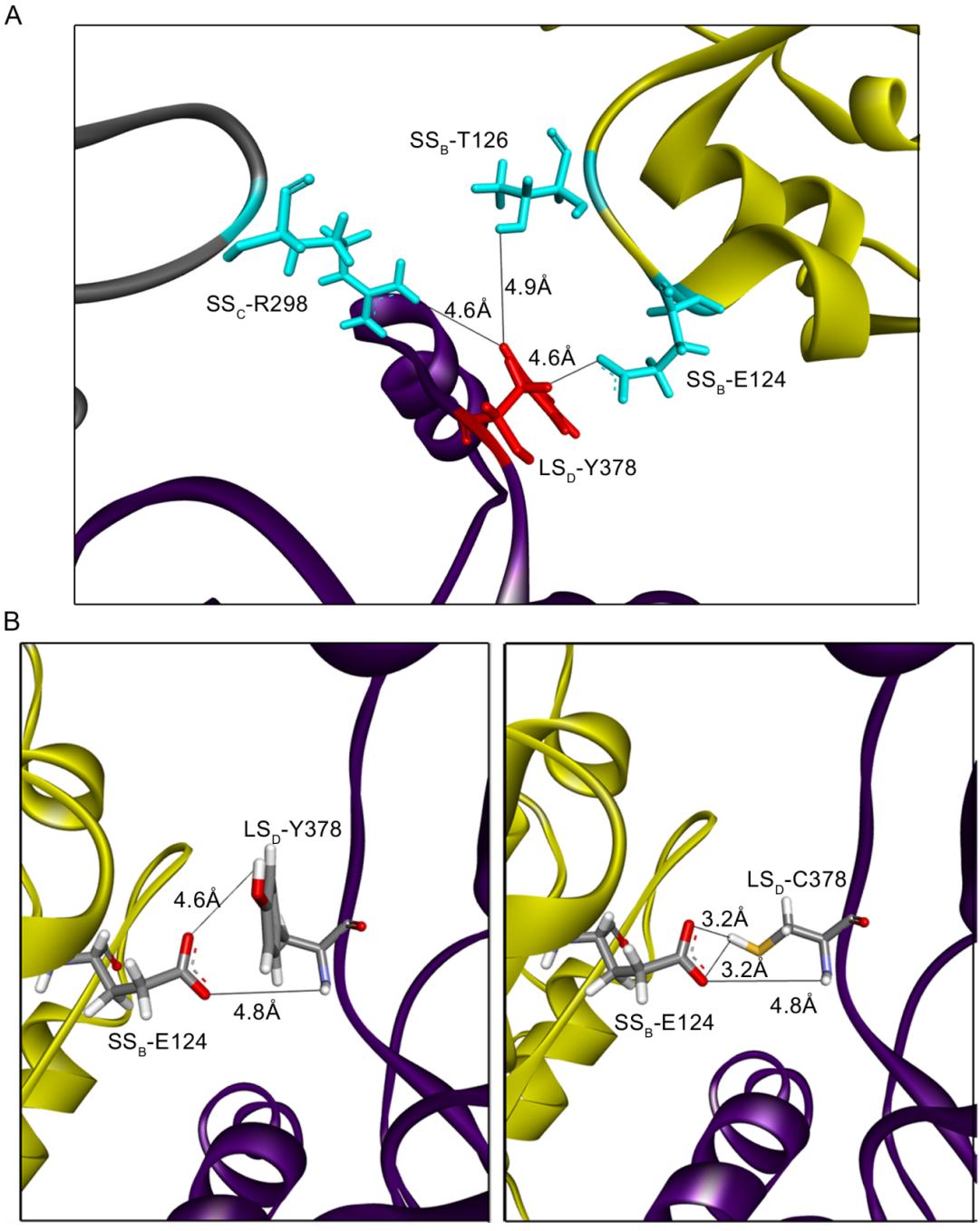

Figure S4 - 6 (A) Location of the LS^{Y378} residue in the heterotetrameric model (Tuncel et al. 2008) and its approximate distance to the SS$_C$-R298, SS$_B$T126 and SS$_B$-E124 residues (B) Comparison of distances between LS^{Y378} and LS^{C378} residues with E124 residue of the SS in the model, respectively.

Supplementray Data – Chapter 5

Table S5 - 1 List of primers used in site directed mutagenesis of rice LS

Primer	Sequence (5'→3')
OsAGPL2 I150V-F	CTTCTCTTAATCGCCATGTCCATCATACATACCTTG
OsAGPL2 I150V-R	CAAGGTATGTATGATGGACATGGCGATTAAGAGAAG
OsAGPL2 Q438C-F	CATGATGATGGGTGCAGATTGCTATGAAACTGAAGAAG
OsAGPL2 Q438C-R	CTTCTTCAGTTTCATAGCAATCTGCACCCATCATCATG

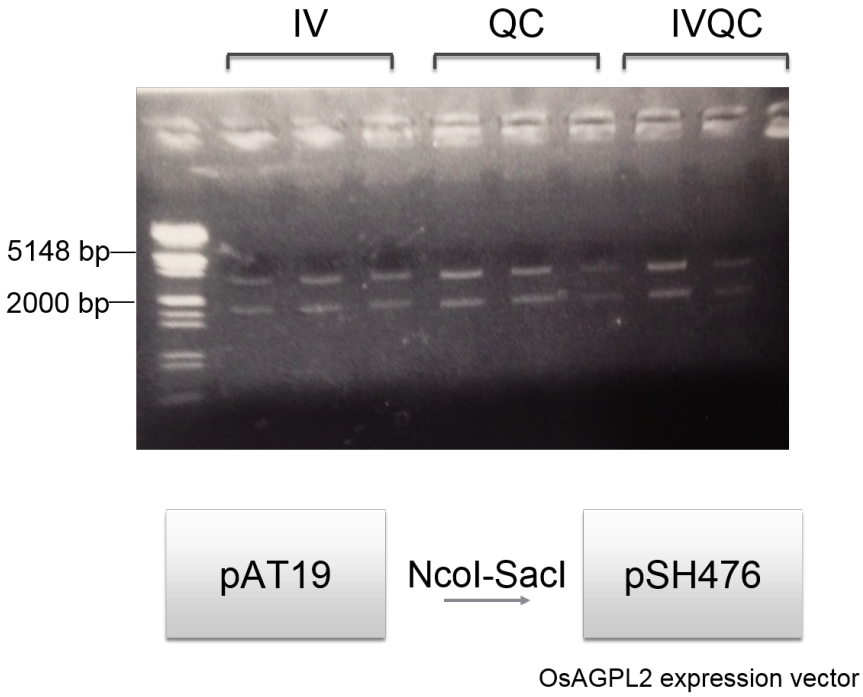

Figure S5 - 1 Sub-cloning of mutated cDNAs on pAT19 plasmid (pUC58 vector having OsAGPL2 cDNA) onto expression vector of OsAGPL2, pSH476, a modified form of pQE30 (Qiagen) containing an N-terminal 6X-His tag. Selected colonies after cloning were digested with NcoI and SacI enzyme to verify presence of the 1560 bp inserts.

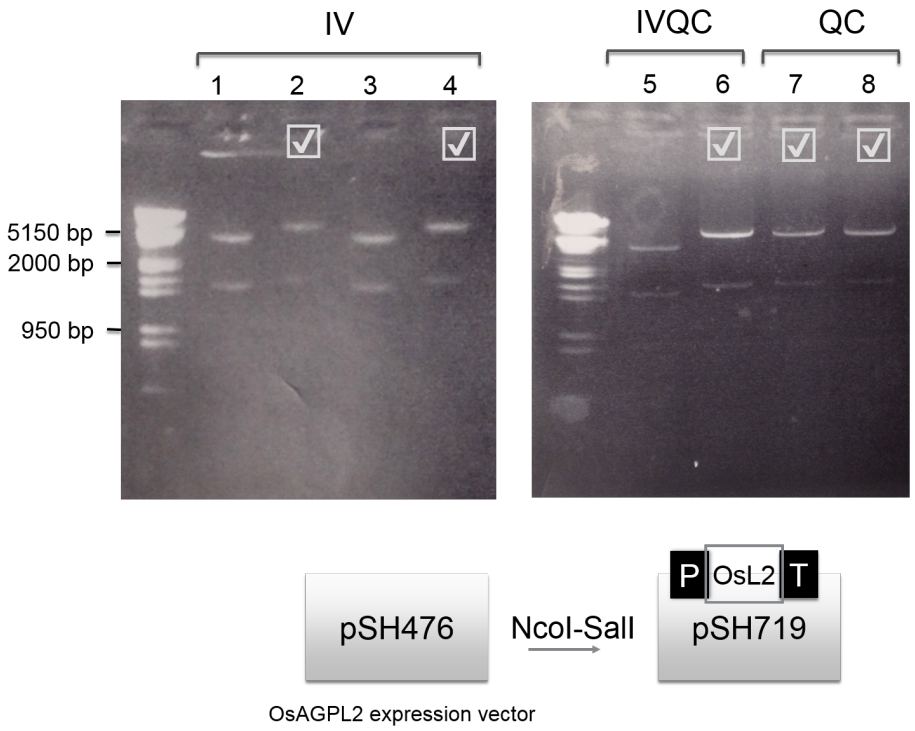

Figure S5 - 2 Sub-cloning of mutant OsAGPL2 cDNAs onto pSH719 vector which contains promoter and terminator sequences of OsAGPL2. After cloning selected colonies were digested with NcoI-SalI enzymes to confirm presence of the 1560 bp inserts. Lane 2, and 4 for show positive constructs for IV, Lane 6 shows positive construct for IVQC and Lane 7-8 show positive constructs for QC

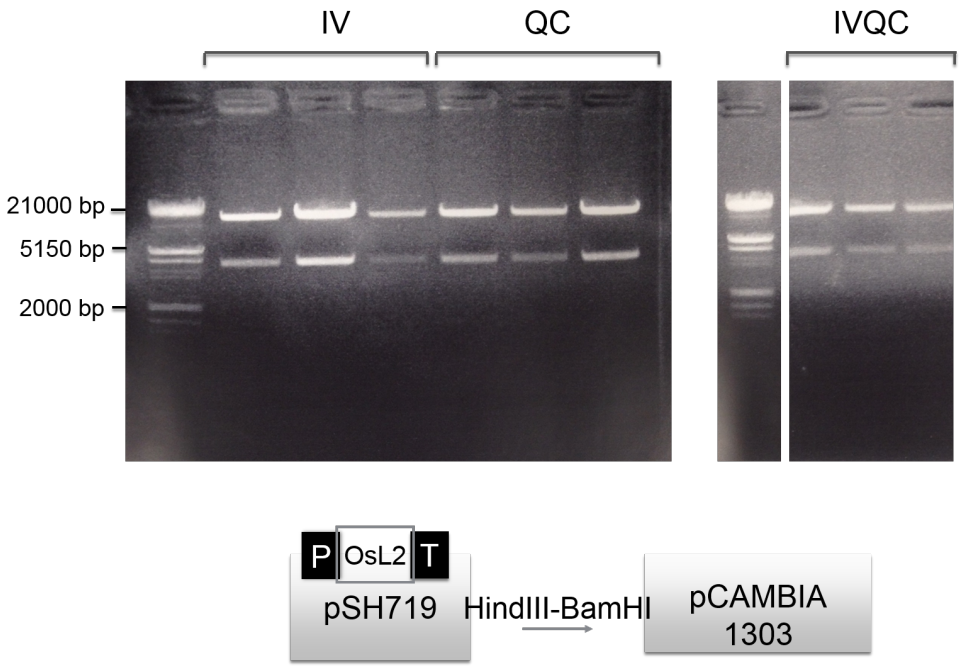

Figure S5 - 3 Sub-cloning of mutant OsAGPL2 constructs along with promoter and terminator sequences onto pCAMBIA1301 binary vector. After cloning selected colonies were digested with HindIII-BamHI enzymes and run in 1% agarose gels to confirm presence of the 4000 bp inserts

Appendix 2

Map of Expression Vectors

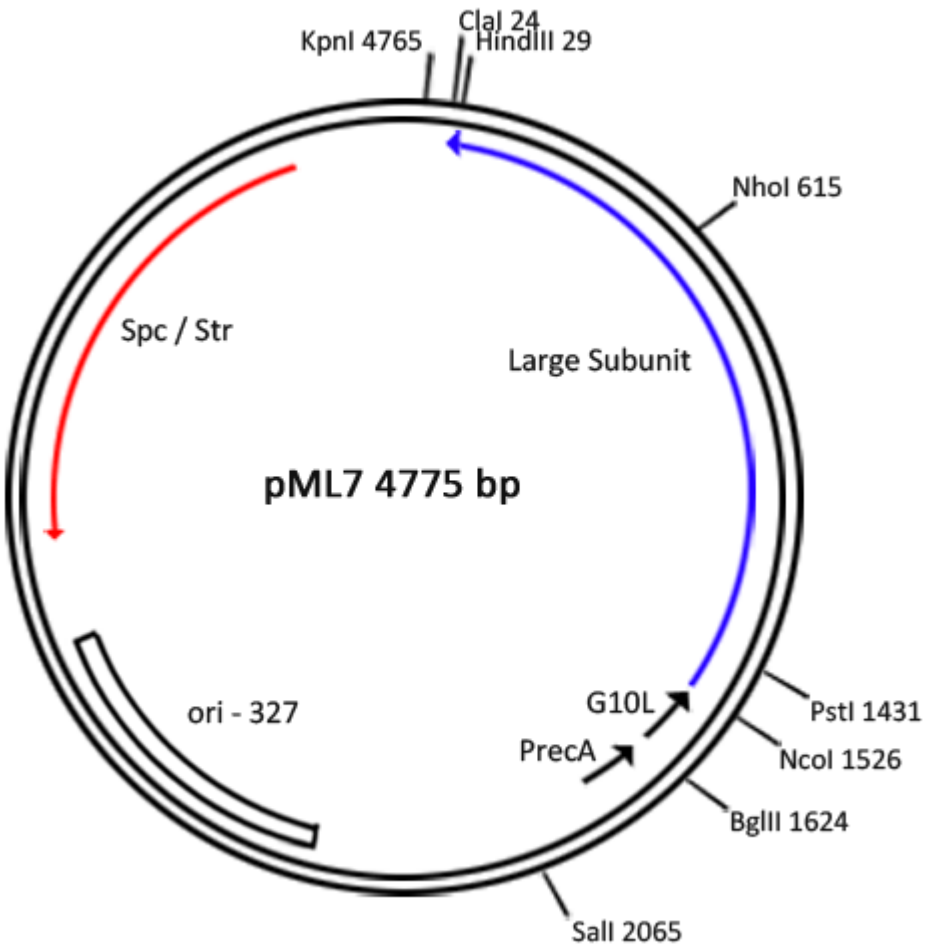

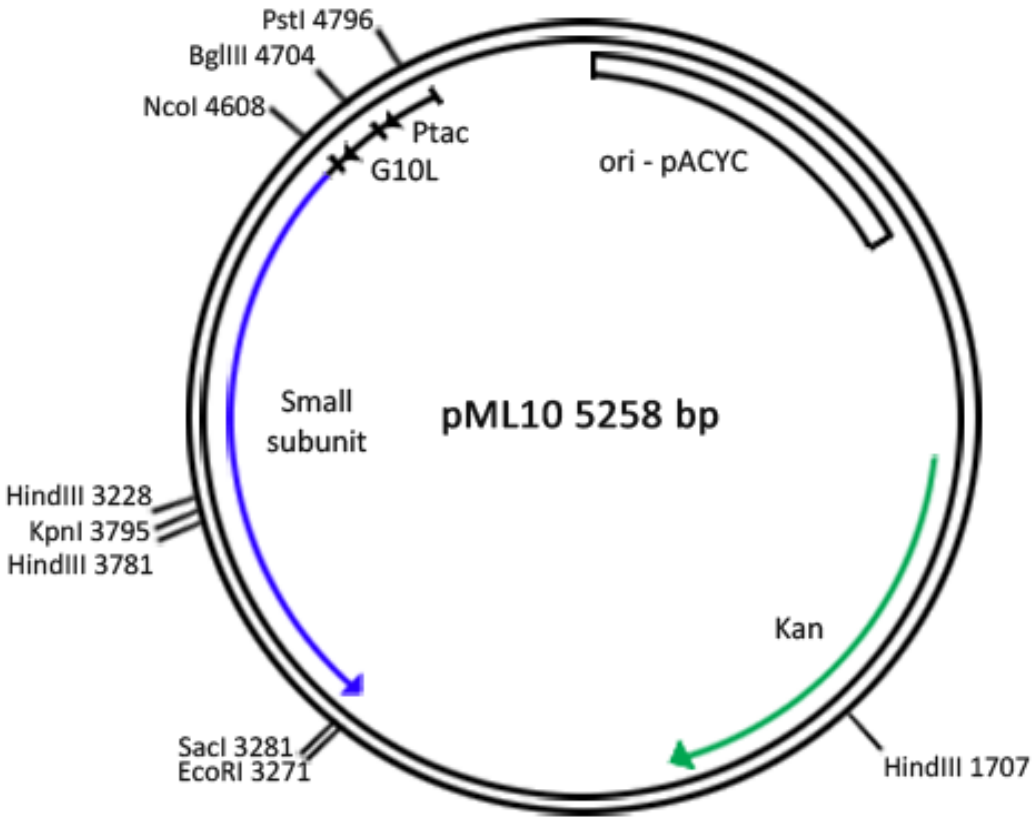
PstI 4796
BglIII 4704
NcoI 4608
Ptac
G10L
ori - pACYC
Small
subunit
pML10 5258 bp
HindIII 3228
KpnI 3795
HindIII 3781
Kan
SacI 3281
EcoRI 3271
HindIII 1707

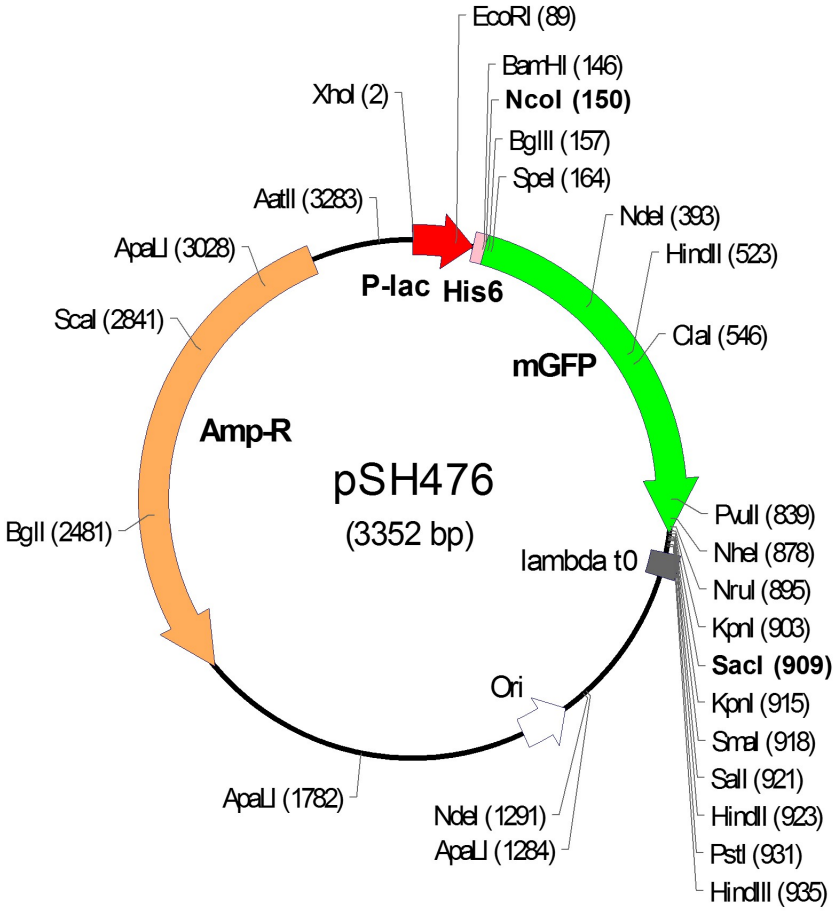
EcoRI (89)
BamHI (146)
NcoI (150)
BglII (157)
SpeI (164)
NdeI (393)
HindII (523)
ClaI (546)
PvuII (839)
NheI (878)
NruI (895)
KpnI (903)
SacI (909)
KpnI (915)
SmaI (918)
SalI (921)
HindII (923)
PstI (931)
HindIII (935)
XhoI (2)
AatII (3283)
ApaLI (3028)
ScaI (2841)
BglI (2481)
ApaLI (1782)
NdeI (1291)
ApaLI (1284)
P-lac
His6
mGFP
Amp-R
pSH476
(3352 bp)
lambda t0
Ori

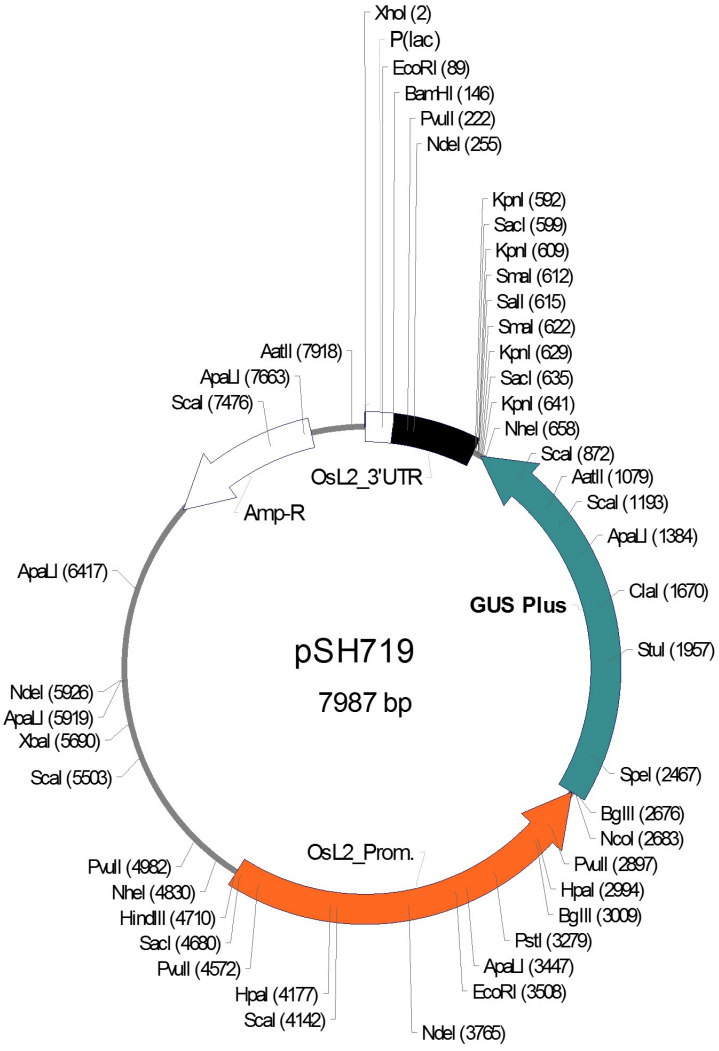
XhoI (2)
P(lac)
EcoRI (89)
BamHI (146)
PvuII (222)
NdeI (255)
KpnI (592)
SacI (599)
KpnI (609)
SmaI (612)
SalI (615)
SmaI (622)
KpnI (629)
SacI (635)
KpnI (641)
NheI (658)
ScaI (872)
AatII (1079)
ScaI (1193)
ApaLI (1384)
ClaI (1670)
StuI (1957)
SpeI (2467)
BglII (2676)
NcoI (2683)
PvuII (2897)
HpaI (2994)
BglII (3009)
PstI (3279)
ApaLI (3447)
EcoRI (3508)
NdeI (3765)
ScaI (4142)
HpaI (4177)
PvuII (4572)
SacI (4680)
HindIII (4710)
NheI (4830)
PvuII (4982)
ScaI (5503)
XbaI (5690)
ApaLI (5919)
NdeI (5926)
ApaLI (6417)
ScaI (7476)
ApaLI (7663)
AatII (7918)
OsL2_3'UTR
Amp-R
GUS Plus
pSH719
7987 bp
OsL2_Prom.

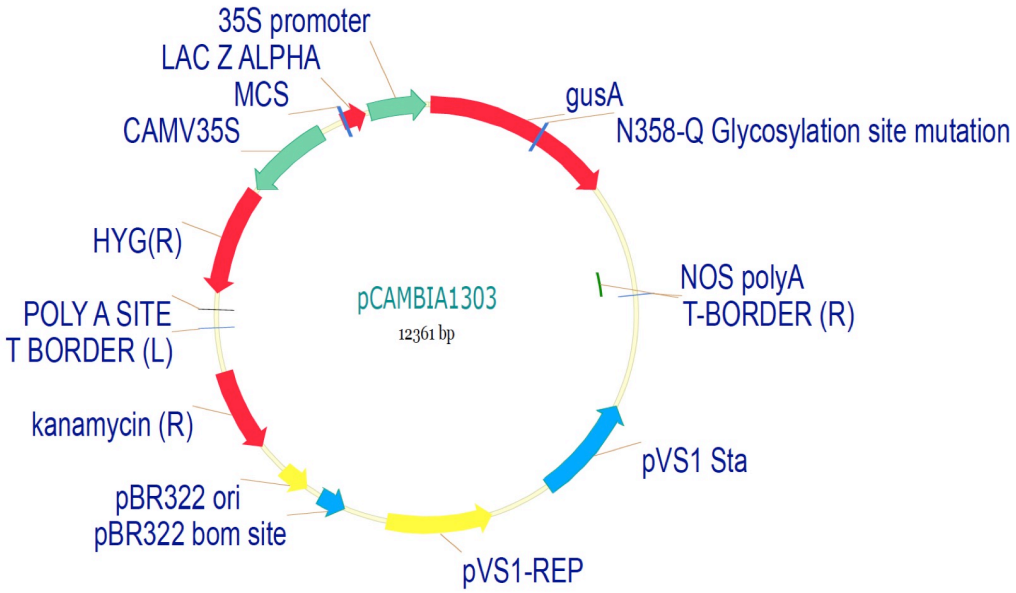
35S promoter
LAC Z ALPHA
MCS
CAMV35S
gusA
N358-Q Glycosylation site mutation
HYG(R)
NOS polyA
T-BORDER (R)
pCAMBIA1303
12361 bp
POLY A SITE
T BORDER (L)
kanamycin (R)
pVS1 Sta
pBR322 ori
pBR322 bom site
pVS1-REP

Appendix 3

DNA and Protein Markers

DNA Molecular Weight Marker

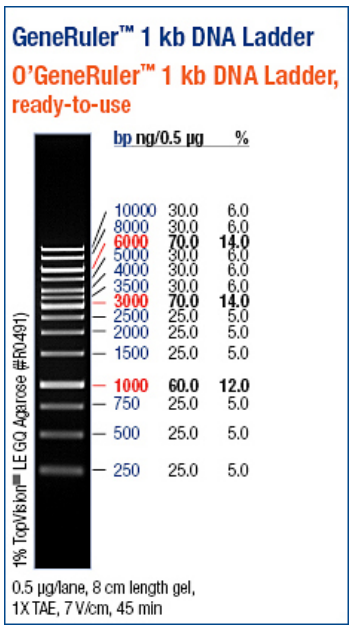

The ladder is a mixture of chromatography-purified individual DNA fragments.

Lambda DNA/EcoRI+HindIII Marker, 3

bp	ng/0.5 µg	%
21226*	218.8	43.8
5148	53.1	10.6
4973	51.3	10.3
4268	44.0	8.8
3530*	36.4	7.3
2027	20.9	4.2
1904	19.6	3.9
1584	16.3	3.3
1375	14.2	2.8
947	9.8	1.95
831	8.6	1.7
564	5.8	1.2

0.5 µg/lane, 8 cm length gel,
1X TAE, 7 V/cm, 45 min

Range

13 fragments (in bp): 21226*, 5148, 4973, 4268, 3530*, 2027, 1904, 1584, 1375, 947, 831, 564, *125 (it comprises 0.3%).*

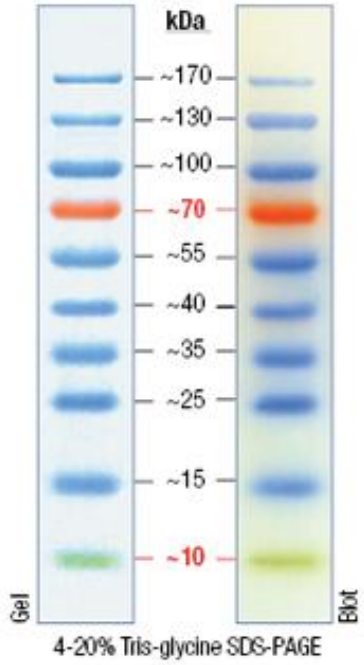

PageRuler Prestained Protein Ladders

Appendix 4

Lab Equipments

Autoclaves	**:** CL-40S/SDP (60L) ALP autoclave
Centrifuges	**:** 4K15, Sigma Laboratory
	: Microfuge 14-15, Sigma Laboratory
Deep freezes and refrigerators	**:** Heto Polar Bear 4410 ultra freezer, JOUAN Nordic A/S, catalog# 003431.
	: 2021 D deep freezer, Arcelik.
	: 1061 M refrigerator, Arcelik.
Electrophoresis equipments	**:** E-C Mini Cell Primo EC320, E-C Apparatus.
	: Mini-PROTEAN 3 Cell and Single-Row AnyGel Stand, Catalog# 165-3321,Bio-Rad.
Gel documentation system	**:** UVIpro GAS7000, UVItec Limited.
Ice Machine	**:** AF 10, Scotsman.
Shaker	**:** Innova 4300 incubator shaker
Magnetic stirrer	**:** Heidolph MR 3001
Pipettes	**:** Pipetteman P10, P 100, P1000, Eppendorf
pH meter	**:** Inolab pH level 1, order# 1A10-1113,
Power supply	**:** PowerPac Basic (300V,400mA,75W) Biorad
Pure water systems	**:** DV25 PureLab Option ELGA
Spectrophotometer	**:** W-1700 PharmaSpec, Shimadzu Corporation.
Vortexing machine	**:** Reax Top, Heidolph2.2.

BIBLIOGRAPHY

1. Slattery, C.J., I.H. Kavakli, and T.W. Okita, *Engineering starch for increased quantity and quality.* Trends in Plant Science, 2000. **5**(7): p. 291-298.
2. Smith, A.M., *Prospects for increasing starch and sucrose yields for bioethanol production.* Plant J, 2008. **54**(4): p. 546-58.
3. Buleon, A., et al., *Starch granules: structure and biosynthesis.* International Journal of Biological Macromolecules, 1998. **23**(2): p. 85-112.
4. Jenkins, J.P.J., R.E. Cameron, and A.M. Donald, *A Universal Feature in the Structure of Starch Granules from Different Botanical Sources.* Starch-Starke, 1993. **45**(12): p. 417-420.
5. Zeeman, S.C., J. Kossmann, and A.M. Smith, *Starch: Its Metabolism, Evolution, and Biotechnological Modification in Plants.* Annual Review of Plant Biology, Vol 61, 2010. **61**: p. 209-234.
6. Rongine De Fekete, M.A., L.F. Leloir, and C.E. Cardini, *Mechanism of starch biosynthesis.* Nature, 1960. **187**: p. 918-9.
7. Nakamura, T., et al., *Characterization of a granule-bound starch synthase isoform found in the pericarp of wheat.* Plant Physiology, 1998. **118**(2): p. 451-459.
8. Vrinten, P.L. and T. Nakamura, *Wheat granule-bound starch synthase I and II are encoded by separate genes that are expressed in different tissues.* Plant Physiology, 2000. **122**(1): p. 255-263.
9. Smith, S.M., et al., *Diurnal changes in the transcriptome encoding enzymes of starch metabolism provide evidence for both transcriptional and posttranscriptional regulation of starch metabolism in arabidopsis leaves.* Plant Physiology, 2004. **136**(1): p. 2687-2699.
10. Wang, S.J., K.W. Yeh, and C.Y. Tsai, *Regulation of starch granule-bound starch synthase I gene expression by circadian clock and sucrose in the source tissue of sweet potato.* Plant Science, 2001. **161**(4): p. 635-644.
11. Smith, A.M., K. Denyer, and C. Martin, *The synthesis of the starch granule.* Annual Review of Plant Physiology and Plant Molecular Biology, 1997. **48**: p. 65-87.
12. Hirose, T. and T. Terao, *A comprehensive expression analysis of the starch synthase gene family in rice (Oryza sativa L.).* Planta, 2004. **220**(1): p. 9-16.
13. Tetlow, I.J., *Understanding storage starch biosynthesis in plants: a means to quality improvement.* Canadian Journal of Botany-Revue Canadienne De Botanique, 2006. **84**(8): p. 1167-1185.

14. Edwards, A., et al., *A combined reduction in activity of starch synthases II and III of potato has novel effects on the starch of tubers.* Plant Journal, 1999. **17**(3): p. 251-261.

15. Lloyd, J.R., V. Landschutze, and J. Kossmann, *Simultaneous antisense inhibition of two starch-synthase isoforms in potato tubers leads to accumulation of grossly modified amylopectin.* Biochemical Journal, 1999. **338**: p. 515-521.

16. Regina, A., et al., *High-amylose wheat generated by RNA interference improves indices of large-bowel health in rats.* Proceedings of the National Academy of Sciences of the United States of America, 2006. **103**(10): p. 3546-3551.

17. Schwall, G.P., et al., *Production of very-high-amylose potato starch by inhibition of SBE A and B.* Nature Biotechnology, 2000. **18**(5): p. 551-554.

18. Heldt, H.-W. and F. Heldt, *Plant biochemistry*. 2005, Elsevier Academic Press: Amsterdam ; Boston. p. 1 online resource (xxvi, 630 p.

19. Burton, R.A., et al., *Starch granule initiation and growth are altered in barley mutants that lack isoamylase activity.* Plant Journal, 2002. **31**(1): p. 97-112.

20. Kawagoe, Y., et al., *Roles of isoamylase and ADP-glucose pyrophosphorylase in starch granule synthesis in rice endosperm.* Plant Journal, 2005. **42**(2): p. 164-174.

21. Ball, S., et al., *From glycogen to amylopectin: A model for the biogenesis of the plant starch granule.* Cell, 1996. **86**(3): p. 349-352.

22. Myers, A.M., et al., *Recent progress toward understanding biosynthesis of the amylopectin crystal.* Plant Physiology, 2000. **122**(4): p. 989-997.

23. Zeeman, S.C., et al., *A mutant of Arabidopsis lacking a chloroplastic isoamylase accumulates both starch and phytoglycogen.* Plant Cell, 1998. **10**(10): p. 1699-1711.

24. Sulpice, R., et al., *Starch as a major integrator in the regulation of plant growth.* Proc Natl Acad Sci U S A, 2009. **106**(25): p. 10348-53.

25. Ballicora, M., A. Iglesias, and J. Preiss, *ADP-Glucose Pyrophosphorylase: A Regulatory Enzyme for Plant Starch Synthesis.* Photosynthesis research, 2004. **79**(1): p. 1-24.

26. Denyer, K., et al., *The major form of ADP-glucose pyrophosphorylase in maize endosperm is extra-plastidial.* Plant Physiology, 1996. **112**(2): p. 779-785.

27. Thorbjornsen, T., et al., *A single gene encodes two different transcripts for the ADP-glucose pyrophosphorylase small subunit from barley (Hordeum vulgare).* Biochem J, 1996. **313 (Pt 1)**: p. 149-54.

28. Mohlmann, T., et al., *ADP-glucose drives starch synthesis in isolated maize endosperm amyloplasts: characterization of starch synthesis and transport*

properties across the amyloplast envelope. Biochem J, 1997. **324 (Pt 2)**: p. 503-9.

29. Caspar, T., S.C. Huber, and C. Somerville, *Alterations in Growth, Photosynthesis, and Respiration in a Starchless Mutant of Arabidopsis thaliana (L.) Deficient in Chloroplast Phosphoglucomutase Activity.* Plant Physiol, 1985. **79**(1): p. 11-7.

30. Lin, T.P., et al., *Isolation and Characterization of a Starchless Mutant of Arabidopsis thaliana (L.) Heynh Lacking ADPglucose Pyrophosphorylase Activity.* Plant Physiol, 1988. **86**(4): p. 1131-5.

31. Tsai, H.L., et al., *Starch synthesis in Arabidopsis is achieved by spatial cotranscription of core starch metabolism genes.* Plant Physiol, 2009. **151**(3): p. 1582-95.

32. Munoz, F.J., et al., *Sucrose synthase controls both intracellular ADP glucose levels and transitory starch biosynthesis in source leaves.* Plant Cell Physiol, 2005. **46**(8): p. 1366-76.

33. Stitt, M. and S.C. Zeeman, *Starch turnover: pathways, regulation and role in growth.* Curr Opin Plant Biol, 2012. **15**(3): p. 282-92.

34. Lu, Y., J.P. Gehan, and T.D. Sharkey, *Daylength and circadian effects on starch degradation and maltose metabolism.* Plant Physiol, 2005. **138**(4): p. 2280-91.

35. Gibon, Y., et al., *Adjustment of growth, starch turnover, protein content and central metabolism to a decrease of the carbon supply when Arabidopsis is grown in very short photoperiods.* Plant Cell Environ, 2009. **32**(7): p. 859-74.

36. Gibon, Y., et al., *Adjustment of diurnal starch turnover to short days: depletion of sugar during the night leads to a temporary inhibition of carbohydrate utilization, accumulation of sugars and post-translational activation of ADP-glucose pyrophosphorylase in the following light period.* Plant J, 2004. **39**(6): p. 847-62.

37. Mugford, S.T., et al., *Regulatory properties of ADP glucose pyrophosphorylase are required for adjustment of leaf starch synthesis in different photoperiods.* Plant Physiol, 2014.

38. Weber, A., et al., *Identification, purification, and molecular cloning of a putative plastidic glucose translocator.* Plant Cell, 2000. **12**(5): p. 787-802.

39. Weise, S.E., A.P. Weber, and T.D. Sharkey, *Maltose is the major form of carbon exported from the chloroplast at night.* Planta, 2004. **218**(3): p. 474-82.

40. Hatzfeld, W.D. and M. Stitt, *A study of the rate of recycling of triose phosphates in heterotrophic Chenopodium rubrum cells, potato tubers, and maize endosperm.* Planta, 1990. **180**(2): p. 198-204.

41. Keeling, P.L., et al., *Starch Biosynthesis in Developing Wheat Grain : Evidence against the Direct Involvement of Triose Phosphates in the Metabolic Pathway.* Plant Physiol, 1988. **87**(2): p. 311-9.

42. Pozueta-Romero, J., et al., *Direct transport of ADPglucose by an adenylate translocator is linked to starch biosynthesis in amyloplasts.* Proc Natl Acad Sci U S A, 1991. **88**(13): p. 5769-73.

43. Tjaden, J., et al., *Expression of a plastidic ATP/ADP transporter gene in Escherichia coli leads to a functional adenine nucleotide transport system in the bacterial cytoplasmic membrane.* J Biol Chem, 1998. **273**(16): p. 9630-6.

44. Patron, N.J., et al., *The lys5 mutations of barley reveal the nature and importance of plastidial ADP-Glc transporters for starch synthesis in cereal endosperm.* Plant Physiol, 2004. **135**(4): p. 2088-97.

45. Shannon, J.C., et al., *Brittle-1, an adenylate translocator, facilitates transfer of extraplastidial synthesized ADP--glucose into amyloplasts of maize endosperms.* Plant Physiol, 1998. **117**(4): p. 1235-52.

46. Bahaji, A., et al., *Starch biosynthesis, its regulation and biotechnological approaches to improve crop yields.* Biotechnol Adv, 2014. **32**(1): p. 87-106.

47. Espada, J., *Enzymic Synthesis of Adenosine Diphosphate Glucose from Glucose 1-Phosphate and Adenosine Triphosphate.* Journal of Biological Chemistry, 1962. **237**(12): p. 3577-3581.

48. Preiss, J. and M.N. Sivak, *Biochemistry, molecular biology and regulation of starch synthesis.* Genet Eng (N Y), 1998. **20**: p. 177-223.

49. Preiss, J., et al., *Regulation of higher plant leaf and reserve tissue starch synthesis.* Plant Biotechnology and in Vitro Biology in the 21st Century, 1999. **36**: p. 315-319.

50. Crevillen, P., et al., *Differential pattern of expression and sugar regulation of Arabidopsis thaliana ADP-glucose pyrophosphorylase-encoding genes.* Journal of Biological Chemistry, 2005. **280**(9): p. 8143-9.

51. Crevillen, P., et al., *Characterization of recombinant ADP-glucose pyrophosphorylases from Arabidopsis thaliana.* Faseb Journal, 2003. **17**(4): p. A568-A568.

52. Georgelis, N., E.L. Braun, and L.C. Hannah, *Duplications and functional divergence of ADP-glucose pyrophosphorylase genes in plants.* Bmc Evolutionary Biology, 2008. **8**.

53. Kuhn, M.L., C.A. Falaschetti, and M.A. Ballicora, *Ostreococcus tauri ADP-glucose pyrophosphorylase reveals alternative paths for the evolution of subunit roles.* J Biol Chem, 2009. **284**(49): p. 34092-102.

54. Weber, H., et al., *Cell-type specific, coordinate expression of two ADP-glucose pyrophosphorylase genes in relation to starch biosynthesis during seed development of Vicia faba L.* Planta, 1995. **195**(3): p. 352-61.

55. Hylton, C. and A.M. Smith, *The rb Mutation of Peas Causes Structural and Regulatory Changes in ADP Glucose Pyrophosphorylase from Developing Embryos.* Plant Physiol, 1992. **99**(4): p. 1626-34.

56. Ball, K. and J. Preiss, *Allosteric sites of the large subunit of the spinach leaf ADPglucose pyrophosphorylase.* J Biol Chem, 1994. **269**(40): p. 24706-11.

57. Morell, M., M. Bloom, and J. Preiss, *Affinity labeling of the allosteric activator site(s) of spinach leaf ADP-glucose pyrophosphorylase.* J Biol Chem, 1988. **263**(2): p. 633-7.

58. Greene, T.W., et al., *Generation of up-regulated allosteric variants of potato ADP-glucose pyrophosphorylase by reversion genetics.* Proceedings of the National Academy of Sciences of the United States of America, 1998. **95**(17): p. 10322-10327.

59. Greene, T.W., et al., *Mutagenesis of the potato ADPglucose pyrophosphorylase and characterization of an allosteric mutant defective in 3-phosphoglycerate activation.* Proc Natl Acad Sci U S A, 1996. **93**(4): p. 1509-13.

60. Greene, T.W., R.L. Woodbury, and T.W. Okita, *Aspartic acid 413 is important for the normal allosteric functioning of ADP-glucose pyrophosphorylase.* Plant Physiol, 1996. **112**(3): p. 1315-20.

61. Kavakli, I.H., et al., *Analysis of allosteric effector binding sites of potato ADP-glucose pyrophosphorylase through reverse genetics.* Journal of Biological Chemistry, 2001. **276**(44): p. 40834-40840.

62. Salamone, P.R., et al., *Directed molecular evolution of ADP-glucose pyrophosphorylase.* Proceedings of the National Academy of Sciences of the United States of America, 2002. **99**(2): p. 1070-1075.

63. Iglesias, A.A., et al., *Expression of the potato tuber ADP-glucose pyrophosphorylase in Escherichia coli.* J Biol Chem, 1993. **268**(2): p. 1081-6.

64. Ballicora, M.A., et al., *Adenosine 5'-Diphosphate-Glucose Pyrophosphorylase from Potato-Tuber - Significance of the N-Terminus of the Small-Subunit for Catalytic Properties and Heat-Stability.* Plant Physiology, 1995. **109**(1): p. 245-251.

65. Cross, J.M., et al., *Both subunits of ADP-glucose pyrophosphorylase are regulatory.* Plant Physiol, 2004. **135**(1): p. 137-44.

66. Cross, J.M., et al., *A polymorphic motif in the small subunit of ADP-glucose pyrophosphorylase modulates interactions between the small and large subunits.* Plant J, 2005. **41**(4): p. 501-11.

67. Hwang, S.K., P.R. Salamone, and T.W. Okita, *Allosteric regulation of the higher plant ADP-glucose pyrophosphorylase is a product of synergy between the two subunits.* FEBS Lett, 2005. **579**(5): p. 983-90.

68. Hwang, S.K., S. Hamada, and T.W. Okita, *Catalytic implications of the higher plant ADP-glucose pyrophosphorylase large subunit.* Phytochemistry, 2007. **68**(4): p. 464-77.

69. Petreikov, M., et al., *Characterization of the AGPase large subunit isoforms from tomato indicates that the recombinant L3 subunit is active as a monomer.* Biochemical Journal, 2010. **428**: p. 201-212.

70. Kleczkowski, L.A., et al., *Kinetic mechanism and regulation of ADP-glucose pyrophosphorylase from barley (Hordeum vulgare) leaves.* J Biol Chem, 1993. **268**(9): p. 6228-33.

71. Paule, M.R. and J. Preiss, *Biosynthesis of Bacterial Glycogen: X. THE KINETIC MECHANISM OF ADENOSINE DIPHOSPHOGLUCOSE PYROPHOSPHORYLASE FROM RHODOSPIRILLUM RUBRUM.* Journal of Biological Chemistry, 1971. **246**(14): p. 4602-4609.

72. Boehlein, S.K., et al., *Deciphering the kinetic mechanisms controlling selected plant ADP-glucose pyrophosphorylases.* Archives of Biochemistry and Biophysics, 2013. **535**(2): p. 215-226.

73. Tiessen, A., et al., *Starch synthesis in potato tubers is regulated by post-translational redox modification of ADP-glucose pyrophosphorylase: a novel regulatory mechanism linking starch synthesis to the sucrose supply.* Plant Cell, 2002. **14**(9): p. 2191-213.

74. Fu, Y., et al., *Mechanism of reductive activation of potato tuber ADP-glucose pyrophosphorylase.* J Biol Chem, 1998. **273**(39): p. 25045-52.

75. Geigenberger, P., *Regulation of starch biosynthesis in response to a fluctuating environment.* Plant Physiol, 2011. **155**(4): p. 1566-77.

76. Hendriks, J.H., et al., *ADP-glucose pyrophosphorylase is activated by posttranslational redox-modification in response to light and to sugars in leaves of Arabidopsis and other plant species.* Plant Physiol, 2003. **133**(2): p. 838-49.

77. Lunn, J.E., et al., *Sugar-induced increases in trehalose 6-phosphate are correlated with redox activation of ADPglucose pyrophosphorylase and higher rates of starch synthesis in Arabidopsis thaliana.* Biochemical Journal, 2006. **397**: p. 139-148.

78. Balmer, Y., et al., *A complete ferredoxin/thioredoxin system regulates fundamental processes in amyloplasts.* Proceedings of the National Academy of Sciences of the United States of America, 2006. **103**(8): p. 2988-2993.

79. Tuncel, A., et al., *The role of the large subunit in redox regulation of the rice endosperm ADP-glucose pyrophosphorylase.* FEBS J, 2014.

80. Jin, X., et al., *Crystal structure of potato tuber ADP-glucose pyrophosphorylase.* EMBO J, 2005. **24**(4): p. 694-704.

81. Cupp-Vickery, J.R., et al., *Structural analysis of ADP-glucose pyrophosphorylase from the bacterium Agrobacterium tumefaciens.* Biochemistry, 2008. **47**(15): p. 4439-4451.

82. Tuncel, A., I.H. Kavakli, and O. Keskin, *Insights into subunit interactions in the heterotetrameric structure of potato ADP-glucose pyrophosphorylase.* Biophys J, 2008. **95**(8): p. 3628-39.

83. Dawar, C., S. Jain, and S. Kumar, *Insight into the 3D structure of ADP-glucose pyrophosphorylase from rice (Oryza sativa L.).* Journal of Molecular Modeling, 2013. **19**(8): p. 3351-3367.

84. Georgelis, N. and L.C. Hannah, *Isolation of a heat-stable maize endosperm ADP-glucose pyrophosphorylase variant.* Plant Science, 2008. **175**(3): p. 247-254.

85. Danishuddin, M., R. Chatrath, and R. Singh, *Insights of interaction between small and large subunits of ADP-glucose pyrophosphorylase from bread wheat (Triticum aestivum L.).* Bioinformation, 2011. **6**(4): p. 144-8.

86. Baris, I., et al., *Investigation of the interaction between the large and small subunits of potato ADP-glucose pyrophosphorylase.* PLoS Comput Biol, 2009. **5**(10): p. e1000546.

87. Greene, T.W. and L.C. Hannah, *Maize endosperm ADP-glucose pyrophosphorylase SHRUNKEN2 and BRITTLE2 subunit interactions.* Plant Cell, 1998. **10**(8): p. 1295-306.

88. Greene, T.W. and L.C. Hannah, *Enhanced stability of maize endosperm ADP-glucose pyrophosphorylase is gained through mutants that alter subunit interactions.* Proc Natl Acad Sci U S A, 1998. **95**(22): p. 13342-7.

89. Ballicora, M.A., et al., *Heat stability of the potato tuber ADP-glucose pyrophosphorylase: role of Cys residue 12 in the small subunit.* Biochem Biophys Res Commun, 1999. **257**(3): p. 782-6.

90. Linebarger, C.R., et al., *Heat stability of maize endosperm ADP-glucose pyrophosphorylase is enhanced by insertion of a cysteine in the N terminus of the small subunit.* Plant Physiol, 2005. **139**(4): p. 1625-34.

91. Boehlein, S.K., et al., *Heat stability and allosteric properties of the maize endosperm ADP-glucose pyrophosphorylase are intimately intertwined.* Plant Physiol, 2008. **146**(1): p. 289-99.

92. Georgelis, N., J.R. Shaw, and L.C. Hannah, *Phylogenetic analysis of ADP-glucose pyrophosphorylase subunits reveals a role of subunit interfaces in the allosteric properties of the enzyme.* Plant Physiol, 2009. **151**(1): p. 67-77.

93. Tuncel, A. and T.W. Okita, *Improving starch yield in cereals by over-expression of ADPglucose pyrophosphorylase: expectations and unanticipated outcomes.* Plant Sci, 2013. **211**: p. 52-60.

94. Sun, J.D., T.W. Okita, and G.E. Edwards, *Modification of carbon partitioning, photosynthetic capacity, and O-2 sensitivity in arabidopsis plants with low ADP-glucose pyrophosphorylase activity.* Plant Physiology, 1999. **119**(1): p. 267-276.

95. Sun, J.D., et al., *Interactions of nitrate and CO2 enrichment on growth, carbohydrates, and rubisco in arabidopsis starch mutants. Significance of starch and hexose.* Plant Physiology, 2002. **130**(3): p. 1573-1583.

96. Obana, Y., et al., *Enhanced turnover of transitory starch by expression of up-regulated ADP-glucose pyrophosphorylases in Arabidopsis thaliana.* Plant Science, 2006. **170**(1): p. 1-11.

97. Gibson, K., et al., *Exploiting leaf starch synthesis as a transient sink to elevate photosynthesis, plant productivity and yields.* Plant Sci, 2011. **181**(3): p. 275-81.

98. Stark, D.M., et al., *Regulation of the amount starch in plant tissues by ADP-glucose pyrophosphorylase.* Science, 1992. **258**: p. 287-292.

99. Giroux, M.J., et al., *A single mutation that increases maize seed weight.* Proc Natl Acad Sci U S A, 1996. **93**(12): p. 5824-9.

100. Wang, Z.Y., et al., *Increasing maize seed weight by enhancing the cytoplasmic ADP-glucose pyrophosphorylase activity in transgenic maize plants.* Plant Cell Tissue and Organ Culture, 2007. **88**(1): p. 83-92.

101. Li, N., et al., *Over-expression of AGPase genes enhances seed weight and starch content in transgenic maize.* Planta, 2011. **233**(2): p. 241-250.

102. Sakulsingharoj, C., et al., *Engineering starch biosynthesis for increasing rice seed weight: the role of the cytoplasmic ADP-glucose pyrophosphorylase.* Plant Science, 2004.

103. Preiss, J. and T. Romeo, *Molecular-Biology and Regulatory Aspects of Glycogen Biosynthesis in Bacteria.* Progress in Nucleic Acid Research and Molecular Biology, Vol 47, 1994. **47**: p. 299-329.

104. Smidansky, E.D., et al., *Expression of a modified ADP-glucose pyrophosphorylase large subunit in wheat seeds stimulates photosynthesis and carbon metabolism.* Planta, 2007. **225**(4): p. 965-976.

105. Smidansky, E.D., et al., *Seed yield and plant biomass increases in rice are conferred by deregulation of endosperm ADP-glucose pyrophosphorylase.* Planta, 2003. **216**(4): p. 656-664.

106. Meyer, F.D., et al., *Field evaluation of transgenic wheat expressing a modified ADP-glucose pyrophosphorylase large subunit.* Crop Science, 2007. **47**(1): p. 336-342.

107. Hannah, L.C., et al., *A shrunken-2 transgene increases maize yield by acting in maternal tissues to increase the frequency of seed development.* Plant Cell, 2012. **24**(6): p. 2352-63.

108. Kang, G., et al., *Increasing the starch content and grain weight of common wheat by overexpression of the cytosolic AGPase large subunit gene.* Plant Physiol Biochem, 2013. **73**: p. 93-8.

109. Ballicora, M.A., A.A. Iglesias, and J. Preiss, *ADP-glucose pyrophosphorylase: a regulatory enzyme for plant starch synthesis.* Photosynthesis Research, 2004. **79**(1): p. 1-24.

110. Kavakli, I.H., et al., *The conversion of carbon and nitrogen into starch and storage proteins in developing storage organs: an overview.* Australian Journal of Plant Physiology, 2000. **27**(6): p. 561-570.

111. Okita, T.W., et al., *Engineering plant starches by the generation of modified plant biosynthetic enzymes.* Engineering Crop Plants for Industrial End Uses, 1998. **14**: p. 99-109

221.

112. Preiss, J., *Regulation of the Biosynthesis and Degradation of Starch.* Annual Review of Plant Physiology and Plant Molecular Biology, 1982. **33**: p. 431-454.

113. Sowokinos, J.R. and J. Preiss, *Pyrophosphorylases in Solanum-Tuberosum .3. Purification, Physical, and Catalytic Properties of Adp-Glucose Pyrophosphorylase in Potatoes.* Plant Physiology, 1982. **69**(6): p. 1459-1466.

114. Nakata, P.A., et al., *Comparison of the Primary Sequences of 2 Potato-Tuber Adp-Glucose Pyrophosphorylase Subunits.* Plant Molecular Biology, 1991. **17**(5): p. 1089-1093.

115. Okita, T.W., et al., *The Subunit Structure of Potato-Tuber Adpglucose Pyrophosphorylase.* Plant Physiology, 1990. **93**(2): p. 785-790.

116. Smithwhite, B.J. and J. Preiss, *Comparison of Proteins of Adp-Glucose Pyrophosphorylase from Diverse Sources.* Journal of Molecular Evolution, 1992. **34**(5): p. 449-464.

117. Kavakli, I.H., et al., *Investigation of subunit function in ADP-glucose pyrophosphorylase.* Biochemical and Biophysical Research Communications, 2001. **281**(3): p. 783-787.

118. Iglesias, A.A., et al., *Expression of the Potato-Tuber Adp-Glucose Pyrophosphorylase in Escherichia-Coli.* Journal of Biological Chemistry, 1993. **268**(2): p. 1081-1086.

119. Salamone, P.R., et al., *Isolation and characterization of a higher plant ADP-glucose pyrophosphorylase small subunit homotetramer.* Febs Letters, 2000. **482**(1-2): p. 113-118.

120. Hwang, S.K., S. Hamada, and T.W. Okita, *ATP binding site in the plant ADP-glucose pyrophosphorylase large subunit.* Febs Letters, 2006. **580**(28-29): p. 6741-6748.

121. Hwang, S.K., et al., *Direct appraisal of the potato tuber ADP-glucose pyrophosphorylase large subunit in enzyme function by study of a novel mutant form.* Journal of Biological Chemistry, 2008. **283**(11): p. 6640-6647.

122. Stitt, M., J. Lunn, and B. Usadel, *Arabidopsis and primary photosynthetic metabolism - more than the icing on the cake.* Plant J, 2010. **61**(6): p. 1067-91.

123. Graf, A. and A.M. Smith, *Starch and the clock: the dark side of plant productivity.* Trends Plant Sci, 2011. **16**(3): p. 169-75.

124. Smith, A.M. and M. Stitt, *Coordination of carbon supply and plant growth.* Plant Cell Environ, 2007. **30**(9): p. 1126-49.

125. Usadel, B., et al., *Global transcript levels respond to small changes of the carbon status during progressive exhaustion of carbohydrates in Arabidopsis rosettes.* Plant Physiol, 2008. **146**(4): p. 1834-61.

126. Mangelsen, E., et al., *Significance of light, sugar, and amino acid supply for diurnal gene regulation in developing barley caryopses.* Plant Physiol, 2010. **153**(1): p. 14-33.

127. Chang, S., J. Puryear, and C. J., *A Simple and Efficient Method for*

Isolating RNA from Pine Trees. Plant Molecular Biology Reporter, 1993. **11**: p. 113-116.

128. Garg, R., et al., *Validation of internal control genes for quantitative gene expression studies in chickpea (Cicer arietinum L.).* Biochem Biophys Res Commun, 2010. **396**(2): p. 283-8.

129. Kavakli, I.H., et al., *Generation, characterization, and heterologous expression of wild-type and up-regulated forms of Arabidopsis thaliana leaf ADP-glucose pyrophosphorylase.* Planta, 2002. **215**(3): p. 430-439.

130. Boehlein, S.K., et al., *Purification and characterization of adenosine diphosphate glucose pyrophosphorylase from maize/potato mosaics.* Plant Physiol, 2005. **138**(3): p. 1552-62.

131. Lee, S.K., et al., *Identification of the ADP-glucose pyrophosphorylase isoforms essential for starch synthesis in the leaf and seed endosperm of rice (Oryza sativa L.).* Plant Molecular Biology, 2007. **65**(4): p. 531-546.

132. Singh, S., et al., *Isolation and characterization of cDNA clones encoding ADP-glucose pyrophosphorylase (AGPase) large and small subunits from chickpea (Cicer arietinum L.).* Phytochemistry, 2002. **59**(3): p. 261-268.

133. Park, S.W. and W.I. Chung, *Molecular cloning and organ-specific expression of three isoforms of tomato ADP-glucose pyrophosphorylase gene.* Gene, 1998. **206**(2): p. 215-221.

134. Villand, P., O.A. Olsen, and L.A. Kleczkowski, *Molecular Characterization of Multiple Cdna Clones for Adp-Glucose Pyrophosphorylase from Arabidopsis-Thaliana.* Plant Molecular Biology, 1993. **23**(6): p. 1279-1284.

135. Emanuelsson, O., H. Nielsen, and G. Von Heijne, *ChloroP, a neural network-based method for predicting chloroplast transit peptides and their cleavage sites.* Protein Science, 1999. **8**(5): p. 978-984.

136. Nakai, K. and M. Kanehisa, *Expert system for predicting protein localization sites in gram-negative bacteria.* Proteins, 1991. **11**(2): p. 95-110.

137. Galasso, I., et al., *Identification and isolation of lectin nucleotide sequences and species relationships in the genus Lens Miller.* Theor Appl Genet, 2004. **108**(6): p. 1098-102.

138. Akihiro, T., K. Mizuno, and T. Fujimura, *Gene expression of ADP-glucose pyrophosphorylase and starch contents in rice cultured cells are cooperatively regulated by sucrose and ABA.* Plant and Cell Physiology, 2005. **46**(6): p. 937-946.

139. Ohdan, T., et al., *Expression profiling of genes involved in starch synthesis in sink and source organs of rice.* Journal of Experimental Botany, 2005. **56**(422): p. 3229-3244.

140. Kwak, M.S., et al., *Two sweetpotato ADP-glucose pyrophosphorylase isoforms are regulated antagonistically in response to sucrose content in storage roots.* Gene, 2006. **366**(1): p. 87-96.

141. Li, X., et al., *Sucrose regulation of ADP-glucose pyrophosphorylase subunit genes transcript levels in leaves and fruits.* Plant Sci, 2002. **162**(2): p. 239-44.

142. Sokolov, L.N., A. Dejardin, and L.A. Kleczkowski, *Sugars and light/dark exposure trigger differential regulation of ADP-glucose pyrophosphorylase genes in Arabidopsis thaliana (thale cress).* Biochem J, 1998. **336 (Pt 3)**: p. 681-7.

143. Matt, P., et al., *Growth of tobacco in short-day conditions leads to high starch, low sugars, altered diurnal changes in the Nia transcript and low nitrate reductase activity, and inhibition of amino acid synthesis.* Planta, 1998. **207**(1): p. 27-41.

144. Singh, S., et al., *Expression, kinetics and regulatory properties of native and recombinant ADP-glucose pyrophosphorylase isoforms from chickpea.* Plant Physiology and Biochemistry, 2003. **41**(5): p. 399-405.

145. Hylton, C. and A.M. Smith, *The Rb Mutation of Peas Causes Structural and Regulatory Changes in Adp Glucose Pyrophosphorylase from Developing Embryos.* Plant Physiology, 1992. **99**(4): p. 1626-1634.

146. Choi, S.B., et al., *Transcriptional expression characteristics and subcellular localization of ADP-glucose pyrophosphorylase in the oil plant Perilla frutescens.* Plant and Cell Physiology, 2001. **42**(2): p. 146-153.

147. Giroux, M.J., et al., *A single gene mutation that inccerases maize seed weight.* Proceedings of the National Academy of Sciences of the United States of America, 1996. **93**: p. 5824-5829.

148. Sun, J.D., G.E. Edwards, and T.W. Okita, *Transient feedback inhibition of photosynthesis and electron transport when shifting to low O-2 in rice plants.* Plant Physiology, 1997. **114**(3): p. 1043-1043.

149. Chia, T., et al., *A cytosolic glucosyltransferase is required for conversion of starch to sucrose in Arabidopsis leaves at night.* Plant Journal, 2004. **37**(6): p. 853-863.

150. Yu, T.S., et al., *The Arabidopsis sex1 mutant is defective in the R1 protein, a general regulator of starch degradation in plants, and not in the chloroplast hexose transporter.* Plant Cell, 2001. **13**(8): p. 1907-1918.

151. Burgess, D., et al., *Molecular cloning and characterization of ADP-glucose pyrophosphorylase cDNA clones isolated from pea cotyledons.* Plant Molecular Biology, 1997. **33**(3): p. 431-444.

152. Weber, H., et al., *Cell-Type-Specific, Coordinate Expression of 2 Adp-Glucose Pyrophosphorylase Genes in Relation to Starch Biosynthesis during Seed Development of Vicia-Faba L.* Planta, 1995. **195**(3): p. 352-361.

153. Villand, P., et al., *ADP-Glucose Pyrophosphorylase Large Subunit cDNA from Barley Endosperm.* Plant Physiol, 1992. **100**(3): p. 1617-8.

154. Okita, T.W., et al., *Engineering plant starches by the generation of modified plant biosynthetic enzymes*. Engineering Crop Plants for Industrial End Uses. Vol. 14. 1998: Portland Press. 221.

155. Hannah, L.C. and M. James, *The complexities of starch biosynthesis in cereal endosperms.* Curr Opin Biotechnol, 2008. **19**(2): p. 160-5.

156. Preiss, J., et al., *Starch synthesis and its bioregulation.* Biochemical Society Trasnduction, 1991. **19**: p. 539-547.

157. Okita, T.W., et al., *The Subunit Structure of Potato Tuber ADPglucose Pyrophosphorylase.* Plant Physiol, 1990. **93**(2): p. 785-90.

158. Ballicora, M.A., et al., *ADP-Glucose pyrophosphorylase from potato tubers. Site-directed mutagenesis studies of the regulatory sites.* Plant Physiol, 1998. **118**(1): p. 265-74.

159. Kim, D., S.K. Hwang, and T.W. Okita, *Subunit interactions specify the allosteric regulatory properties of the potato tuber ADP-glucose pyrophosphorylase.* Biochem Biophys Res Commun, 2007. **362**(2): p. 301-6.

160. Ventriglia, T., et al., *Two Arabidopsis ADP-glucose pyrophosphorylase large subunits (APL1 and APL2) are catalytic.* Plant Physiol, 2008. **148**(1): p. 65-76.

161. Hwang, S.K., S. Hamada, and T.W. Okita, *ATP binding site in the plant ADP-glucose pyrophosphorylase large subunit.* FEBS Lett, 2006. **580**(28-29): p. 6741-8.

162. Hwang, S.K., et al., *Direct appraisal of the potato tuber ADP-glucose pyrophosphorylase large subunit in enzyme function by study of a novel mutant form.* J Biol Chem, 2008. **283**(11): p. 6640-7.

163. Sowokinos, J.R. and J. Preiss, *Pyrophosphorylases in Solanum tuberosum: III. PURIFICATION, PHYSICAL, AND CATALYTIC PROPERTIES OF ADPGLUCOSE PYROPHOSPHORYLASE IN POTATOES.* Plant Physiol, 1982. **69**(6): p. 1459-66.

164. Kavakli, I.H., et al., *Analysis of allosteric effector binding sites of potato ADP-glucose pyrophosphorylase through reverse genetics.* J Biol Chem, 2001. **276**(44): p. 40834-40840.

165. Greene, T.W., et al., *Generation of up-regulated allosteric variants of potato ADP-glucose pyrophosphorylase by reversion genetics.* Proc Natl Acad Sci U S A, 1998. **95**(17): p. 10322-7.

166. Sowokinos, J.R., *Pyrophosphorylases in Solanum tuberosum: I. Changes in ADP-Glucose and UDP-Glucose Pyrophosphorylase Activities Associated with Starch Biosynthesis during Tuberization, Maturation, and Storage of Potatoes.* Plant Physiol, 1976. **57**(1): p. 63-8.

167. Seferoglu, A.B., et al., *Transcriptional regulation of the ADP-glucose pyrophosphorylase isoforms in the leaf and the stem under long and short photoperiod in lentil.* Plant Sci, 2013. **205-206**: p. 29-37.

168. Seferoglu, A.B., *Identification of important residues for modulation of allosteric properties of potato ADP glucose pyrophosphorylase* in *Chemical and Biological Engineering*. 2011, Koc University.

169. Iglesias, A.A., et al., *Characterization of the kinetic, regulatory, and structural properties of ADP-glucose pyrophosphorylase from Chlamydomonas reinhardtii.* Plant Physiol, 1994. **104**(4): p. 1287-94.

170. Boehlein, S.K., et al., *Probing allosteric binding sites of the maize endosperm ADP-glucose pyrophosphorylase.* Plant Physiol, 2010. **152**(1): p. 85-95.

171. Lee, S.M., et al., *Characterization of the potato upreg1gene, encoding a mutated ADP-glucose pyrophosphorylase large subunit, in transformed rice.* Plant Cell Tissue and Organ Culture, 2010. **102**(2): p. 171-179.

172. Seferoglu, A.B., et al., *Enhanced heterotetrameric assembly of potato ADP-glucose pyrophosphorylase using reverse genetics.* Plant Cell Physiol, 2014. **55**(8): p. 1473-83.

173. *Food and Agriculture Organization of the United Nations* 2013 [cited 2014 15 October 2014]; Available from: http://faostat.fao.org/site/567/default.aspx - ancor

174. Singh, R. and B.O. Juliano, *Free sugars in relation to starch accumulation in developing rice grain.* Plant Physiol, 1977. **59**(3): p. 417-21.

175. Ohdan, T., et al., *Expression profiling of genes involved in starch synthesis in sink and source organs of rice.* J Exp Bot, 2005. **56**(422): p. 3229-44.

176. Akihiro, T., K. Mizuno, and T. Fujimura, *Gene expression of ADP-glucose pyrophosphorylase and starch contents in rice cultured cells are cooperatively regulated by sucrose and ABA.* Plant Cell Physiol, 2005. **46**(6): p. 937-46.

177. Cook, F.R., B. Fahy, and K. Trafford, *A rice mutant lacking a large subunit of ADP-glucose pyrophosphorylase has drastically reduced starch content in the culm but normal plant morphology and yield.* Functional Plant Biology, 2012. **39**(12): p. 1068-1078.

178. Tuncel, A., et al., *The rice endosperm ADP-glucose pyrophosphorylase large subunit is essential for optimal catalysis and allosteric regulation of the heterotetrameric enzyme.* Plant Cell Physiol, 2014. **55**(6): p. 1169-83.

179. Yan, J.Q., et al., *Quantitative trait loci analysis for the developmental behavior of tiller number in rice (Oryza sativa L.).* Theoretical and Applied Genetics, 1998. **97**(1-2): p. 267-274.